AdriaClim

Climate change information, monitoring and management tools for adaptation strategies in Adriatic coastal areas

Project ID: 10252001

Report on

D.3.3.4 Validation for relevant models used in A3.2

PP12 – ISPRA

D.3.4.1 Integration and assessment of monitoring (observations and models) components information for each Pilot

PP1 – CNR-ISMAR

Final version, June 2023

Deliverable:	D3.3.4 [Validation report for relevant models used in A3.2] D3.4.1 [Report on Integration and assessment of monitoring (observations and models) components information for each Pilot]
Due month	M42 [June 2023]
Delivery Date	30/06/2023
Document status	V0.1
Authors	CNR-ISMAR: Christian Ferrarin, Maria Letizia Vitelletti, Fabio Raicich ISPRA: Sara Morucci, Tommaso Petochi, Andrea Bonometto, Antonello Bruschi, Paolo Gyssels, Gianfranco Calise, Alì Pourzangbar, Maria Paola Campolunghi, Francesco Lalli, Giovanna Marino CMCC: Viviana Piermattei, Vladimir Santos Da Costa, Giorgia Verri APULIA REGION: Pietro Calabrese IOF: Gordana Beg Paklar, Tomislav Džoić, Branka Grbec, Hrvoje Mihanović, Petra Zemunik
Reviewers	

Table of contents

1. Aims and content of document

The main aim of the present document is to provide information about model validation procedures and the main results gathered by the comparison of observed historical time series and simulations (3.3.4) and to provide the list of quality-checked information (observations and model outputs) available for each of the project's Pilot areas (3.4.1) (Fig.1).
Since the contents of these two deliverables are similar and belong to the same activities, they have been merged in a single report in order to facilitate comprehension, completeness and to avoid redundance.
Moreover, these deliverables aim at providing an overview of the climate variability in the past/present time and in the future scenarios through the computation of specific climate indicators (e.g., trends) in the referring period (1992-2011).

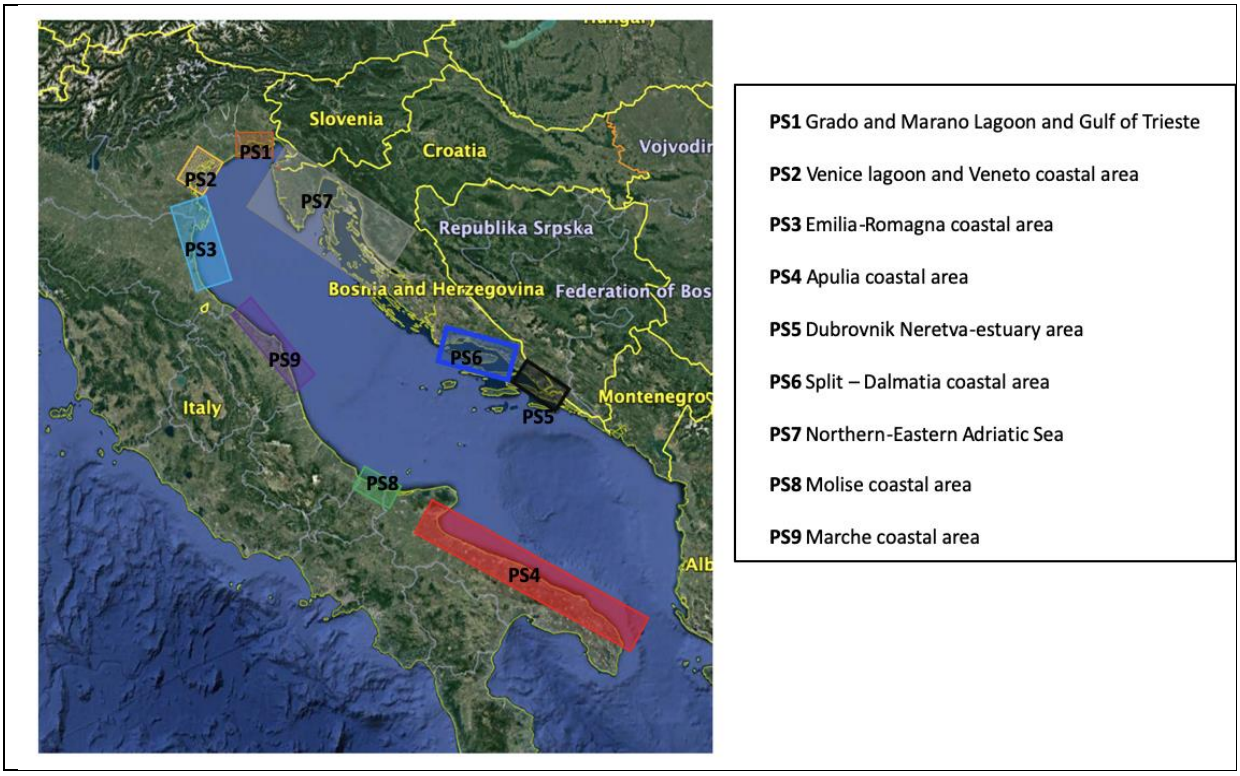

Fig. 1. The AdriaClim pilot areas in the Adriatic basin.

2. Available datasets for each Pilot area

The list of available information has been derived from deliverables 3.1.1. and 3.2.1 for the observations and the model outputs, respectively. The datasets should be subjected to the quality check protocols described in deliverable 3.3.1 and distributed through the AdriaClim information system (see deliverable 4.1.1.).

It is noteworthy that the Regional Earth System Model over the Adriatic Sea area implemented in the AdriaClim project will provide atmospheric, hydrologic and oceanographic information for all pilot areas.

2.1 PS1 Grado and Marano Lagoon and Gulf of Trieste

Involved partners: ARPA FVG, UNIBO, CNR-ISMAR.

Table 1: Available observations and model results at PS1.

Type	Name	Description
Observation	ISPRA RMN Tide-gauge at Trieste	*Variables: sea-level height, water temperature, air temperature, atmospheric pressure, wind speed, wind direction, relative humidity* *Sampling frequency: 10 min*
Observation	ISPRA RMLV Tide-gauge at Grado	*Variables: sea-level height* *Sampling frequency: 10 min*
Observation	CNR tide-gauge station al Molo Sartorio	*Variables: sea-level height, atmospheric pressure.* *Sampling frequency: 10 min/ hourly*
Observation	CNR Meteorological station at Molo F. Bandiera	*Variables: 10 m air temperature and wind, sea temperature at 0.4, 2 and 6 m.* *Sampling frequency: 10 min/ hourly*
Observation	ARPA FVG coastal meteorological station at Trieste, Fossalon di Grado, Grado and Lignano Sabbiadoro	*Variables: precipitation, wind speed and direction, temperature, relative humidity and global solar radiation.* *Sampling frequency: 10 min/ hourly*
Observation	ARPA FVG open sea stations located in the Gulf of Trieste (16 stations)	*Variables: temperature, salinity, dissolved oxygen, turbidity and chlorophyll-a, dissolved nitrogen forms, dissolved phosphorus, silicate, total nitrogen and total phosphorus.* *Sampling frequency: monthly*
Observation	ARPA FVG transitional waters stations located in the Lagoon of Marano-Grado (16 stations)	*Variables: temperature, salinity, dissolved oxygen, turbidity and chlorophyll-a, dissolved nitrogen forms, dissolved phosphorus, silicate, total nitrogen and total phosphorus.* *Sampling frequency: 10 min/ hourly*
Model	SHYFEM application to the Gulf of Trieste and the Lagoon of Marano-Grado	*Variables: sea level height, current velocity, water temperature and salinity.* *Output frequency: hourly.*

		Numerical domain and resolution: the numerical computation is performed on a spatial domain that represents part of the northern Adriatic Sea and the lagoon of Marano-Grado by means of an unstructured grid. To adequately resolve the river-sea continuum, the unstructured grid also includes the lower part of the other major rivers flowing into the considered system. The numerical grid consists of 33,100 triangular elements with a resolution that varies from 4 km in the open sea to a few hundred metres along the coast and tens of metres in the inner lagoon channels.

2.2 PS2 Venice Lagoon / City of Venice / Veneto coastal area

Involved partners: Arpa Veneto, CNR-ISMAR, AUSSL3 Serenissima, ISPRA, City of Venice.

Table 2: Available observations and model results at PS2.

Type	Name	Description
Observation	*ISPRA RMLV tide-gauge and meteorological stations in the North Adriatic Sea and the Venice lagoon (26 monitoring stations)*	*Variables: sea level height and meteo-marine parameters* *Sampling frequency: 10 minutes*
Observation	ARPAV Environmental quality network of Veneto coastal and marine waters (76 sampling stations)	*Variables: multiparametric probe, nutrients, phytoplankton, chemical analysis of the water and sediment and biota matrix* *Sampling frequency: seven campaigns per year*
Observation	ARPAV Marine Strategy network	*Variables: analysis of the water, sediment and biota matrix* *Sampling frequency: six campaigns per year*
Observation	ARPAV environmental quality network of the Venice lagoon (30 sampling stations)	*Variables: ecological quality* *Sampling frequency: four campaigns per year*
Observation	ISPRA RON wave buoy Venice	*Variables: significant wave height, wave direction, wave mean period, wave peak period, wind speed, wind direction, water temperature, air temperature, atmospheric pressure, relative humidity* *Sampling frequency: 10 min/ hourly*
Observation	CNR-ISMAR Acqua Alta oceanographic platform	*Variables: wind speed and direction, air temperature, humidity, solar radiation, precipitation, sea temperature, sea level, ADCP currents, waves* *Sampling frequency: 10 min/ hourly*

Observation	ARPAV meteorological network	*Variables: meteorological parameters precipitation, temperature, wind speed and direction, humidity, solar radiation, surface pressure* *Sampling frequency: 5 to 15 min depending on the variable*
Model	SHYFEM application to the Venice Lagoon and Veneto coast	*Variables: sea level height, current velocity, water temperature and salinity.* *Output frequency: hourly.* *Numerical domain and resolution: the numerical computation is performed on a spatial domain that represents the entire Lagoon and its adjacent shore. The numerical grid consists of about 32,000 triangular elements with a resolution that varies from 2 km in the open sea to a few hundred metres along the coast and tens of metres in the inner lagoon channels.*

2.3 PS3 Emilia-Romagna area

Involved partners: ARPAE, RER, UNIBO, CNR-ISMAR, CMCC, ISPRA.

Table 3: Available observations and model results at PS3.

Type	Name	Description
Observation	ISPRA RMN Tide-gauge at Ravenna	*Variables: sea-level height, water temperature, air temperature, atmospheric pressure, wind speed, wind direction, relative humidity* *Sampling frequency: 10 min*
Observation	ARPAE real-time coastal and marine network (four stations in the Goro and Sacca di Goro Area and other four located in the Valli di Comacchio)	*Variables: Dissolved oxygen, pH, salinity and temperature* *Sampling frequency: hourly*
Observation	ARPAE monitoring in the Sacca di Goro (20 stations)	*Variables: Dissolved oxygen, pH, salinity and temperature* *Sampling frequency: undefined, only from June to September*
Observation	ARPAE Integrated station of Porto Garibaldi	*Variables: sea level, water quality, air temperature and humidity, wind direction and velocity, atmospheric pressure, pluviosity, vertical land movement parameters* *Sampling frequency: hourly*
Observation	ARPAE Nausicaa buoy	*Variables: sea temperature, significant wave height, wave direction, wave mean period, wave peak period* *Sampling frequency: hourly*

Observation	ARPAE idro-meteo monitoring network	*Variables: Rain gauges (233), hydrometric levels (182), temperature (176), relative humidity (67), wind (36), solar radiation (27), snow depth (18), radars (2), and an automatic radio sounder (1)* *Sampling frequency: hourly*
Observation	ARPAE Daphne Oceanographic Structure (35 sampling stations located along eight transects perpendicular to the coast)	*Variables: sea temperature, salinity, dissolved oxygen, pH, chlorophyll-a, nutrients (nitrate, phosphate and silicate) and phytoplankton communities.* *Sampling frequency: two times a month (weekly from June to September)*
Observation	IZSLER Environmental and sanitary monitoring network of shellfish production areas of Emilia Romagna (on 24 sampling stations)	*Variables: salinity, oxygen, pH, water and air temperature, faecal bacteria (Escherichia coli; Salmonella spp.)* *Sampling frequency: weekly/monthly/yearly*
Observation	ARPAE Daphne Oceanographic Structure for shellfish life and productions (most of the 35 sampling stations for the classification of the trophic status of coastal marine waters)	*Variables: pH, T°, oxygen, salinity, suspended solids, colour, metals, hydrocarbons, organ halogenated substances, faecal coliforms and saxitoxin and other substances which can influence the flavour of shellfish* *Sampling frequency: unknown*
Model	SHYFEM application to the Emilia Romagna coast	*Variables: sea level height, current velocity, water temperature, salinity.* *Output frequency: hourly.* *Numerical domain and resolution: the numerical computation is performed on a spatial domain that represents the Emilia-Romagna coast and its adjacent shore. The numerical grid consists of 15,392 triangular elements with a resolution that increases towards the coast.*

2.4 PS4 Apulia region

Involved partners: Apulia region, CMCC.

Table 4: Available observations and model results at PS4.

Type	Name	Description
Observation	ISPRA RMN Tide-gauge at Bari and Otranto	*Variables: sea-level height, water temperature, air temperature, atmospheric pressure, wind speed, wind direction, relative humidity* *Sampling frequency: 10 min*

Observation	ISPRA RON wave buoy at Monopoli	*Variables: significant wave height, wave direction, wave mean period, wave peak period, wind speed, wind direction, water temperature, air temperature, atmospheric pressure, relative humidity* *Sampling frequency: 10 min/ hourly*
Observation	CMCC buoy at Torre Guaceto Marine Protected Area	*Variables: temperature, conductivity (calculated salinity, density), dissolved oxygen, turbidity* *Sampling frequency: 10 minutes*
Model	CMCC-EBM application for the Ofanto river	*Variables: salinity, volume flux, salt wedge intrusion length.* *Output frequency: daily.* *Numerical domain and resolution: The EBM is a 1D box model applied to the target estuary volume. Moreover, a 3D implementation of the finite element model Shyfem will cover the Ofanto river-sea continuum and will be used as benchmark*

2.5 PS5 Dubrovnik Neretva area

Involved partners: DUNEA, IOF, CMCC, CNR-ISMAR.

Table 5: Available observations and model results at PS5.

Type	Name	Description
Observation	Slano Bay monitoring network (3 stations)	*Variables: salinity, temperature and bacterial (Escherichia coli, Enterococcus)* *Sampling frequency: seasonally*
Observation	Automatic meteo-oceanographic station in the Slano Bay	*Variables: sea level, sea temperature, air temperature, air pressure, humidity, wind speed and direction, precipitation, solar radiation.* *Sampling frequency: 15 minutes*
Observation	Permanent national oceanographic monitoring	*Variables: temperature, conductivity (salinity), dissolved oxygen, Chlorophyll A, nutrients (N, P, Si)* *Sampling frequency: monthly or seasonally*
Observation	Regular Neretva estuary monitoring by a research vessel BIOS DVA	*Variables: sea temperature, salinity, transparency, oxygen, copper, zinc, phytoplankton pigments, phytoplankton species, nutrient salts, pH, DOC (Dissolved organic carbon), priority substances in water, biota and sediment, microalgae, microzooplankton, mesozooplankton, marine seagrass, menthic invertebrates* *Sampling frequency: seasonally*

Observation	Automatic meteo-oceanographic station in the Metković harbour	*Variables: wind speed and direction, air temperature, relative humidity, air pressure, water temperature, conductivity, hydrostatic pressure and sea level.* *Sampling frequency: meteorological parameters and water level - one minute; water temperature, conductivity and hydrostatic pressure - 10 minutes.*
Observation	Autonomous sensors for water temperature, conductivity and dissolved oxygen content at four locations in the Neretva River estuary (Metković, Opuzen, Komin, Rogotin)	*Variables: water temperature, conductivity and dissolved oxygen content* *Sampling frequency: 10 minutes*
Model	ROMS-Ichthyop application to the Dubrovnik Neretva area	*Variables: sea level height, current velocity, water temperature, salinity and dispersion of passive particles.* *Output frequency: daily.* *Numerical domain and resolution: the model domain covers the Neretva estuary and adjacent coastal sea with a horizontal resolution of 200 m.*
Model	CMCC-EBM application for the Neretva River	*Variables: salinity, volume flux, salt wedge intrusion length.* *Output frequency: daily.* *Numerical domain and resolution: The EBM is a 1D box model applied to the Neretva River estuary.*

2.6 PS6 Split – Dalmatia area

Involved partners: RERA, IOF, RB, CMCC, CNR-ISMAR

Table 6: Available observations and model results at PS6.

Type	Name	Description
Observation	IOF T/S long-term monitoring at Split-Vis transect	*Variables: water temperature and salinity* *Sampling frequency: monthly*
Observation	IOF phytoplankton and microbiological monitoring at Stončica and Kaštela Bay stations	*Variables: sea temperature, salinity, chlorophyll-a concentration, phytoplankton community composition, abundance and production of heterotrophic bacteria (with different DNA content, i.e. High- DNA bacteria and Low-DNA bacteria), abundances of two cyanobacteria groups, i.e. Prochlorococcus and Synechococcus), abundances of pico-eukaryotic algae and abundances of protistan grazers (heterotrophic nanoflagellates).*

		Sampling frequency: monthly or seasonally
Observation	Sediment monitoring at Stončica and Kaštela Bay stations	*Variables: grain size composition, the content of organic matter (loss of ignition) and carbonates were determined at all stations, while the content of N and P in surface subsamples 2 cm thick and the content of org C.* *Sampling frequency: monthly or seasonally*
Observation	Tide gauge at Jurana cape	*Variables: sea level height* *Sampling frequency: hourly*
Model	ROMS-Ichthyop application to the Split-Dalmatia area	*Variables: sea level height, current velocity, water temperature, salinity and dispersion of passive particles.* *Output frequency: daily.* *Numerical domain and resolution: the model domain covers the middle Adriatic coastal area with a horizontal resolution of 165 m in the E-W direction and 231.5 m in the N-S direction.*

2.7 PS7 Northern-Eastern Adriatic Sea

Involved partners: IRB

Table 7: Available observations and model results at PS7.

Type	Name	Description
Observation	IRB Center for Marine Research (CMR) oceanographic buoys - meteorological sensors	*Variables: wind direction and speed, air temperature, relative humidity, atmospheric pressure, solar irradiation, precipitation and air visibility* *Sampling frequency: 10 min*
Observation	IRB Center for Marine Research (CMR) oceanographic buoys - physical, chemical and biological sensors	*Variables: Acoustic Doppler Current Profiler (ADCP), wave sensor, surface current measurement, PCO2, sea temperature, conductivity (salinity), dissolved oxygen, light transmission, pH, soluble organic fluorescence (FDOM), phytoplankton pigment (phycocyanin, phycoerythrin, Chlorophyll A and backscatter Red sensor, backscatter blue sensor)* *Sampling frequency: 10 min*
Observation	Permanent national oceanographic monitoring	*Variables: temperature, conductivity (salinity), dissolved oxygen, Chlorophyll A,* nutrients (N, P, Si) *Sampling frequency: monthly or seasonally*

2.8 PS8 Marche area

Involved partners: Regione Marche.

Table 8: Available observations and model results at PS8.

Type	Name	Description
Observation	SPCSL meteorological network	*Variables: precipitation, temperature, humidity, wind, air pressure, hydrometric level of watercourse* *Sampling frequency: hourly*
Observation	ASSAM meteorological network	*Variables: precipitation, temperature, humidity, wind, air pressure* *Sampling frequency: hourly*
Observation	ISPRA RMN Tide-gauge at Ancona and San Benedetto del Tronto	*Variables: sea-level height, water temperature, air temperature, atmospheric pressure, wind speed, wind direction, relative humidity* *Sampling frequency: 10 min*
Observation	CNR-IRBIM Meda Senigallia	*Variables: air temperature, humidity, wind, air pressure, sea level height, current speed and direction, significant wave height, mean wave period, mean wave direction, chlorophyll a, turbidity, sea temperature, salinity, dissolved oxygen,* *Sampling frequency: hourly*
Observation	ARPAM Algal surveillance monitoring (35 stations)	*Variables: sea temperature, salinity, pH, dissolved oxygen, concentration of chlorophyll-a, reactive silica and transparency, phytoplankton component (composition, density, reporting of blooms of potentially toxic species), nutrients (soluble inorganic nitrogen and total phosphorus)* *Sampling frequency: monthly*
Observation	ARPAM Monitoring of coastal marine water bodies (12 transects, each consisting of 2 stations)	*Variables: sea temperature, salinity, pH, dissolved oxygen, chlorophyll a, reactive silica and transparency, phytoplankton component (composition, density, reporting of blooms of potentially toxic species), nutrients (soluble inorganic nitrogen and total phosphorus), macrobenthonic component* *Sampling frequency: monthly*

2.9 PS9 Molise area

Involved partners: Regione Molise.

Table 9: Available observations and model results at PS9.

Type	Name	Description
Observation	Civil protection hydro-meteorological monitoring network	*Variables: equivalent precipitation, hydrometric level, air temperature, relative humidity of the air, wind speed and wind direction, solar radiation, the height of the snow cover, normalised pressure at sea level, sea temperature, salinity, pH, dissolved oxygen, turbidity, significant wave height, wave direction, wave mean period, wave peak period, phenological network* *Sampling frequency: 10 min*

3. Assessing climate variability for each Pilot area

The objective of the second part of this study is to identify useful statistical indicators from measured and modelled datasets for assessing the climate variability in the investigated pilot area. The climate variability trends have been computed applying time-series analysis methodologies to selected monitoring variables, here grouped in three main categories: 1) physical and chemical marine variables (sea temperature, salinity, sea level, wind-wave energy and height, oxygen, nutrients), 2) atmospheric and hydrological variables (air temperature, wind speed, mean sea level pressure, precipitation, river discharge), 3) biotic variables (chlorophyll-a and phytoplankton) (Chust et al., 2022).

Traditionally, time series methods decompose the temporal data into the following components: cyclical fluctuation, trend, and random error (Mudelsee, 2019). For the present study, we suggest using the non-parametric Mann–Kendall test to assess the significance of trends in the climate data on monthly, seasonal, and annual scales. The null hypothesis in the test is that there is no significant trend within the time series and when this hypothesis is rejected it indicates a trend, which can be either positive or negative as described by its score.

The analysis will be performed for investigating:

- changes in the mean values of the variable;
- changes in extreme events; here an appropriate metric needs to be defined (e.g., intensity, duration or frequency of the event) before the trend analysis.
- changes in seasonality, which in classical decomposition methods is assumed to be constant over the years.

Data have been first decomposed to remove seasonal effects using LOESS (Cleveland et al., 1990). For the purpose of the AdriaClim project, we decided to limit the trend analysis to the 20-year periods considered in the model simulations: 1992-2011 and 2031-2050 for the historical and climate change scenarios, respectively. In Table 10, we listed the trend analyses to be applied to the measured timeseries and to model output timeseries extracted at site-specific monitoring station locations. Some of the computed trends overlap with the indicators for changes in the climate systems proposed within Activity 3.5. The trends will be computed with the software developed in Activity 4.2.
For each pilot site, some additional analyses have been carried out depending on the site-specific peculiarities.

Table 10: List of variables and analyses to be performed on the timeseries.

Category	Variable	Units	Analysis description
Physical and chemical marine	Sea temperature	°C	*Trend in daily/monthly/yearly mean values; Trend in monthly/yearly extreme values (95th percentile)*
Physical and chemical marine	Salinity		*Trend in daily/monthly/yearly mean values*
Physical and chemical marine	Sea level	m	*Trend in daily/monthly/yearly mean values; Trend in monthly/yearly extreme values (95th percentile); Trend in number of peaks over site-specific threshold per year*
Physical and chemical marine	Significant wave height	m	*Trend in daily/monthly/yearly mean values; Trend in monthly/yearly extreme values (95th percentile)*
Physical and chemical marine	Dissolved oxygen	mg l^{-1}	*Trend in monthly/yearly mean values*
Physical and chemical marine	Nutrients (NH4, PO4, NO2, NO3, SiO4)	mg l^{-1}	*Trend in monthly/yearly mean values*
Atmospheric and hydrological	Air temperature	°C	*Trend in daily/monthly/yearly mean values; Trend in monthly/yearly extreme values (10th and 95th percentiles); Trend in number of days with T over/below threshold (25°C for warm and 0°C for cold days) per year*
Atmospheric and hydrological	Wind speed	m s^{-1}	*Trend in daily/monthly/yearly mean values; Trend in monthly/yearly extreme values (95th percentile)*
Atmospheric and hydrological	Mean sea level pressure	mbar	*Trend in daily/monthly/yearly mean values; Trend in monthly/yearly extreme values (95th percentile)*
Atmospheric and hydrological	Precipitation	mm day^{-1}	*Trend in annual accumulated values; Trend in yearly extreme values (95th percentile); Trend in number of days with P over threshold (10 mm/day); Trend in number of days without precipitation*
Atmospheric and hydrological	River flow	m^3 s^{-1}	*Trend in monthly/yearly mean values; Trend in monthly/yearly extreme values (95th percentile)*
Biotic	Chlorophyll a	mg l^{-1}	*Trend in monthly/yearly mean values*
Biotic	Phytoplankton	mg m^{-3}	*Trend in monthly/yearly mean values*

3.1 PS1 Grado and Marano Lagoon and Gulf of Trieste

Table 11: Statistics computed for PS1 from observations (Obs 1991-2020), reanalysis scenario (REA 1991-2020), historical climate scenario (Hist 1992-2011) and climate change RCP85 scenario (RCP8.5 2031-2050).

Station	Variable	Trend (units/year)				
		Description	Obs 1991-2020	REA 1991-2019	Hist 1992-2011	RCP8.5 2031-2050
Trieste	Sea surface temperature (°C)	*Trend in monthly mean values*	*0.037 ± 0.000*	*0.041 ± 0.000*		
		Trend in monthly extreme (p95) values	*0.033 ± 0.000*	*0.048 ± 0.000*		
	Surface salinity	*Trend in monthly mean values*	-	*0.016 ± 0.000*		
	Sea surface height (mm)	*Trend in monthly mean values*	*3.38 ± 0.03*	*3.55 ± 0.03*	*3.36 ± 0.03*	*NoSignTrend*
		Trend in monthly extreme (p95) values	*3.59 ± 0.05*	*3.47 ± 0.05*	*2.01 ± 0.04*	*NoSignTrend*
		Number of hours over the X.X m threshold per year				

3.2 PS2 Venice Lagoon / City of Venice / Veneto coastal area

One of the most important variables for the hydrodynamics in the Lagoon of Venice and Veneto coastal area is the sea level, which is the result of several drivers acting a different spatial and temporal scales (astronomic tide, seiche, inter-decadal, inter-annual and seasonal variability, planetary atmospheric waves, mesoscale and synoptic air pressure and wind forcing, meteotsunami, waves, …). In the Lagoon of Venice, the astronomic tide plays a crucial role in determining the daily sea level variability, circulation and exchange with the open sea. Extreme sea levels, mostly determined by storm surges induced by Scirocco winds, are causing flooding in the City of Venice and the nearby coastal area (Ferrarin et al., 2022).

Table 12: Statistics computed for PS2 from observations (Obs 1991-2020), reanalysis scenario (REA 1991-2020), historical climate scenario (Hist 1991-2011) and climate change RCP85 scenario (RCP8.5 2031-2050).

Station	Variable	Trend (units/year)				
		Description	Obs 1991-2020	REA 1991-2020	Hist 1992-2011	RCP8.5 2031-2050
AAOT	Sea surface temperature (°C)	*Trend in monthly mean values*	-	*0.040 ± 0.000*		
		Trend in monthly extreme (p95) values	-	*0.044 ± 0.000*		
	Surface salinity	*Trend in monthly mean values*	-	*no*		
	Sea level height (mm)	*Trend in monthly mean values*	*4.66 ± 0.03*	*3.69 ± 0.03*	*4.00 ± 0.03*	*2.59 ± 0.03*
		Trend in monthly extreme (p95) values	*5.52 ± 0.05*	*3.90 ± 0.04*	*3.26 ± 0.04*	*1.51 ± 0.04*
Venice Punta della Salute	Sea surface height (mm)	*Trend in monthly mean values*	*4.94 ± 0.03*			
		Trend in monthly extreme (p95) values	*4.43 ± 0.04*			

3.3 PS3 Emilia-Romagna area

The results obtained from the sub regional downscaling performed during the AdriaClim project are analyzed here by addressing the differences between the available datasets for the Emilia-Romagna region measuring stations and the results of the NEMO and WRF-Hydro models. By analyzing the results of the historical subregional simulations together with observations it was possible to check the general performance of the sub regional downscaling technique.

In what refers to the oceanographic sub regional downscaling performed with the NEMO model, Arpae collected and organized the data available for the measuring stations shown in Figure x1A in terms of salinity and temperature. Then, the results of the NEMO model were extracted for the closest domain points relative to stations 1014, 2014, 1019, 604, 619, 614, 2004, and 1004 which are shown in Figure x1B. The subsequent step involved plotting boxplots and empirical cumulative distribution functions (ECDFs) using the difference between the measured values and the historical simulation results. The extraction of the model results and the organization of the plots (http://interreg.c3hpc.exact-lab.it/AdriaClim/Med_CORDEX_analysis/NEMO_model_validation_arpae.php) was done by ARPA-FVG which provided technical support and structured the graphs in the same way as developed for their pilot site.

Table 13: Statistics computed for PS3 from observations (Obs 1991-2020), reanalysis scenario (REA 1991-2020), historical climate scenario (Hist 1991-2011) and climate change RCP85 scenario (RCP8.5 2031-2050).

Station	Variable	Trend (units/year)				
		Description	Obs 1991-2020	REA 1991-2020	Hist 1992-2011	RCP8.5 2031-2050
Porto Garibaldi	Sea surface temperature (°C)	*Trend in monthly mean values*	*No Sign.Trend*		*0.032*	*0.016*
		Trend in monthly extreme (p95) values	*No Sign.Trend*		*0.041*	*0.009*
	Surface salinity (psu)	*Trend in monthly mean values*	*No Sign.Trend*		*-0.079*	*0.153*

		Trend in monthly extreme (p95) values	*No Sign.Trend*		*-0.074*	*0.077*
	Sea level height (mm)	*Trend in monthly mean values*	*No Sign.Trend*		*4.86 ± 0.03*	*2.98 ± 0.04*
		Trend in monthly extreme (p95) values	*No Sign.Trend*		*4.64 ± 0.05*	*2.26 ± 0.05*

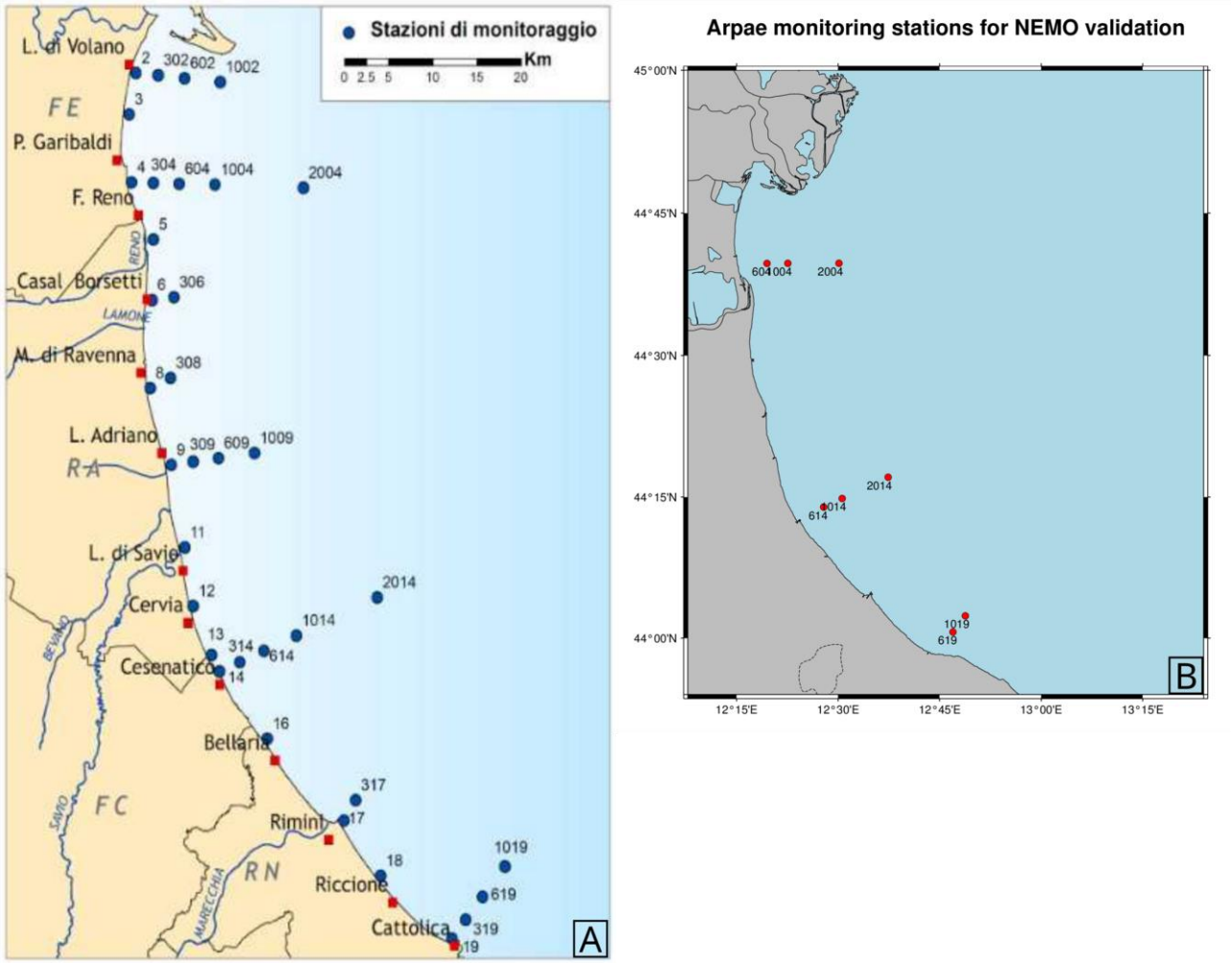

Figure x1: A) monitoring stations done by Arpae on a regular or almost regular basis. B) Stations that were used to analyze the results of the sub regional NEMO downscaling results

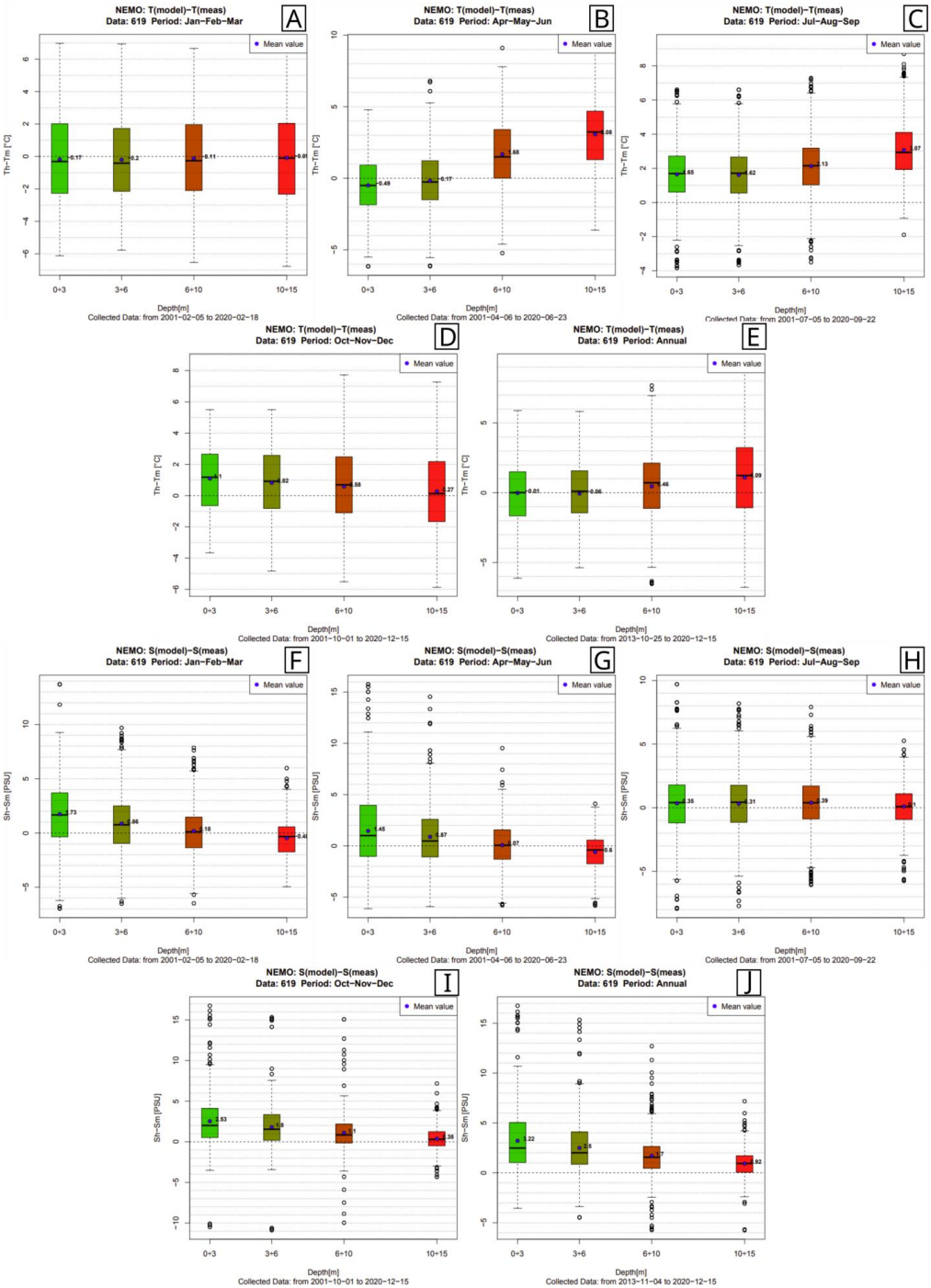

Figure x2: Boxplots of the difference between modeled and measured values for temperature (from subfigures A to E) and salinity (subfigures F to J) for station 619. Subfigures A) and F) represent January-February-March; Subfigures B) and G) April-May-June; Subfigures C) and H) July-August-September; Subfigures D) and I) October-November-December; and Subfigures E) and J) represent the annual values.

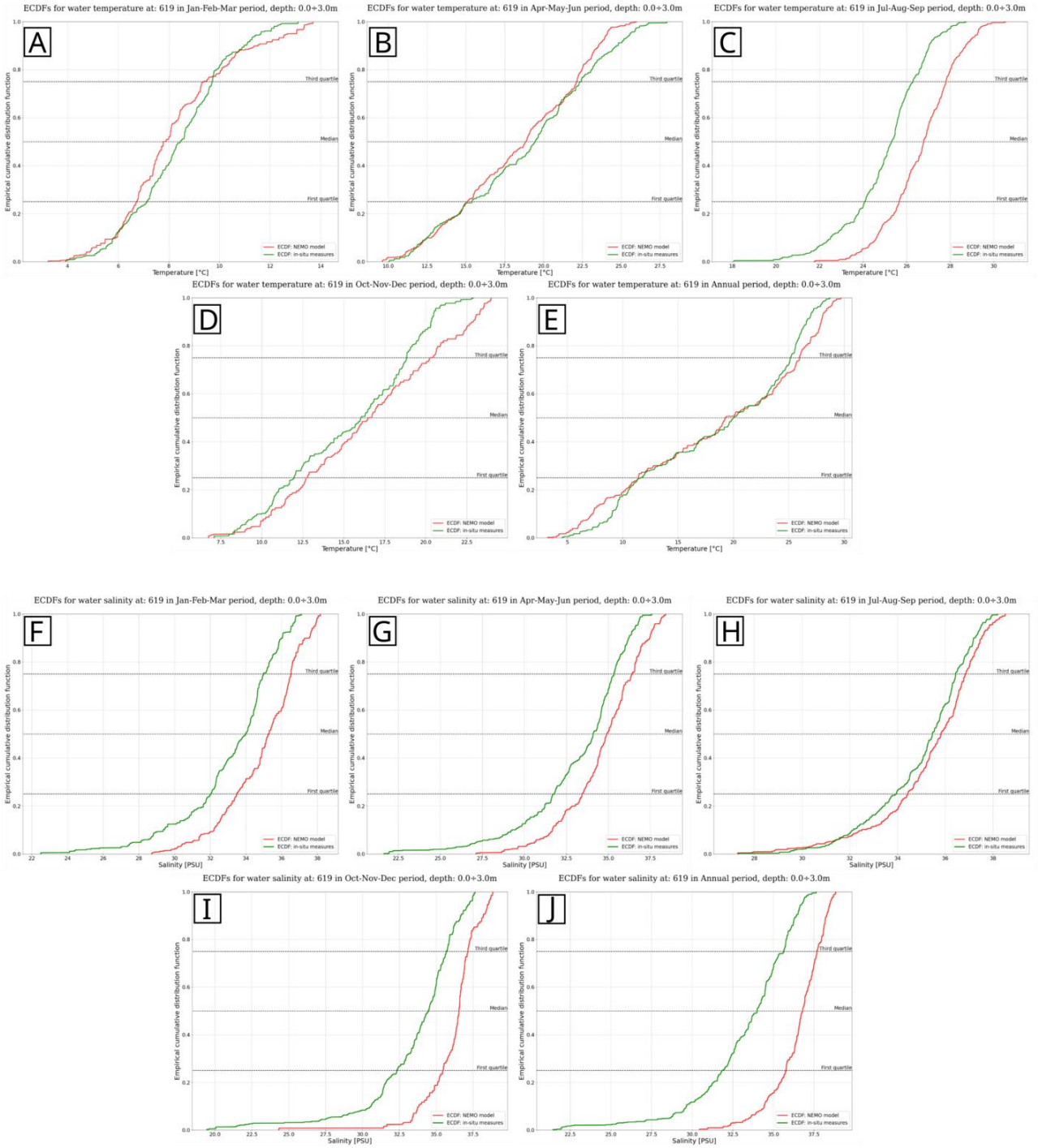

Figure x3: ECDFs of the difference between modeled and measured values for temperature (from subfigures A to E) and salinity (subfigures F to J) for station 619 (between 0 and 3.0m depth). Subfigures A) and F) represent January-February-March; Subfigures B) and G) April-May-June; Subfigures C) and H) July-August-September; Subfigures D) and I) October-November-December; and Subfigures E) and J) represent the annual values.

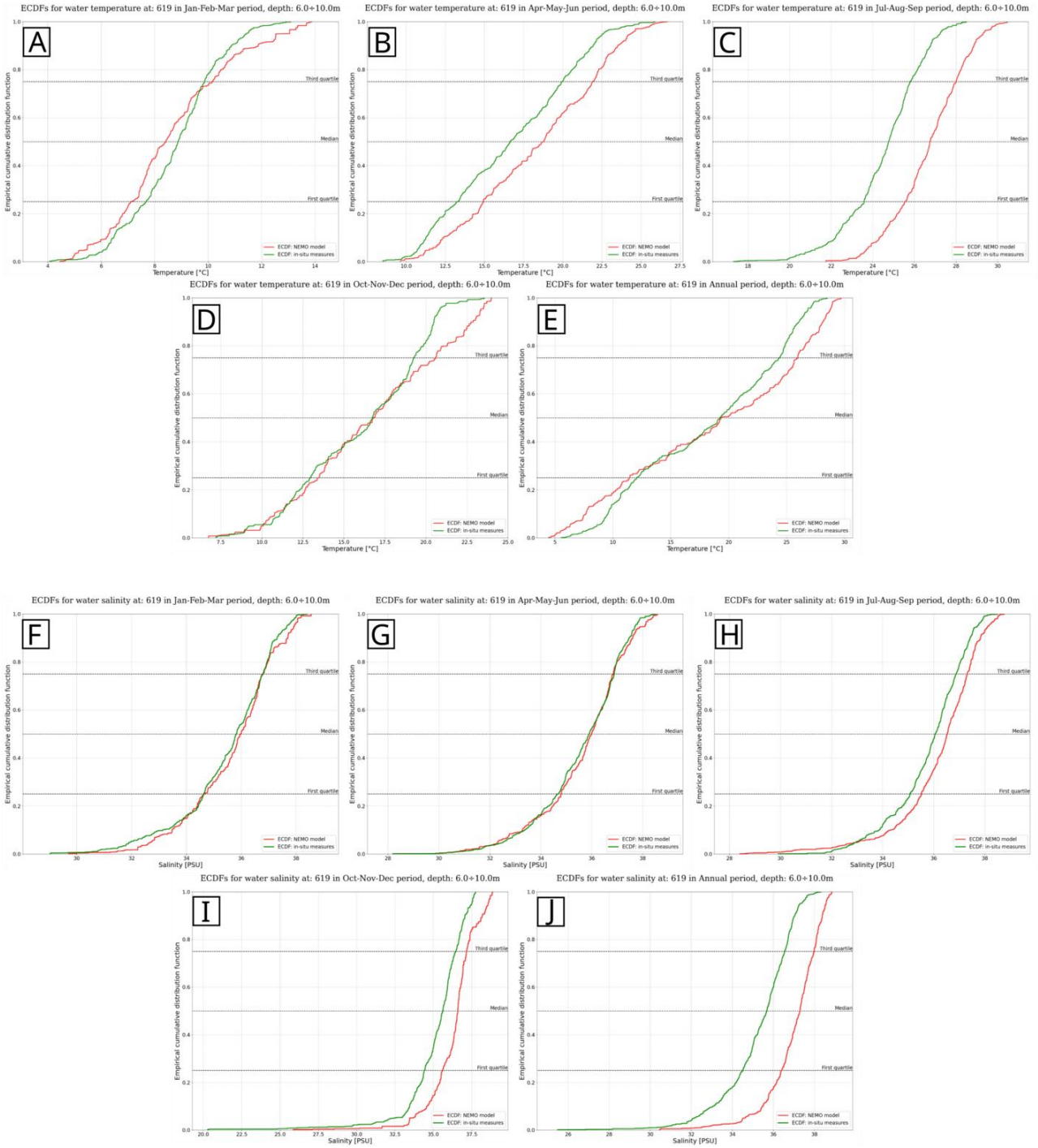

Figure x4: ECDFs of the difference between modeled and measured values for temperature (from subfigures A to E) and salinity (subfigures F to J) for station 619 (between 6 and 10.0m depth). Subfigures A) and F) represent January-February-March; Subfigures B) and G) April-May-June; Subfigures C) and H) July-August-September; Subfigures D) and I) October-November-December; and Subfigures E) and J) represent the annual values.

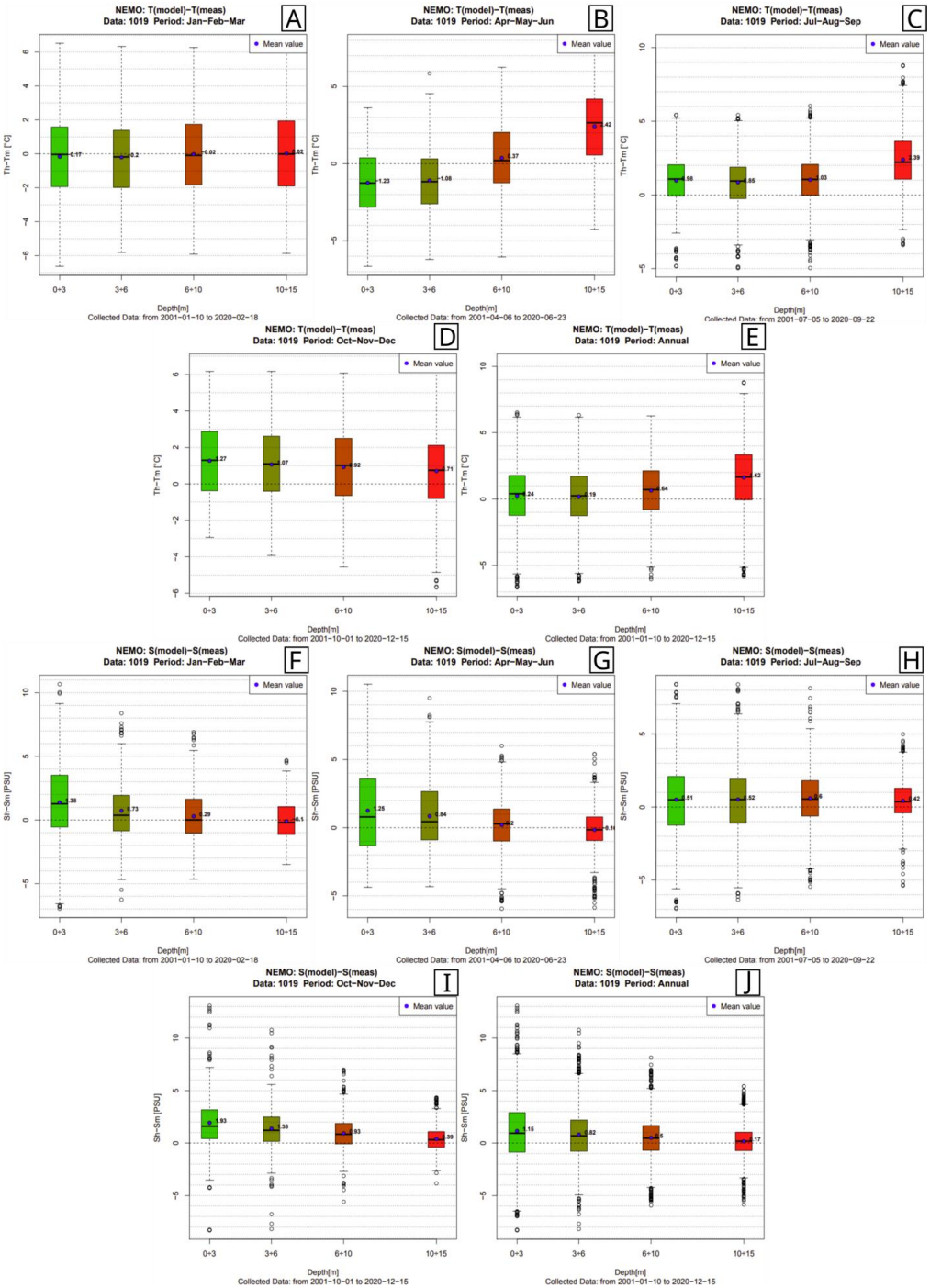

Figure x5: Boxplots of the difference between modeled and measured values for temperature (from subfigures A to E) and salinity (subfigures F to J) for station 1019. Subfigures A) and F) represent January-February-March; Subfigures B) and G) April-May-June; Subfigures C) and H) July-August-September; Subfigures D) and I) October-November-December; and Subfigures E) and J) represent the annual values.

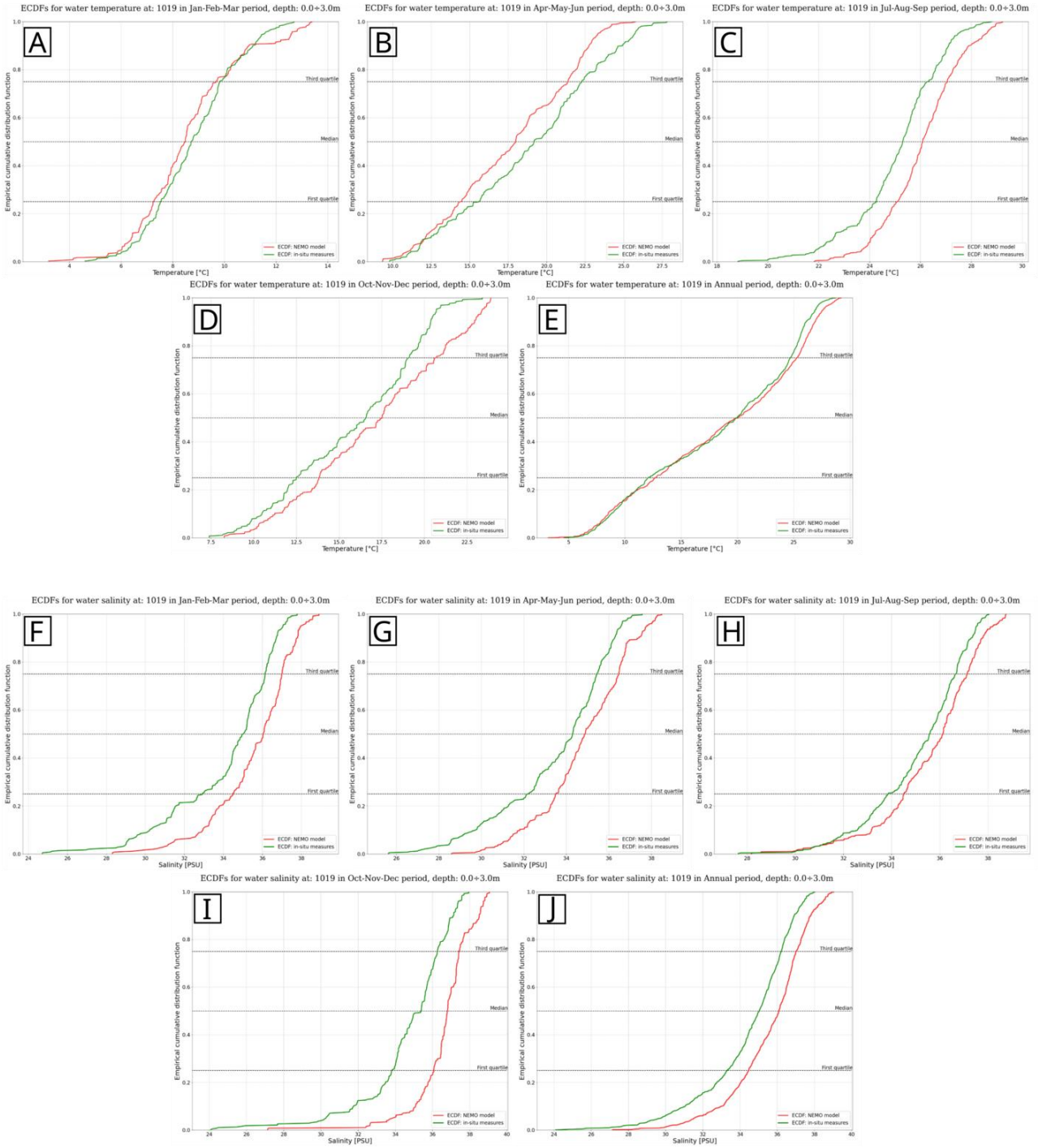

Figure x6: ECDFs of the difference between modeled and measured values for temperature (from subfigures A to E) and salinity (subfigures F to J) for station 1019 (between 0 and 3.0m depth). Subfigures A) and F) represent January-February-March; Subfigures B) and G) April-May-June; Subfigures C) and H) July-August-September; Subfigures D) and I) October-November-December; and Subfigures E) and J) represent the annual values.

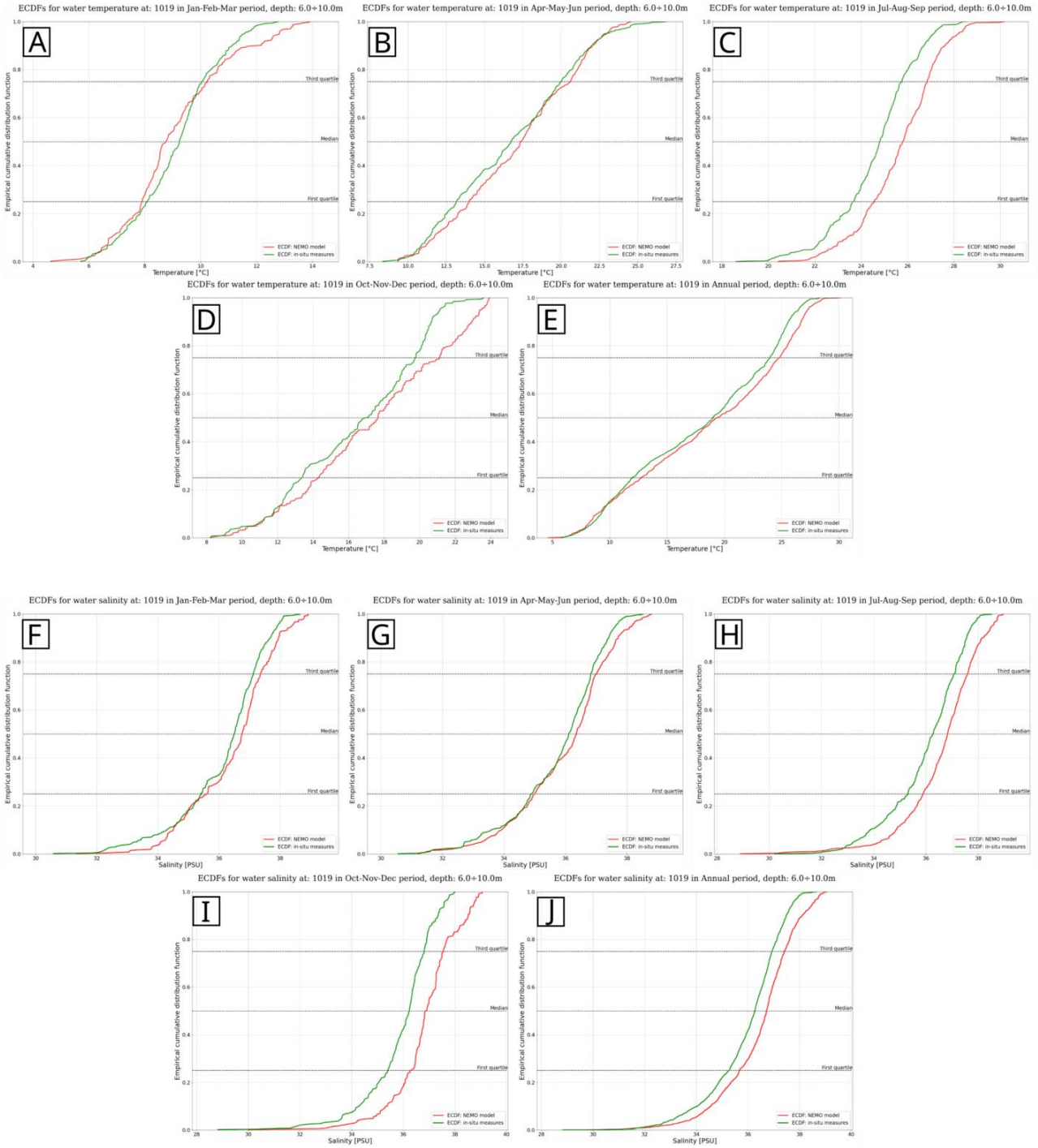

Figure x7: ECDFs of the difference between modeled and measured values for temperature (from subfigures A to E) and salinity (subfigures F to J) for station 1019 (between 6 and 10.0m depth). Subfigures A) and F) represent January-February-March; Subfigures B) and G) April-May-June; Subfigures C) and H) July-August-September; Subfigures D) and I) October-November-December; and Subfigures E) and J) represent the annual values.

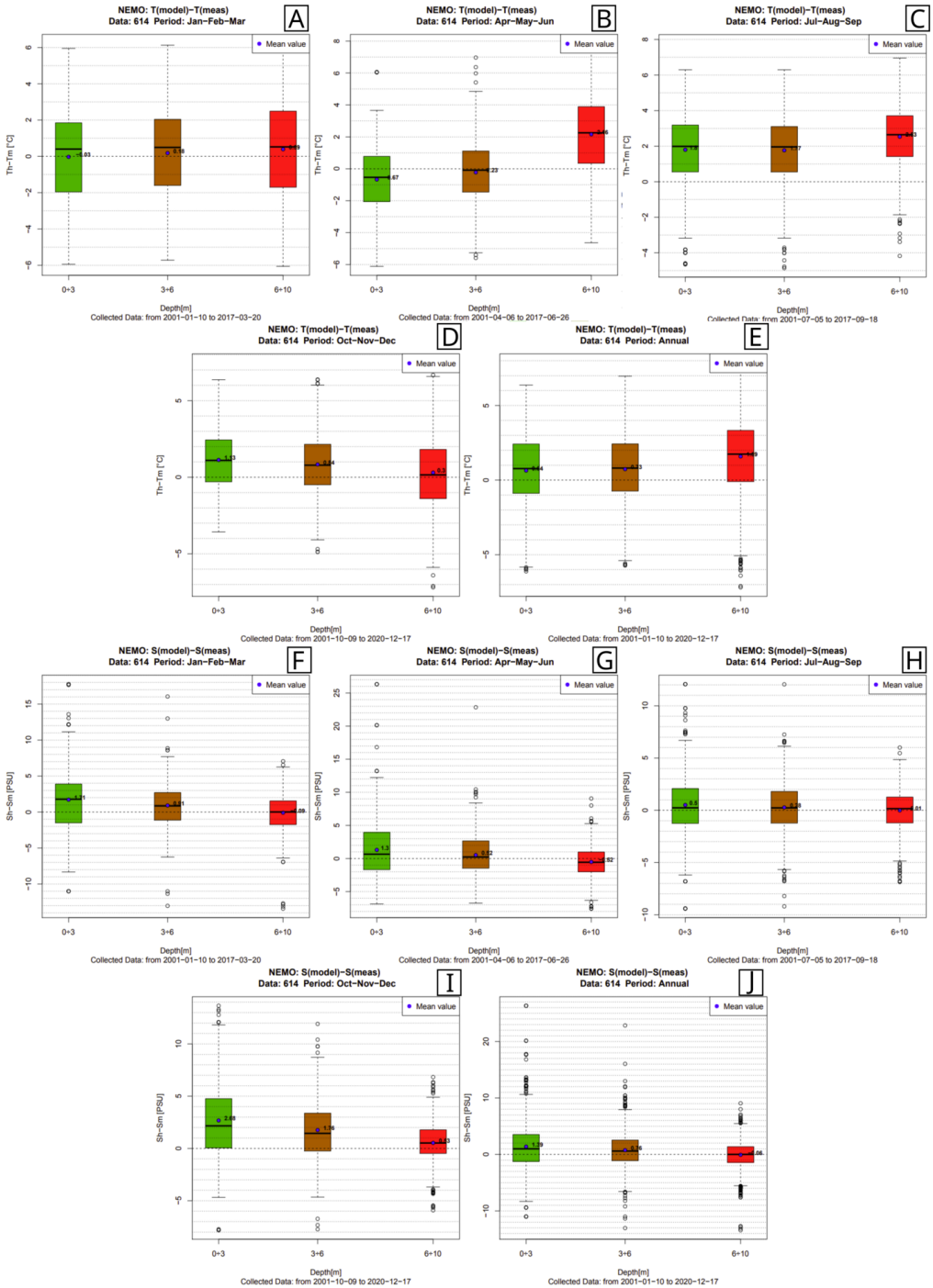

Figure x8: Boxplots of the difference between modeled and measured values for temperature (from subfigures A to E) and salinity (subfigures F to J) for station 614. Subfigures A) and F) represent January-February-March; Subfigures B) and G) April-May-June; Subfigures C) and H) July-August-September; Subfigures D) and I) October-November-December; and Subfigures E) and J) represent the annual values.

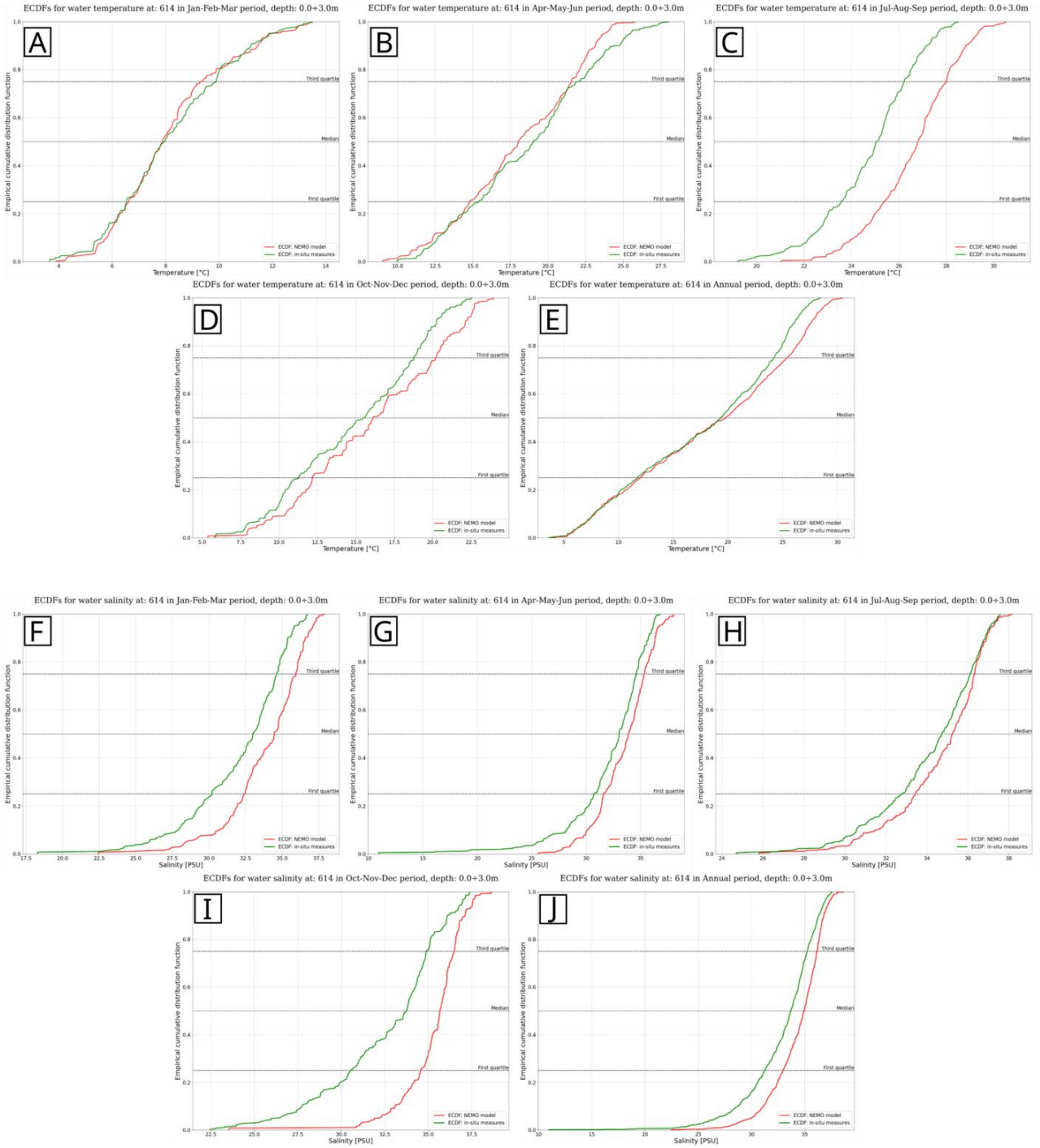

Figure x9: ECDFs of the difference between modeled and measured values for temperature (from subfigures A to E) and salinity (subfigures F to J) for station 614 (between 0 and 3.0m depth). Subfigures A) and F) represent January-February-March; Subfigures B) and G) April-May-June; Subfigures C) and H) July-August-September; Subfigures D) and I) October-November-December; and Subfigures E) and J) represent the annual values.

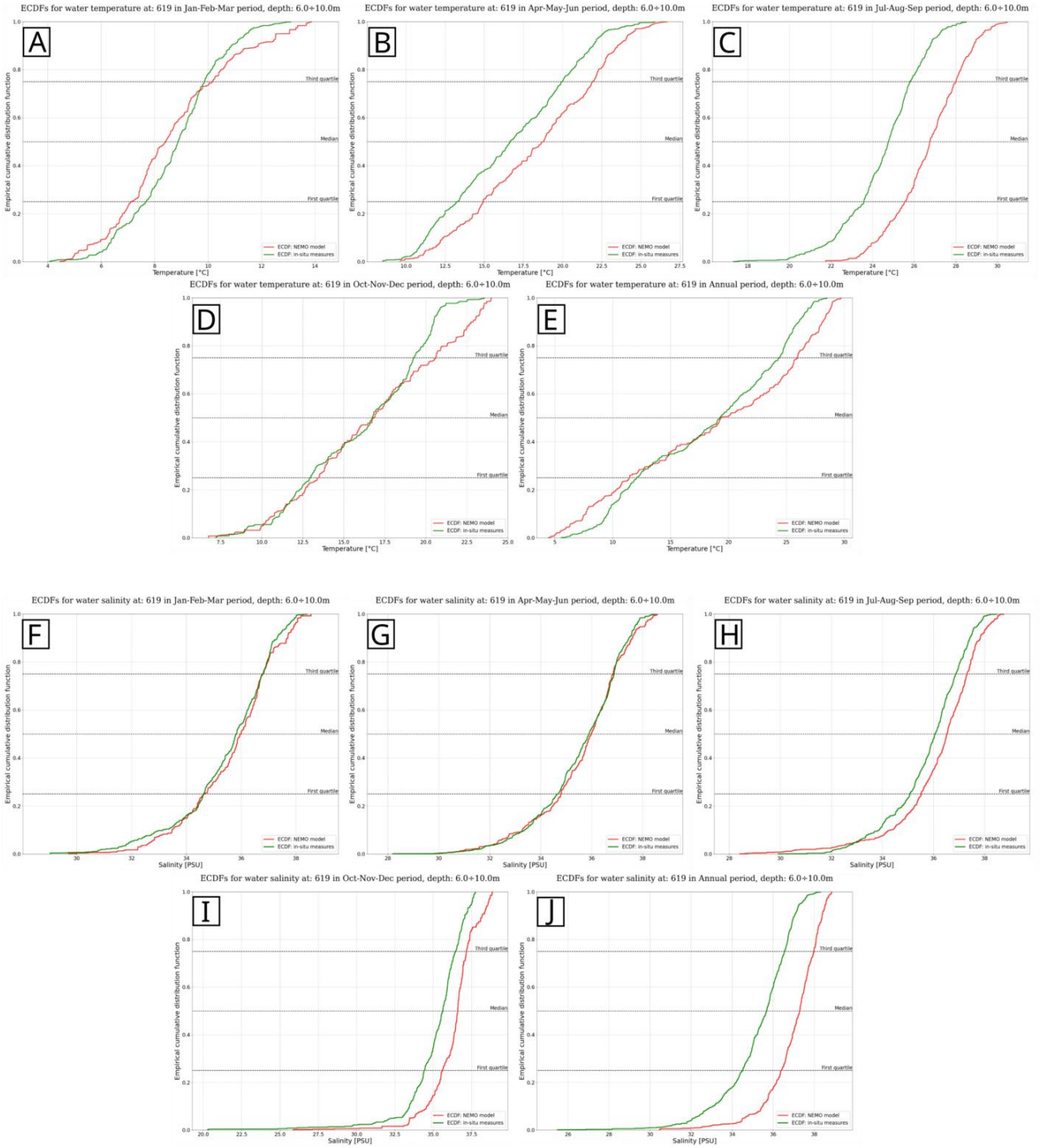

Figure x10: ECDFs of the difference between modeled and measured values for temperature (from subfigures A to E) and salinity (subfigures F to J) for station 614 (between 6 and 10.0m depth). Subfigures A) and F) represent January-February-March; Subfigures B) and G) April-May-June; Subfigures C) and H) July-August-September; Subfigures D) and I) October-November-December; and Subfigures E) and J) represent the annual values.

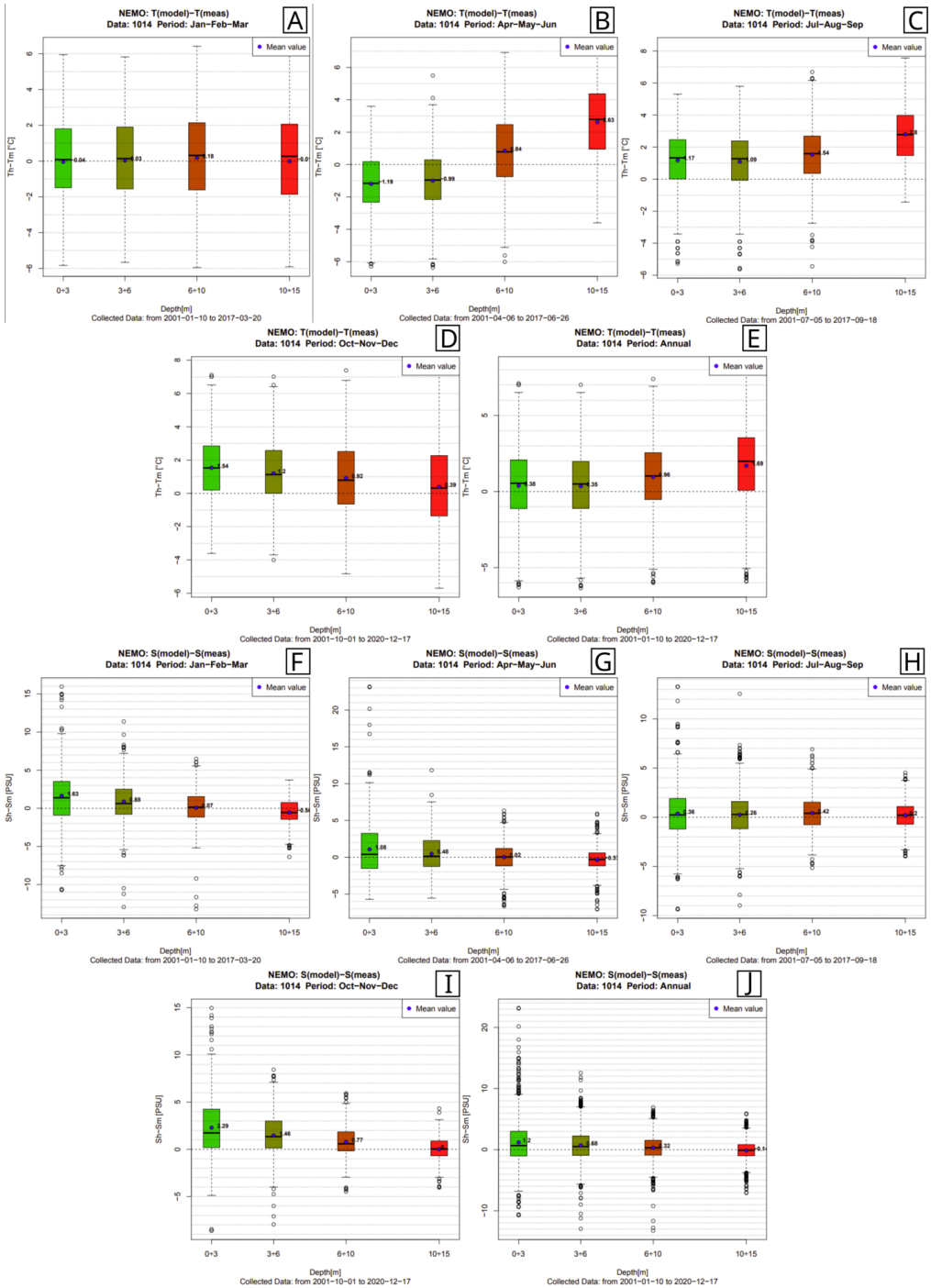

Figure x11: Boxplots of the difference between modeled and measured values for temperature (from subfigures A to E) and salinity (subfigures F to J) for station 1014. Subfigures A) and F) represent January-February-March; Subfigures B) and G) April-May-June; Subfigures C) and H) July-August-September; Subfigures D) and I) October-November-December; and Subfigures E) and J) represent the annual values.

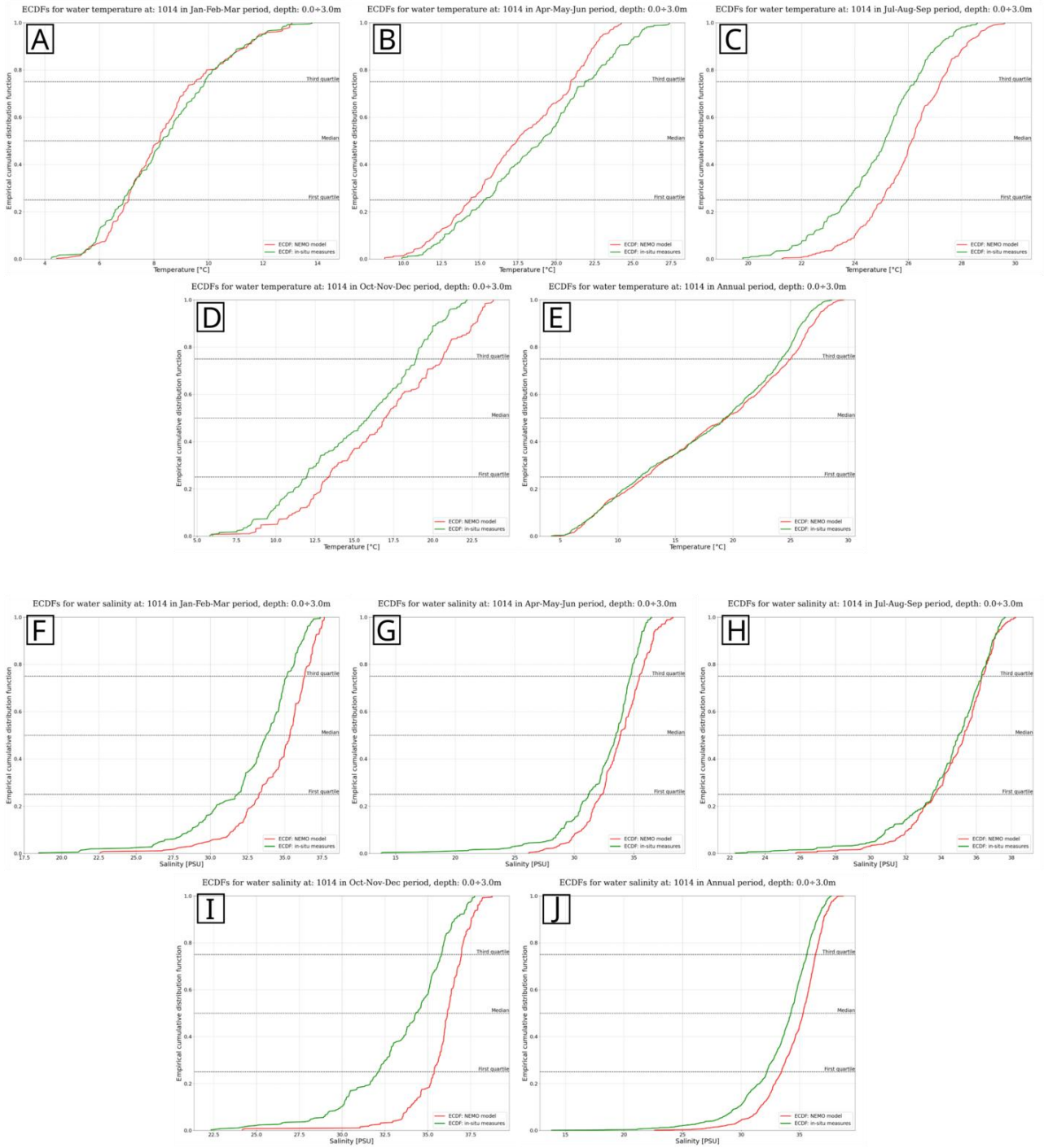

Figure x12: ECDFs of the difference between modeled and measured values for temperature (from subfigures A to E) and salinity (subfigures F to J) for station 1014 (between 0 and 3.0m depth). Subfigures A) and F) represent January-February-March; Subfigures B) and G) April-May-June; Subfigures C) and H) July-August-September; Subfigures D) and I) October-November-December; and Subfigures E) and J) represent the annual values.

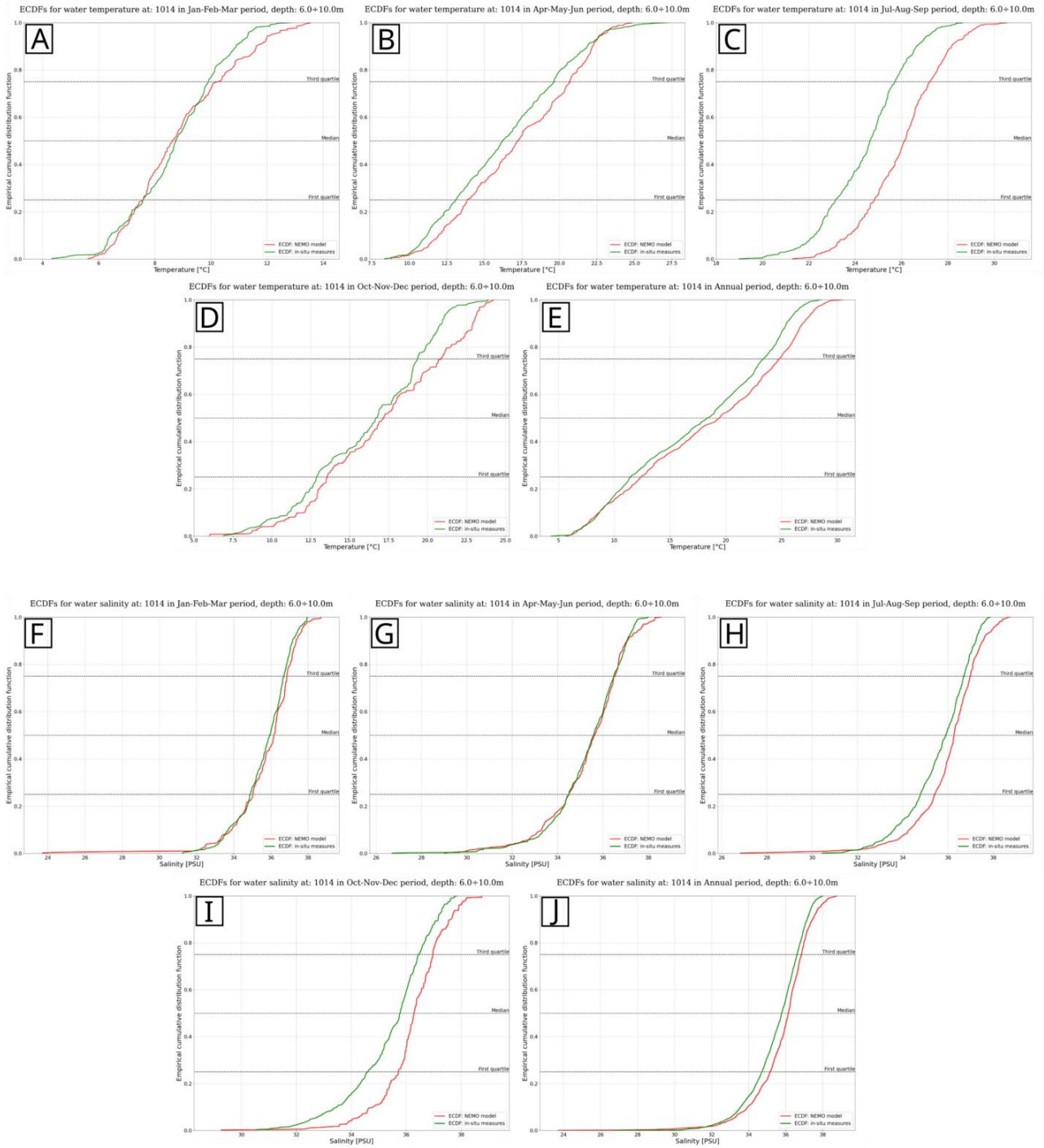

Figure x13: ECDFs of the difference between modeled and measured values for temperature (from subfigures A to E) and salinity (subfigures F to J) for station 1014 (between 6.0 and 10.0m depth). Subfigures A) and F) represent January-February-March; Subfigures B) and G) April-May-June; Subfigures C) and H) July-August-September; Subfigures D) and I) October-November-December; and Subfigures E) and J) represent the annual values.

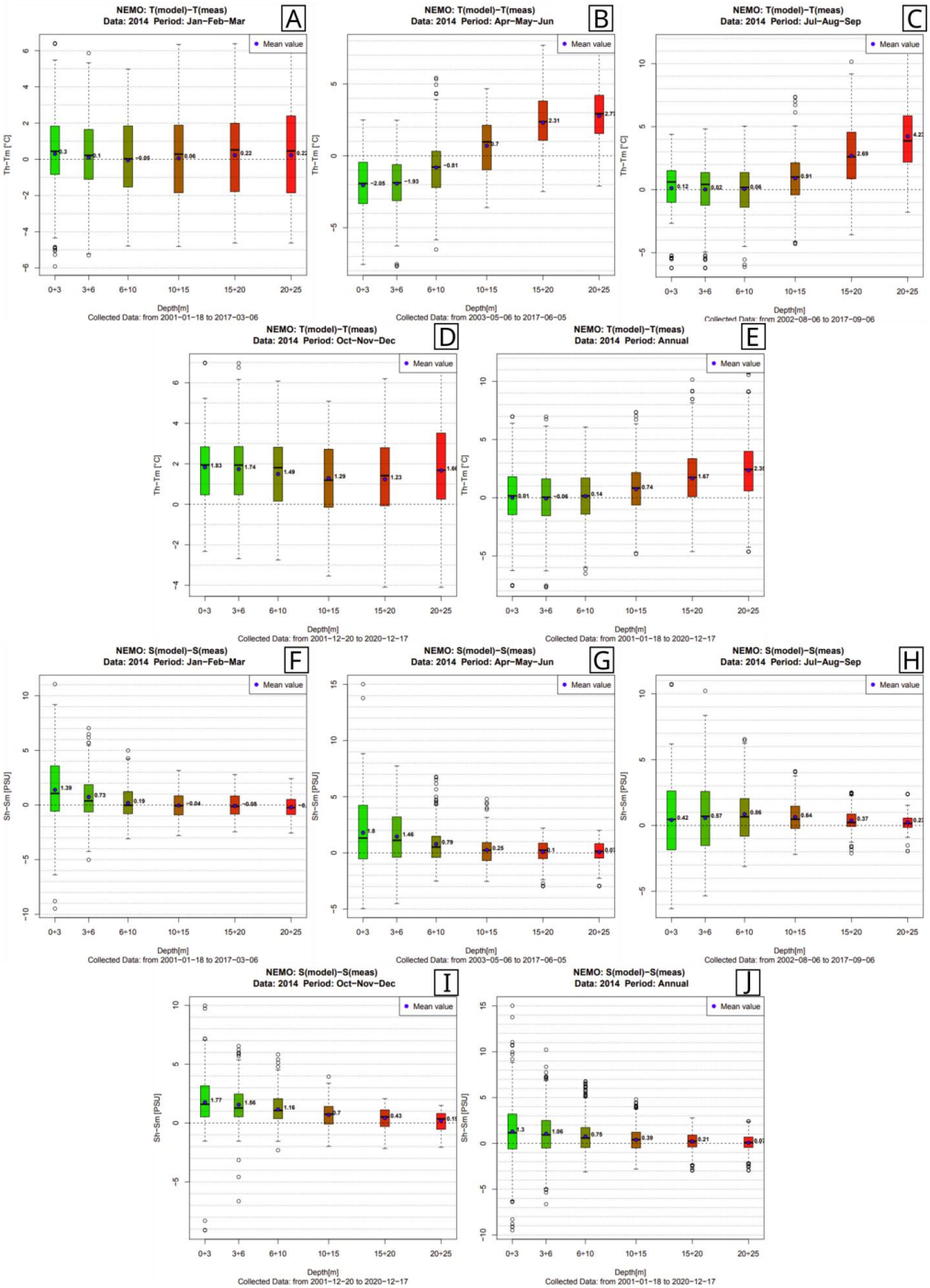

Figure x14: Boxplots of the difference between modeled and measured values for temperature (from subfigures A to E) and salinity (subfigures F to J) for station 2014. Subfigures A) and F) represent January-February-March; Subfigures B) and G) April-May-June; Subfigures C) and H) July-August-September; Subfigures D) and I) October-November-December; and Subfigures E) and J) represent the annual values.

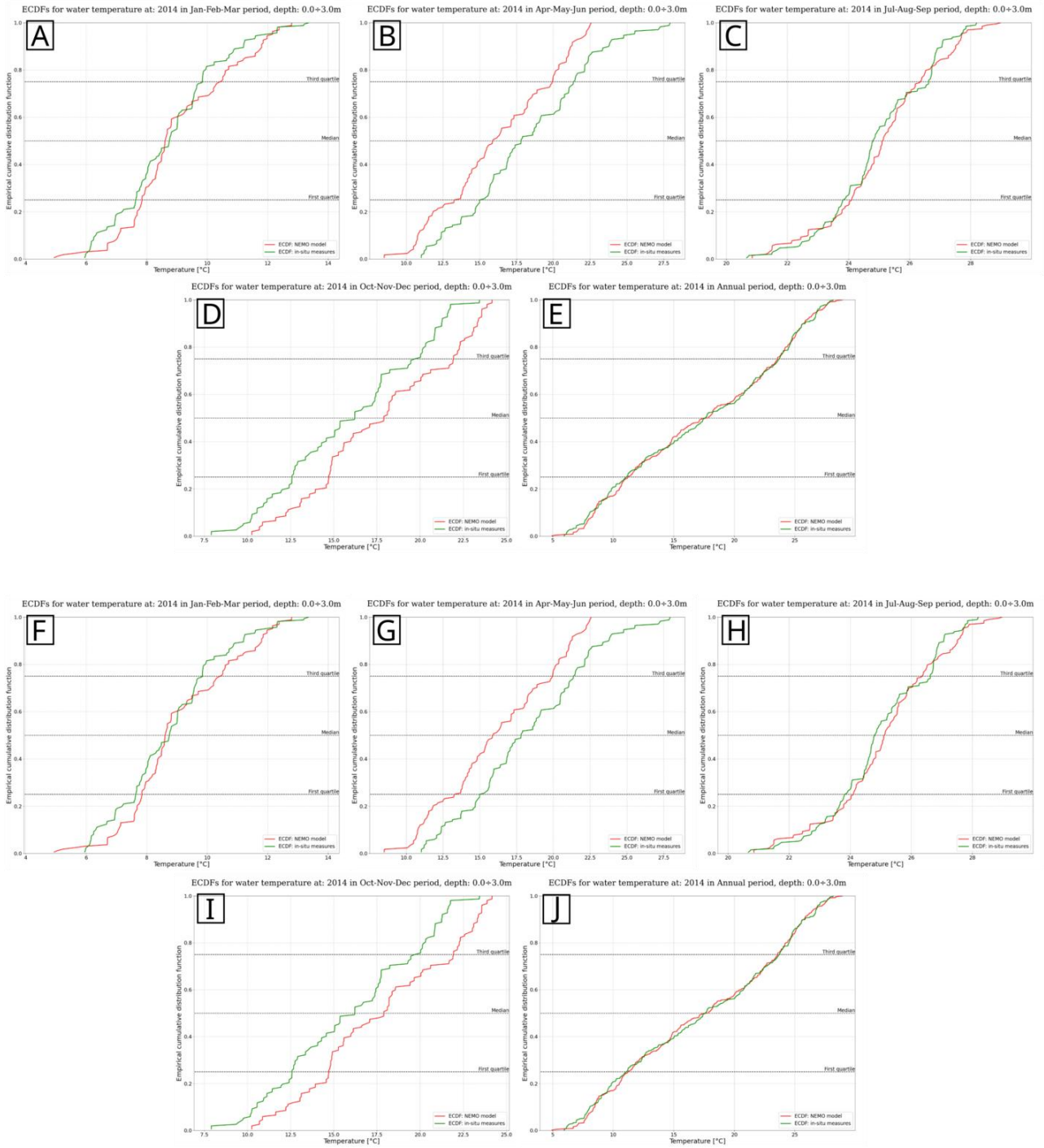

Figure x15: ECDFs of the difference between modeled and measured values for temperature (from subfigures A to E) and salinity (subfigures F to J) for station 2014 (between 0 and 3.0m depth). Subfigures A) and F) represent January-February-March; Subfigures B) and G) April-May-June; Subfigures C) and H) July-August-September; Subfigures D) and I) October-November-December; and Subfigures E) and J) represent the annual values.

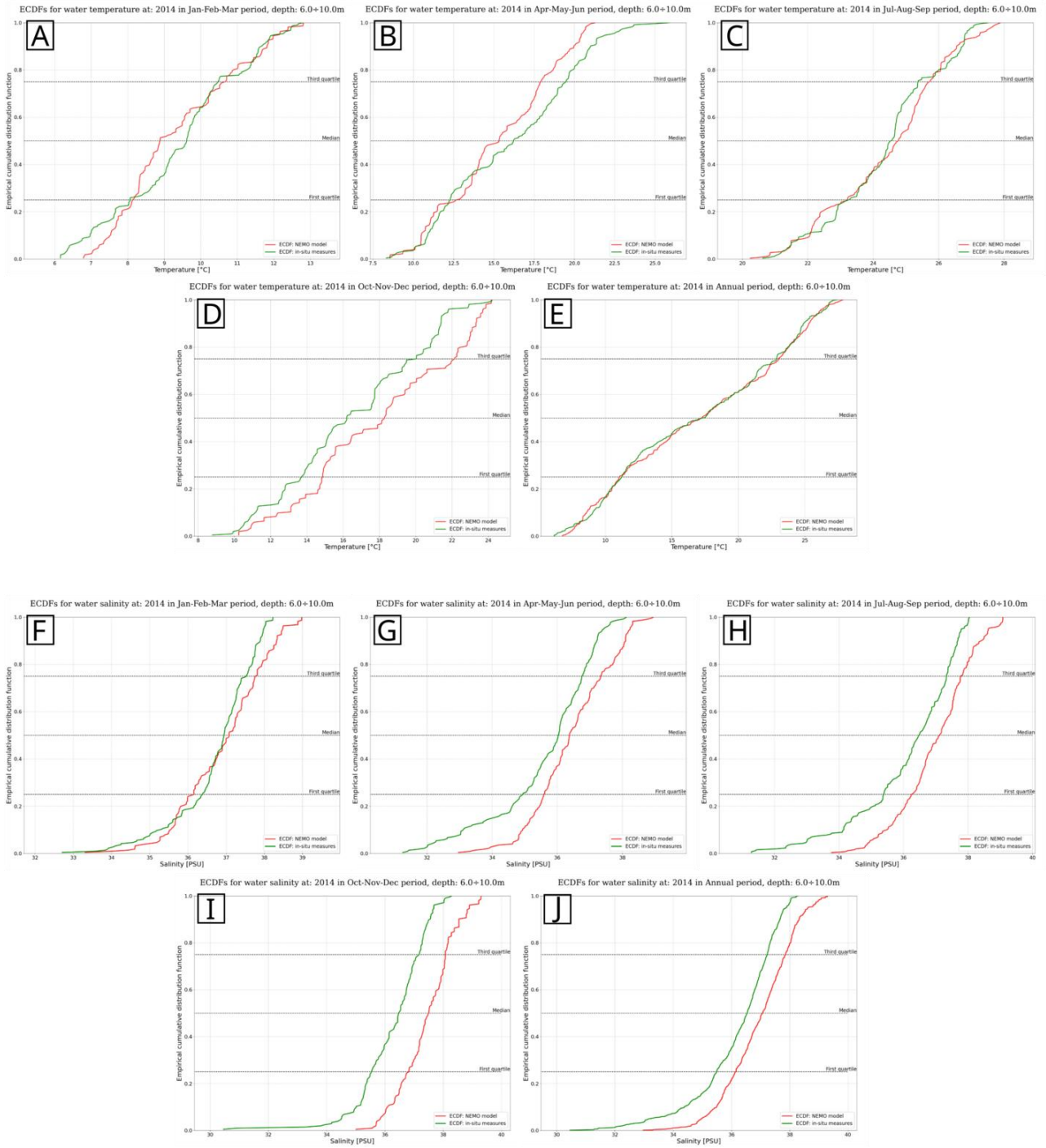

Figure x16: ECDFs of the difference between modeled and measured values for temperature (from subfigures A to E) and salinity (subfigures F to J) for station 2014 (between 6.0 and 10.0m depth). Subfigures A) and F) represent January-February-March; Subfigures B) and G) April-May-June; Subfigures C) and H) July-August-September; Subfigures D) and I) October-November-December; and Subfigures E) and J) represent the annual values.

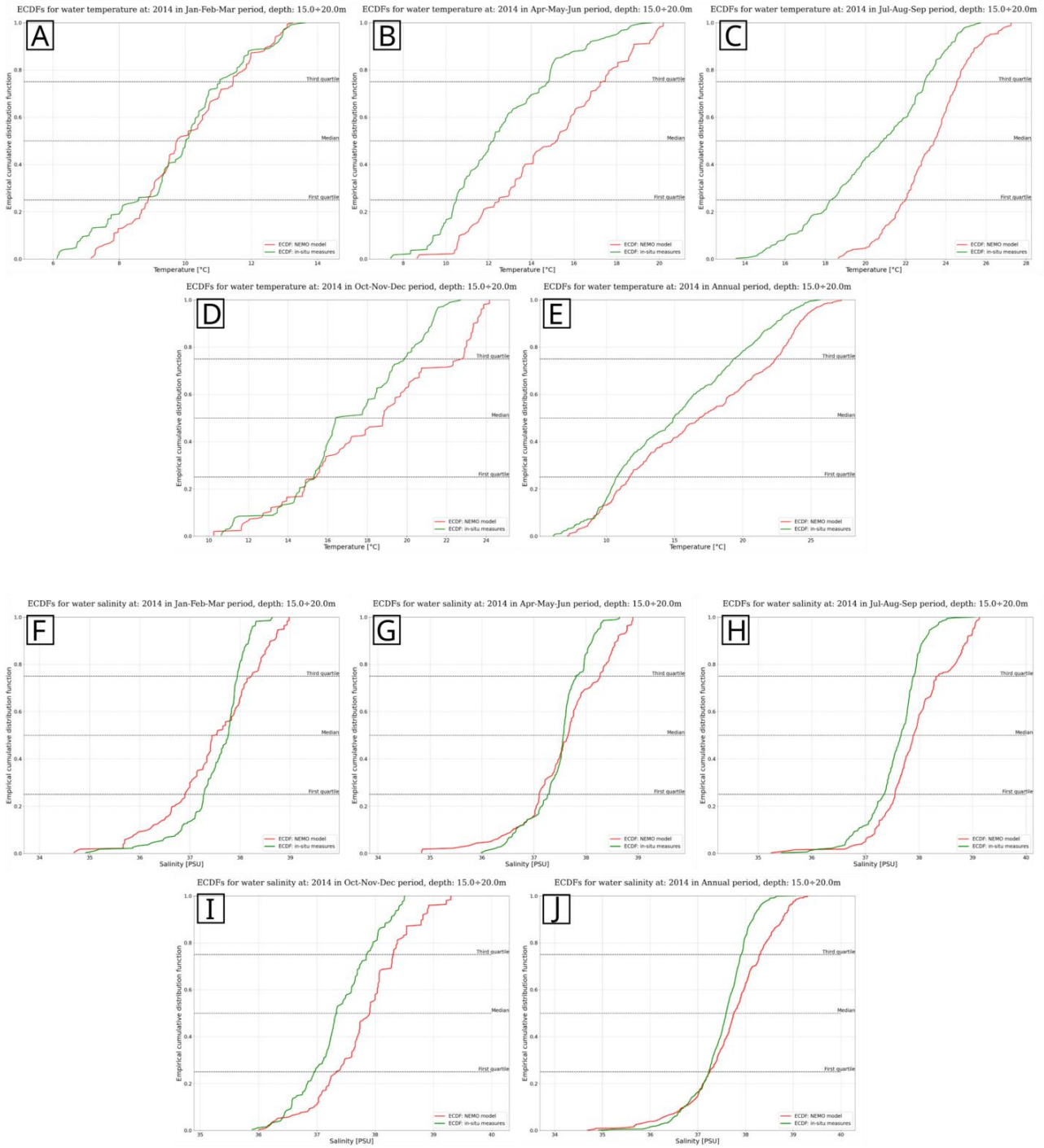

Figure x17: ECDFs of the difference between modeled and measured values for temperature (from subfigures A to E) and salinity (subfigures F to J) for station 2014 (between 15.0 and 20.0m depth). Subfigures A) and F) represent January-February-March; Subfigures B) and G) April-May-June; Subfigures C) and H) July-August-September; Subfigures D) and I) October-November-December; and Subfigures E) and J) represent the annual values.

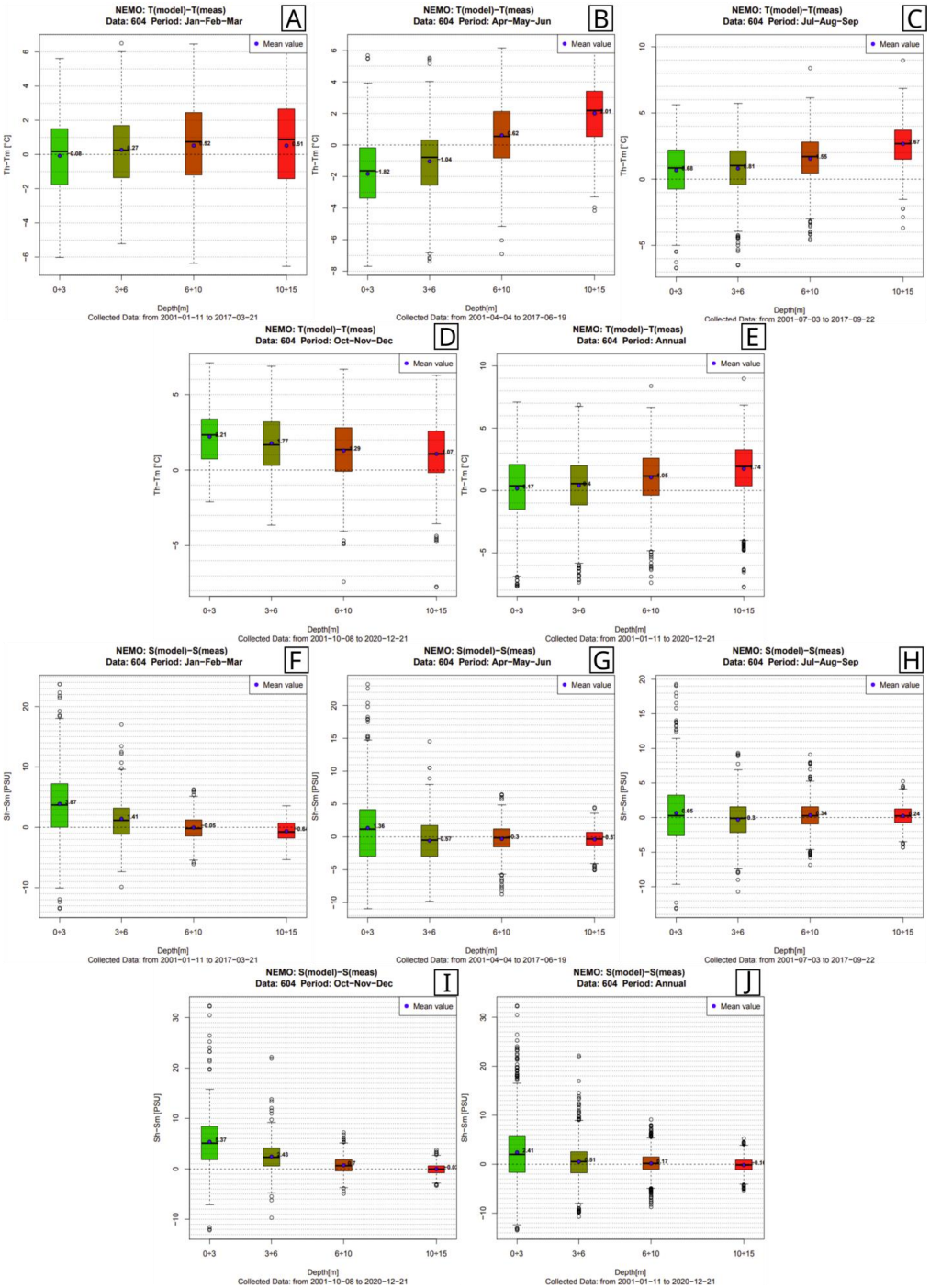

Figure x18: Boxplots of the difference between modeled and measured values for temperature (from subfigures A to E) and salinity (subfigures F to J) for station 604. Subfigures A) and F) represent January-February-March; Subfigures B) and G) April-May-June; Subfigures C) and H) July-August-September; Subfigures D) and I) October-November-December; and Subfigures E) and J) represent the annual values.

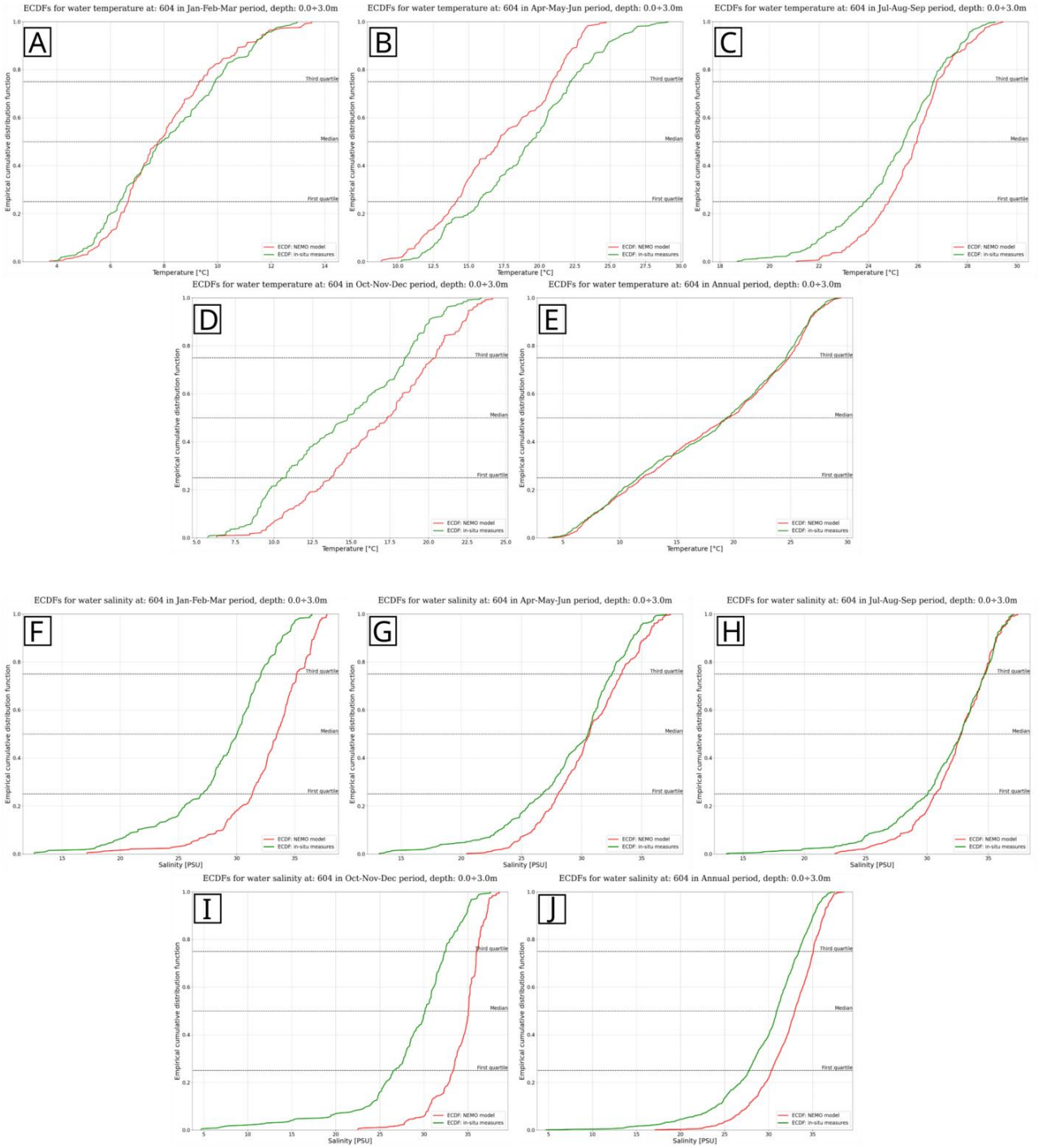

Figure x19: ECDFs of the difference between modeled and measured values for temperature (from subfigures A to E) and salinity (subfigures F to J) for station 604 (between 0 and 3.0m depth). Subfigures A) and F) represent January-February-March; Subfigures B) and G) April-May-June; Subfigures C) and H) July-August-September; Subfigures D) and I) October-November-December; and Subfigures E) and J) represent the annual values.

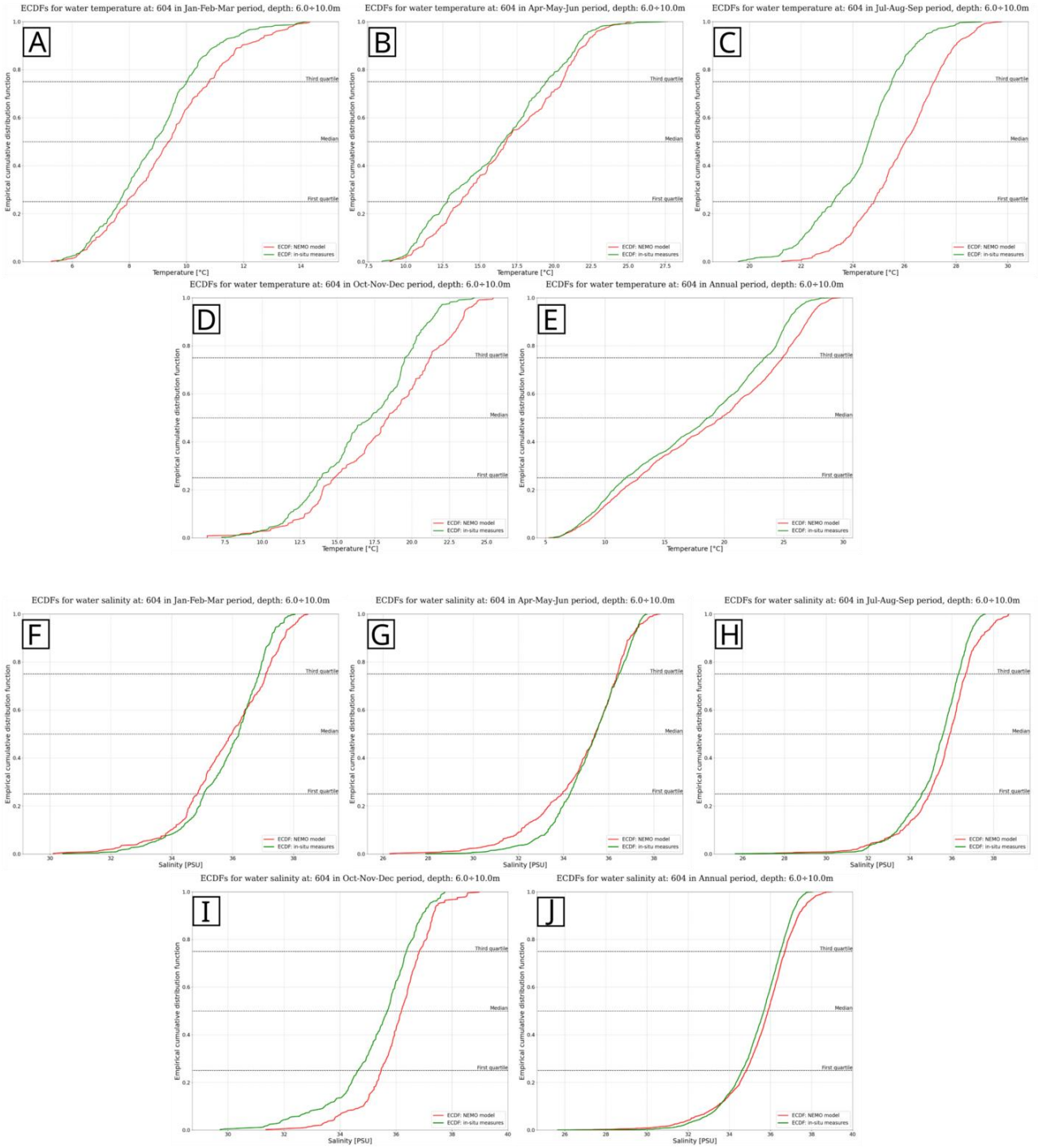

Figure x20: ECDFs of the difference between modeled and measured values for temperature (from subfigures A to E) and salinity (subfigures F to J) for station 604 (between 6.0 and 10.0m depth). Subfigures A) and F) represent January-February-March; Subfigures B) and G) April-May-June; Subfigures C) and H) July-August-September; Subfigures D) and I) October-November-December; and Subfigures E) and J) represent the annual values.

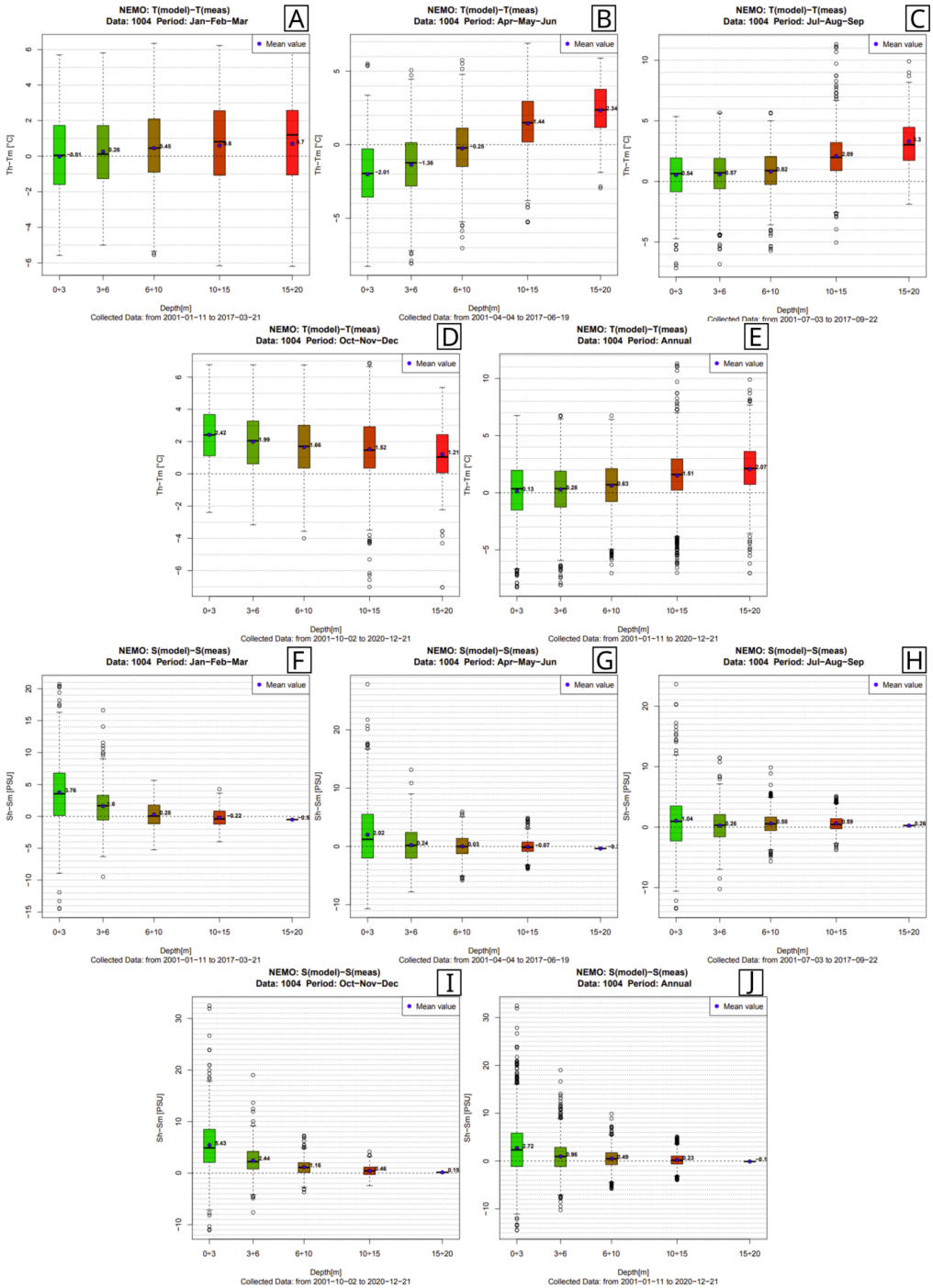

Figure x21: Boxplots of the difference between modeled and measured values for temperature (from subfigures A to E) and salinity (subfigures F to J) for station 1004. Subfigures A) and F) represent January-February-March; Subfigures B) and G) April-May-June; Subfigures C) and H) July-August-September; Subfigures D) and I) October-November-December; and Subfigures E) and J) represent the annual values.

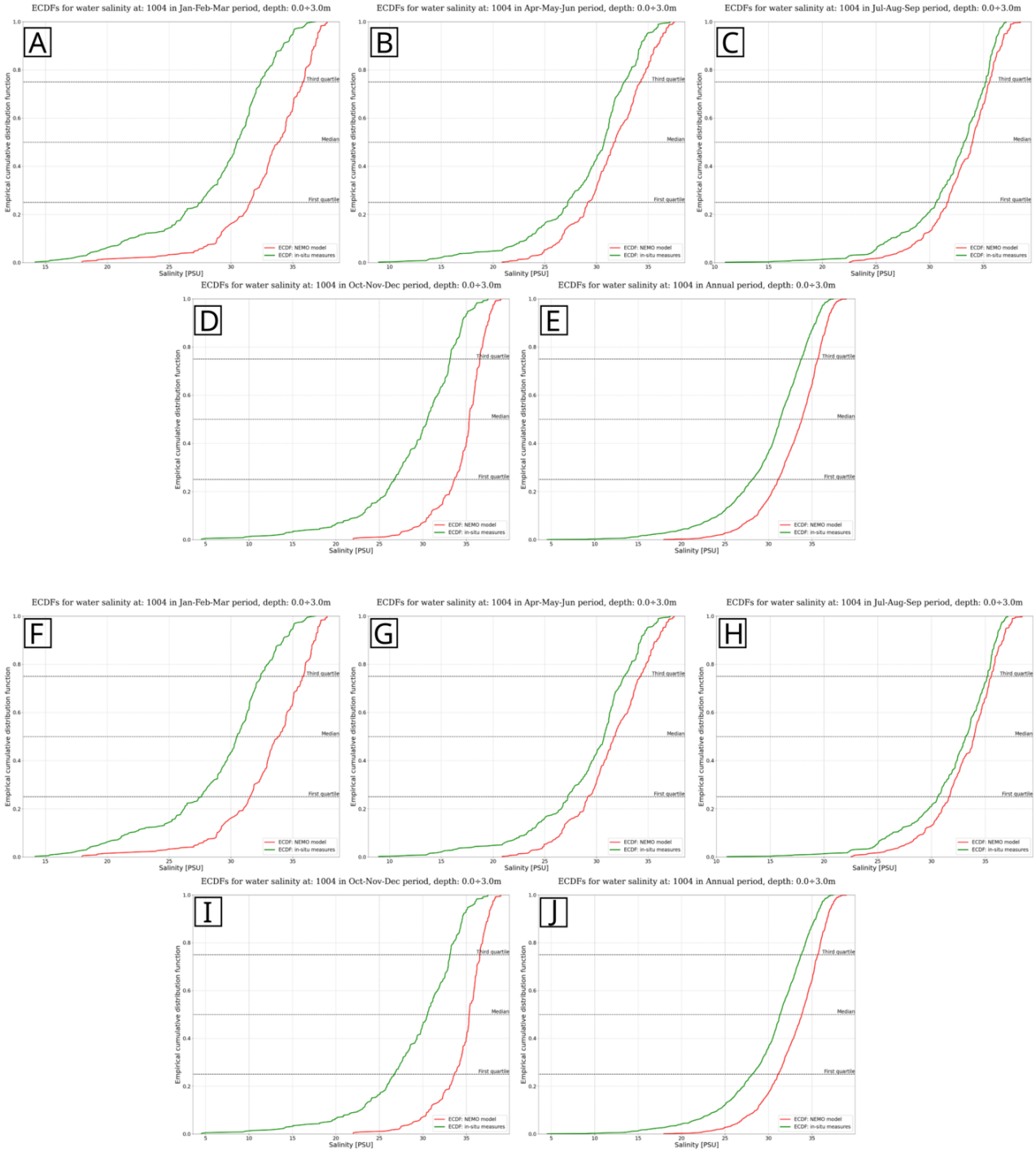

Figure x22: ECDFs of the difference between modeled and measured values for temperature (from subfigures A to E) and salinity (subfigures F to J) for station 1004 (between 0 and 3.0m depth). Subfigures A) and F) represent January-February-March; Subfigures B) and G) April-May-June; Subfigures C) and H) July-August-September; Subfigures D) and I) October-November-December; and Subfigures E) and J) represent the annual values.

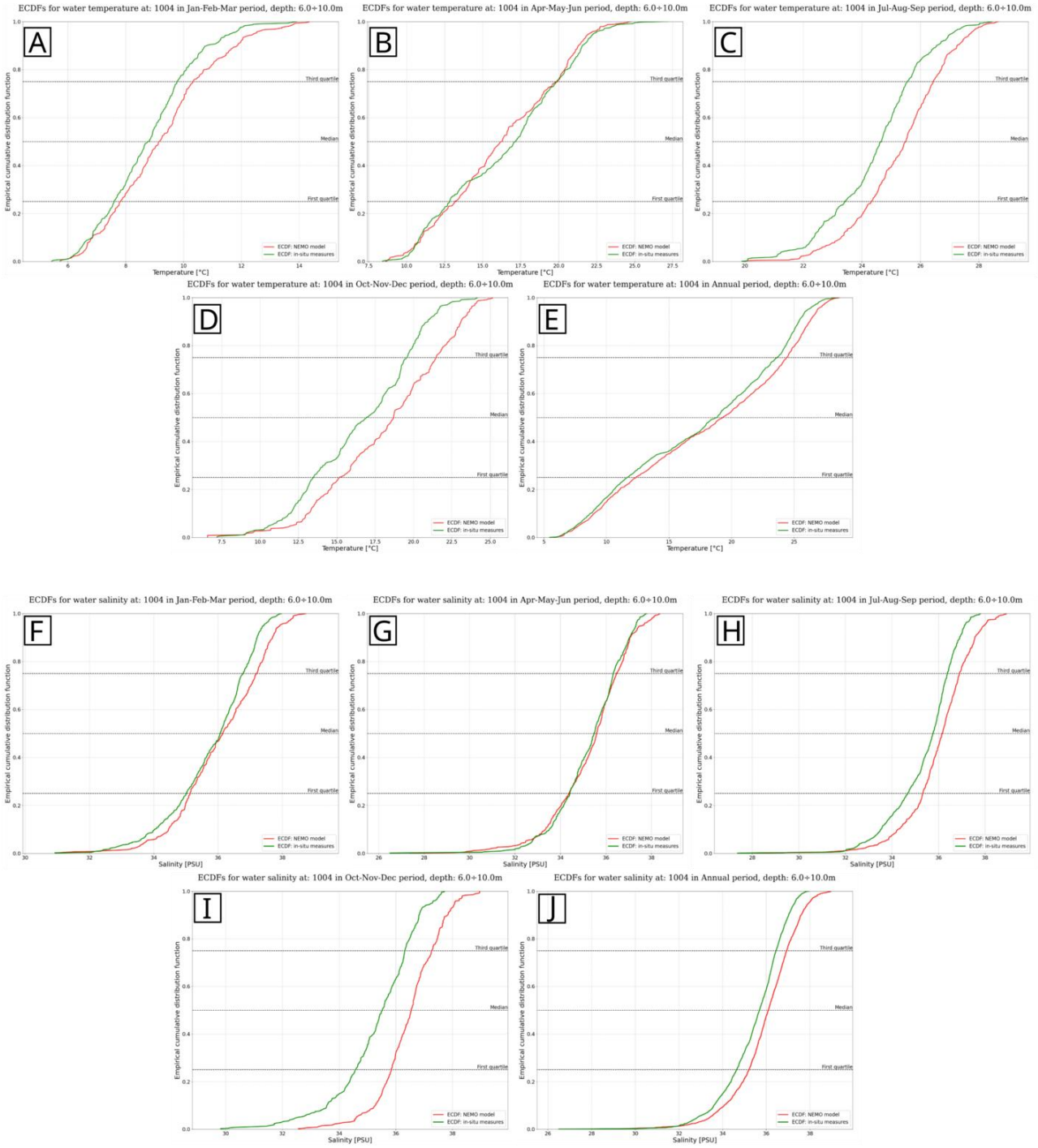

Figure x23: ECDFs of the difference between modeled and measured values for temperature (from subfigures A to E) and salinity (subfigures F to J) for station 1004 (between 6.0 and 10.0m depth). Subfigures A) and F) represent January-February-March; Subfigures B) and G) April-May-June; Subfigures C) and H) July-August-September; Subfigures D) and I) October-November-December; and Subfigures E) and J) represent the annual values.

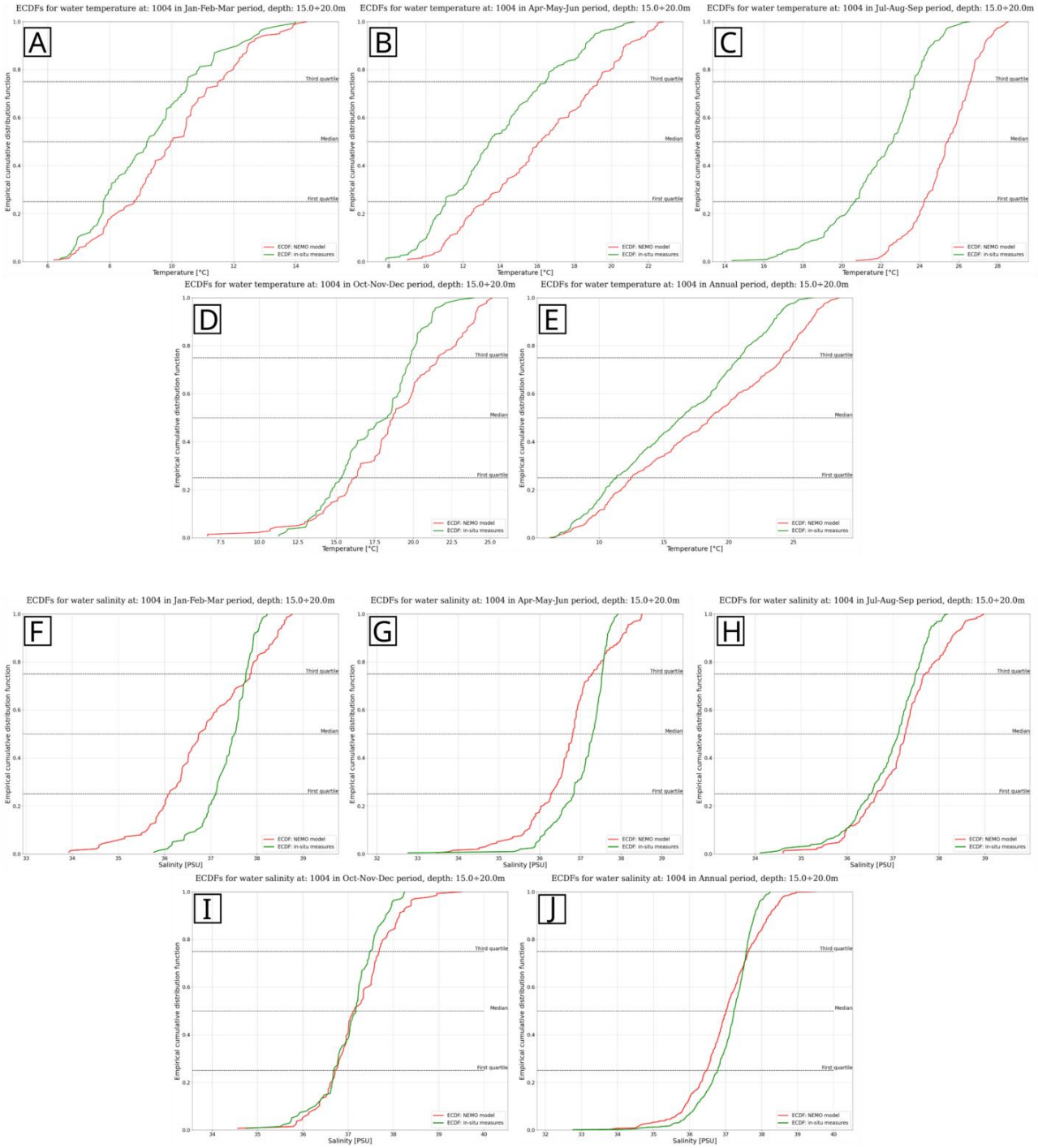

Figure x24: ECDFs of the difference between modeled and measured values for temperature (from subfigures A to E) and salinity (subfigures F to J) for station 1004 (between 15.0 and 20.0m depth). Subfigures A) and F) represent January-February-March; Subfigures B) and G) April-May-June; Subfigures C) and H) July-August-September; Subfigures D) and I) October-November-December; and Subfigures E) and J) represent the annual values.

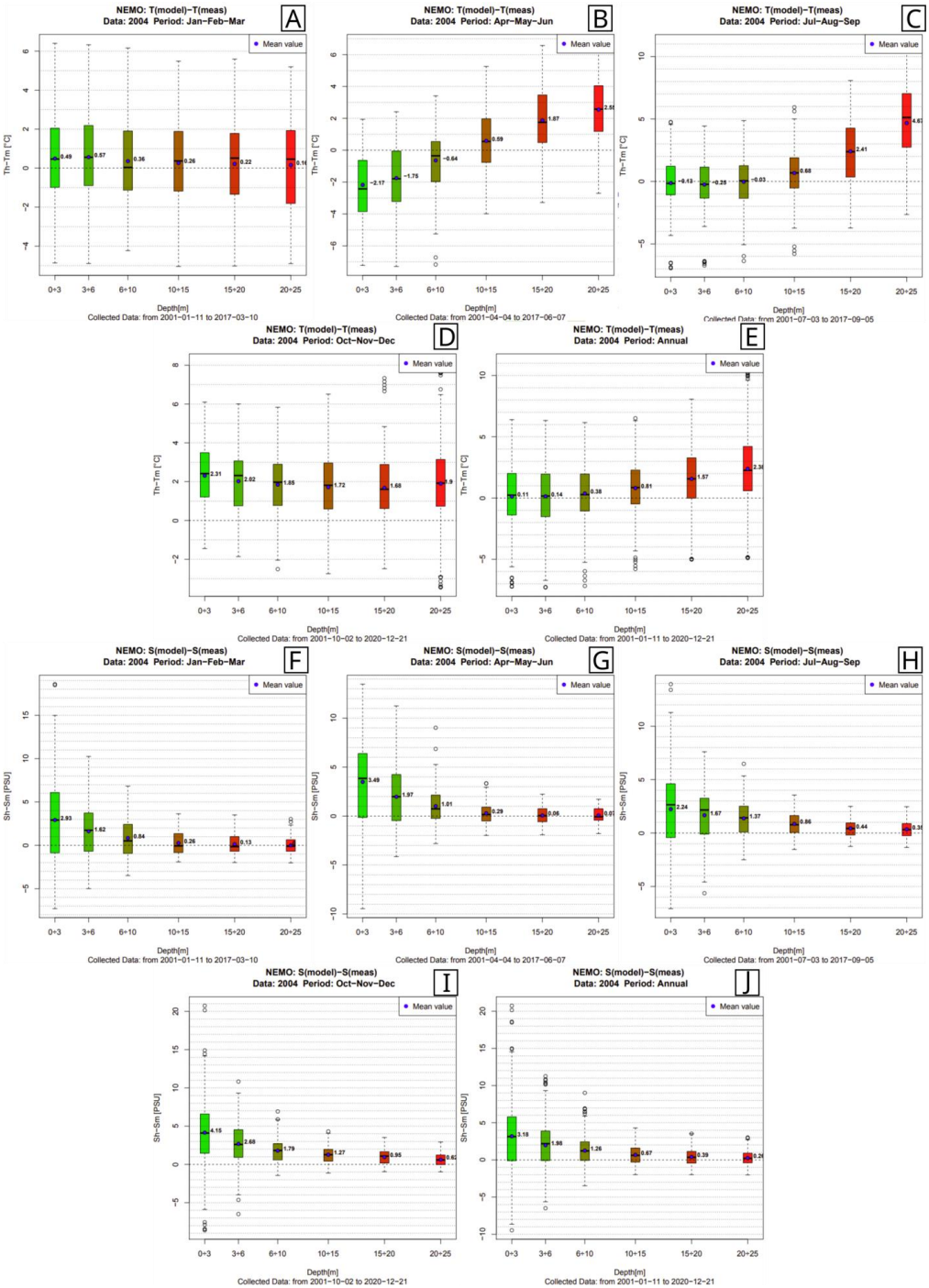

Figure x25: Boxplots of the difference between modeled and measured values for temperature (from subfigures A to E) and salinity (subfigures F to J) for station 2004. Subfigures A) and F) represent January-February-March; Subfigures B) and G) April-May-June; Subfigures C) and H) July-August-September; Subfigures D) and I) October-November-December; and Subfigures E) and J) represent the annual values.

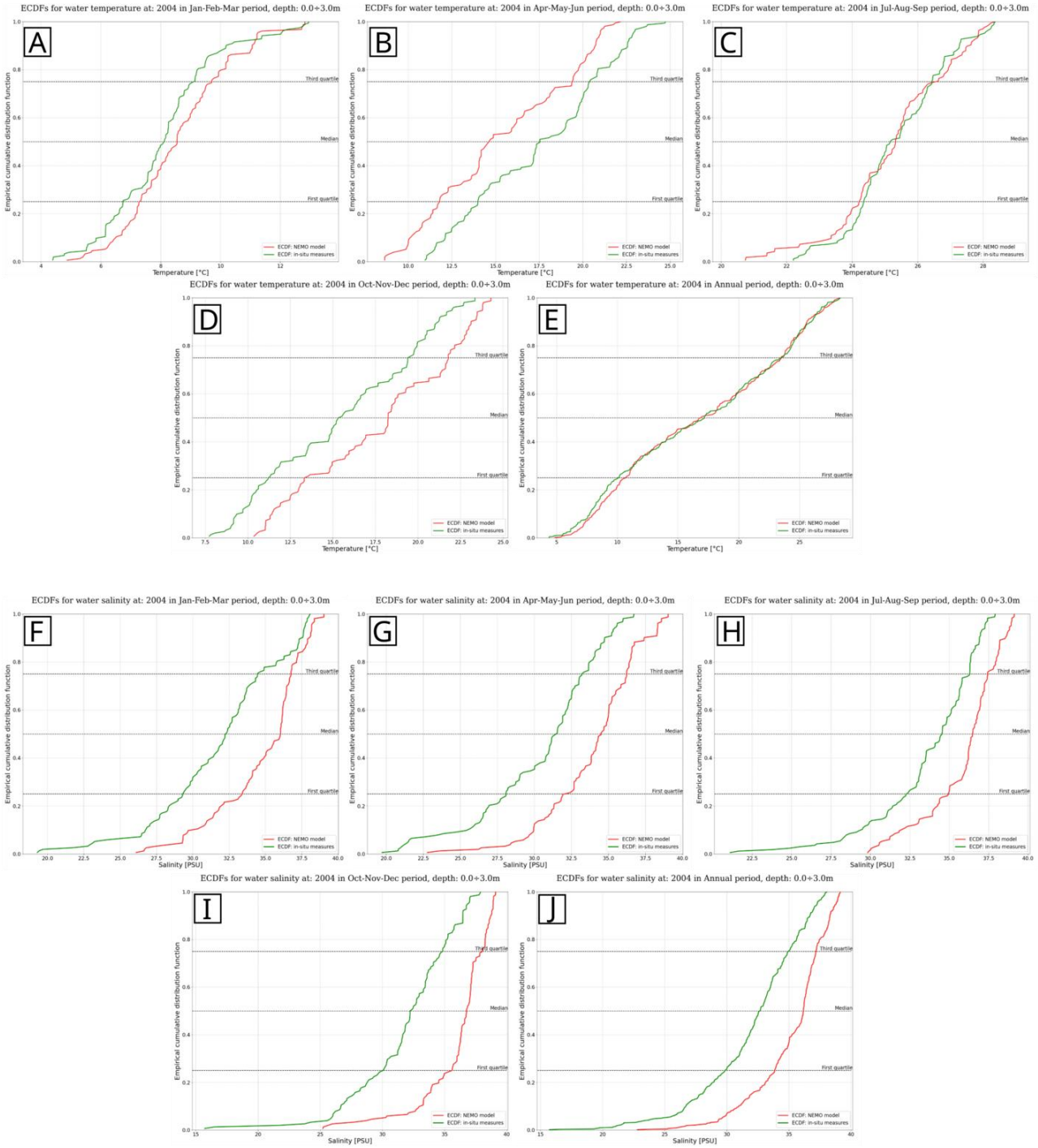

Figure x26: ECDFs of the difference between modeled and measured values for temperature (from subfigures A to E) and salinity (subfigures F to J) for station 2004 (between 0 and 3.0m depth). Subfigures A) and F) represent January-February-March; Subfigures B) and G) April-May-June; Subfigures C) and H) July-August-September; Subfigures D) and I) October-November-December; and Subfigures E) and J) represent the annual values.

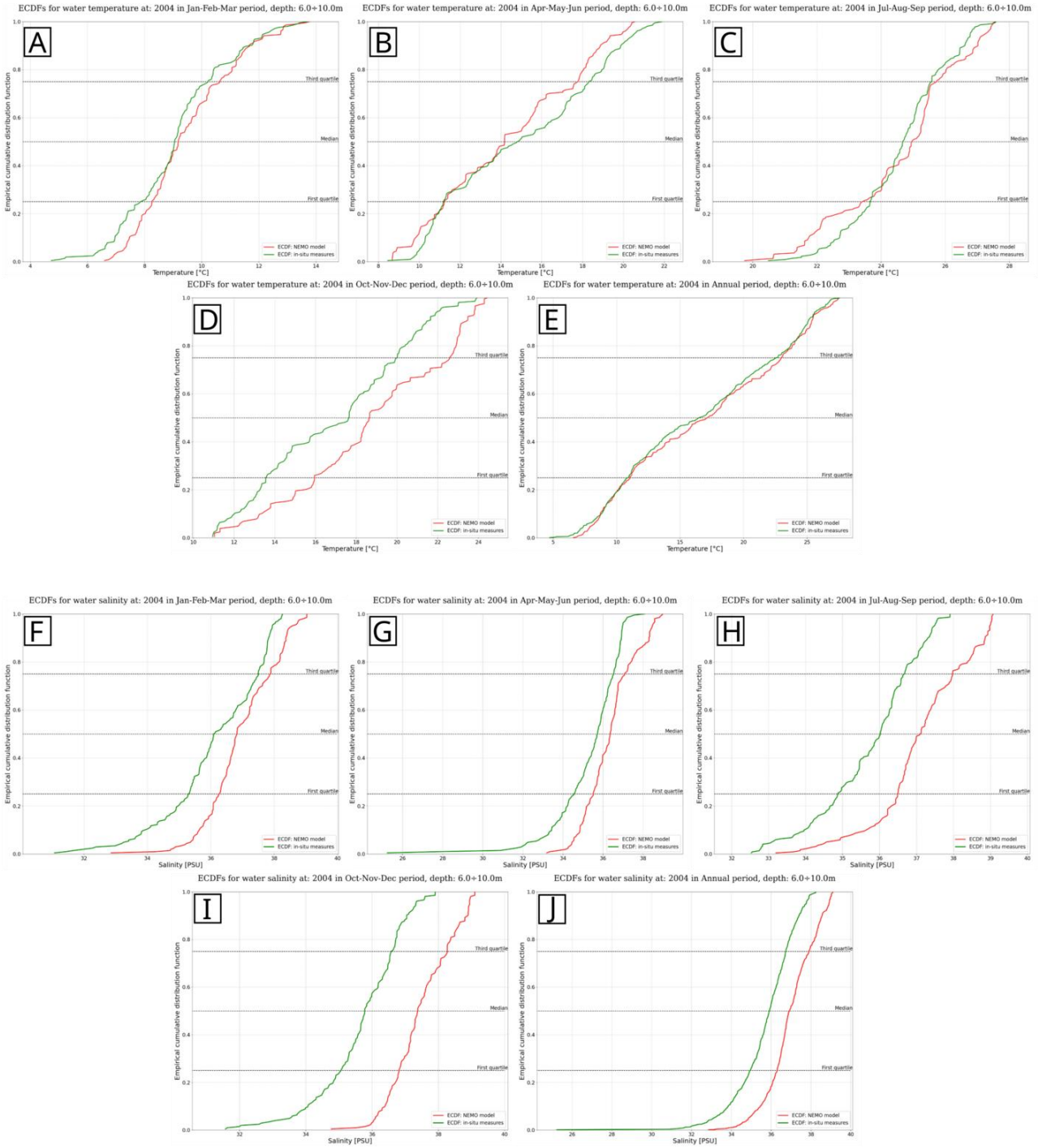

Figure x27: ECDFs of the difference between modeled and measured values for temperature (from subfigures A to E) and salinity (subfigures F to J) for station 2004 (between 6.0 and 10.0m depth). Subfigures A) and F) represent January-February-March; Subfigures B) and G) April-May-June; Subfigures C) and H) July-August-September; Subfigures D) and I) October-November-December; and Subfigures E) and J) represent the annual values.

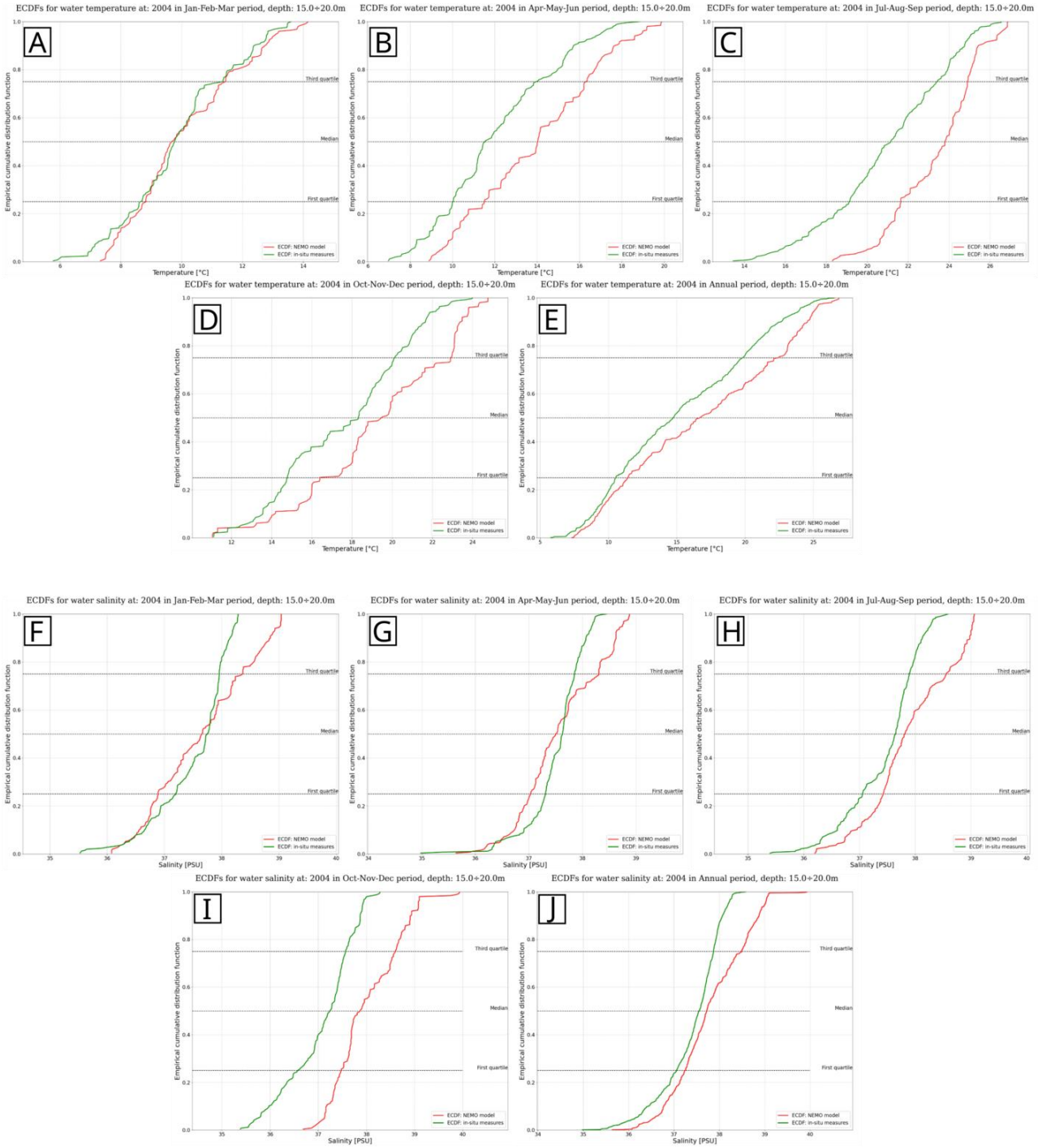

Figure x28: ECDFs of the difference between modeled and measured values for temperature (from subfigures A to E) and salinity (subfigures F to J) for station 2004 (between 15.0 and 20.0m depth). Subfigures A) and F) represent January-February-March; Subfigures B) and G) April-May-June; Subfigures C) and H) July-August-September; Subfigures D) and I) October-November-December; and Subfigures E) and J) represent the annual values.

For the validation of the river discharge values, Arpae collected historical data from the Po river at the measuring station of Pontelagoscuro and analyzed it together with the outputs of the river discharges modeled by WRF-Hydro. In Figures x29-x, the results of the analyses are shown.

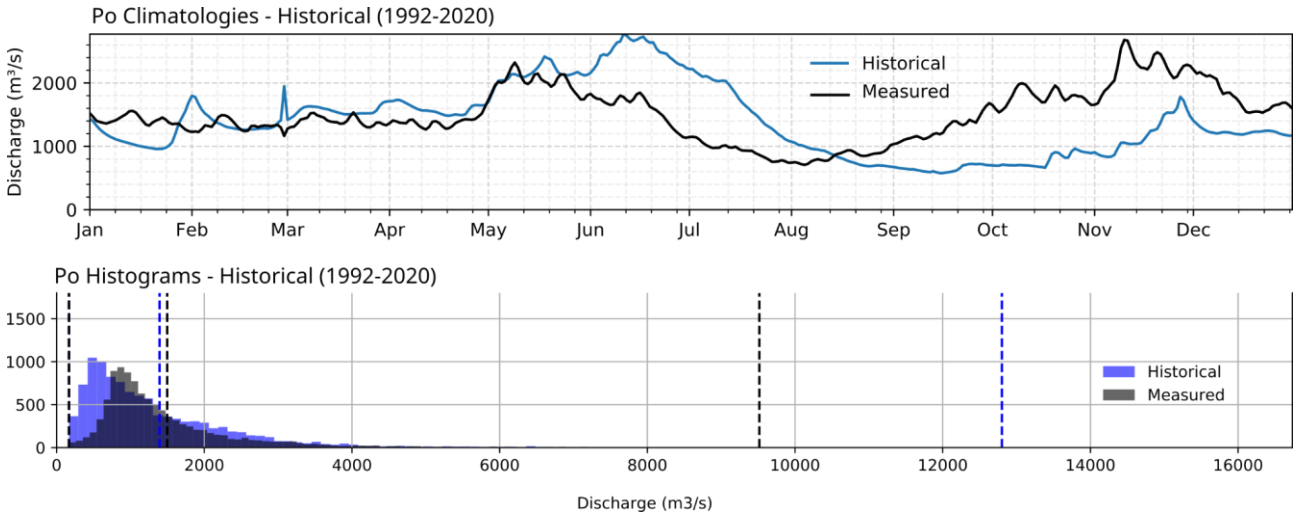

Figure x29: Upper graph presents the climatological values for the historical simulation (blue solid line) and measurements (black solid line) covering the 1992-2020 timespan. In the bottom graph, the histogram for the same timeseries are shown with the historical simulation values presented as blue bars and the measurements as black bars. The vertical dashed lines represent, from left to right, the minimum, average and maximum values either for the simulations (blue dashed lines) or the measurements (black dashed lines).

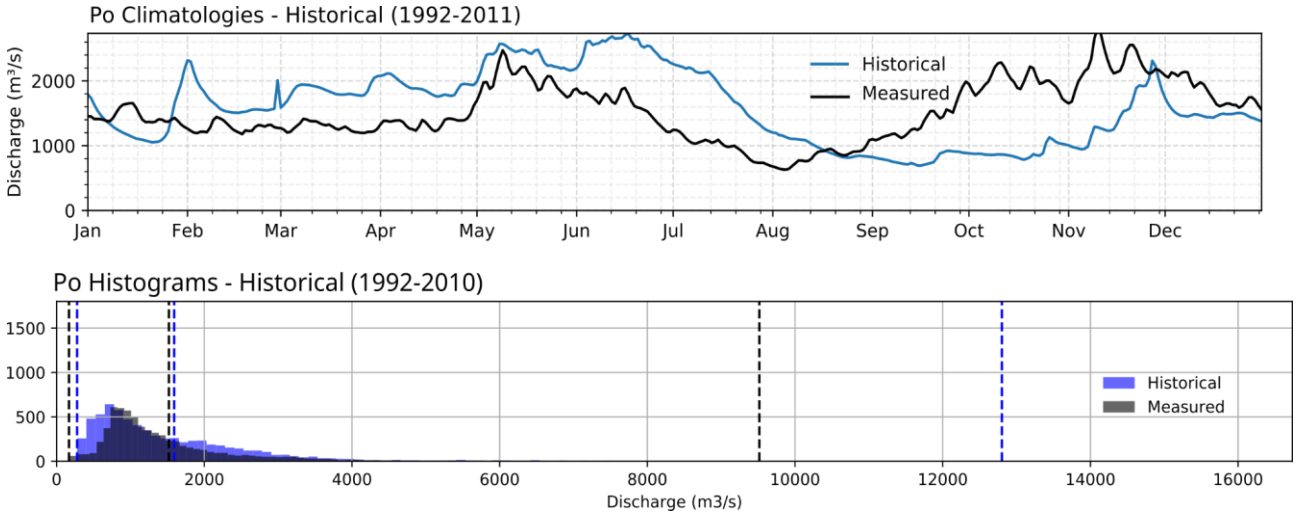

Figure x30: same as Figure x29 but for the timeseries covering from 1992-2010.

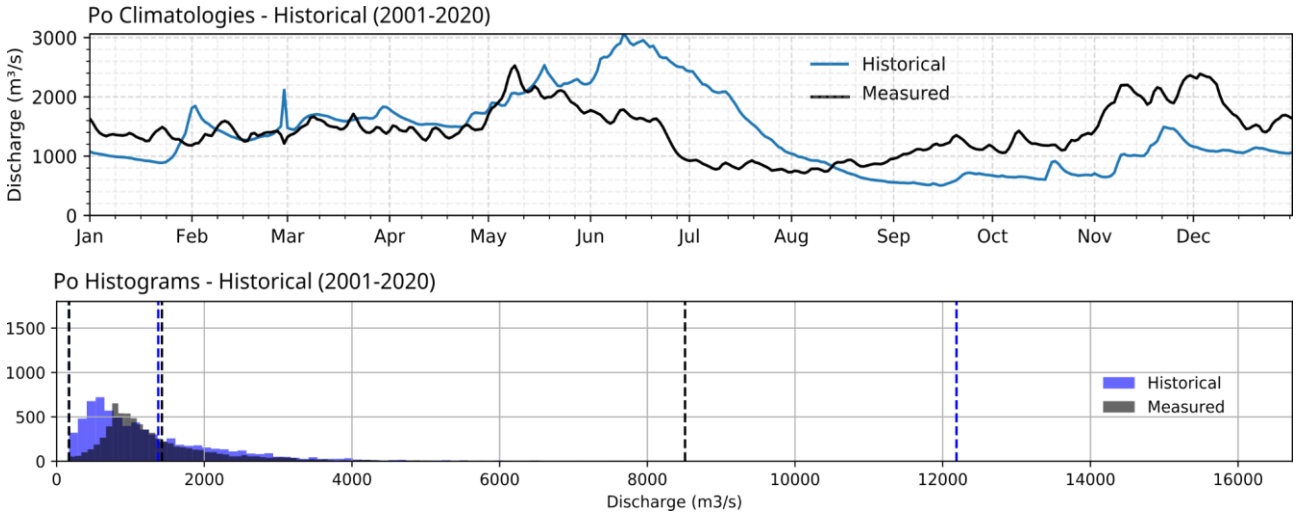

Figure x31: same as Figure x29 but for the timeseries covering from 2001-2020.

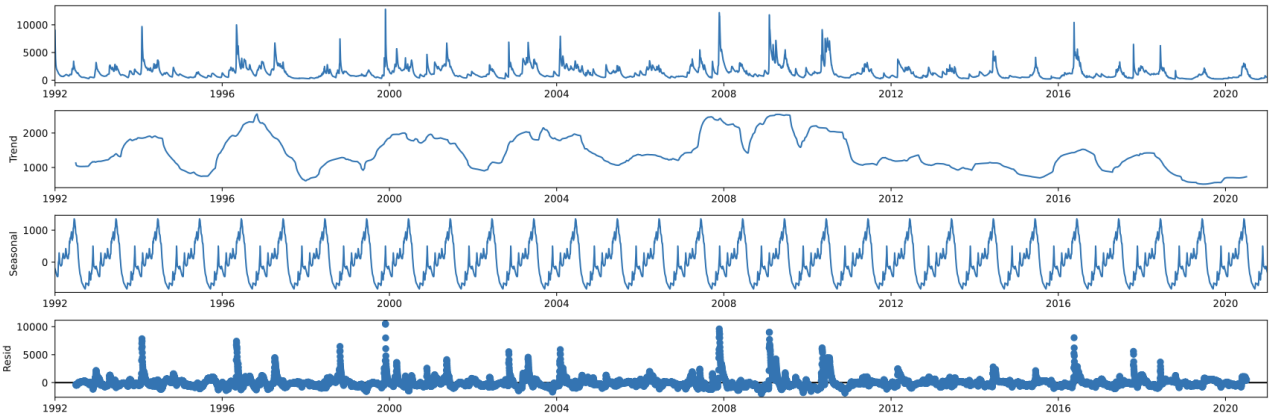

Figure x32: decomposition of the WRF historical simulation (1992-2020) using a moving average of 365 days. The upper graph shows the timeseries while the second, third, and fourth graphs present the trend, seasonal, and residual components once the timeseries decomposition was performed.

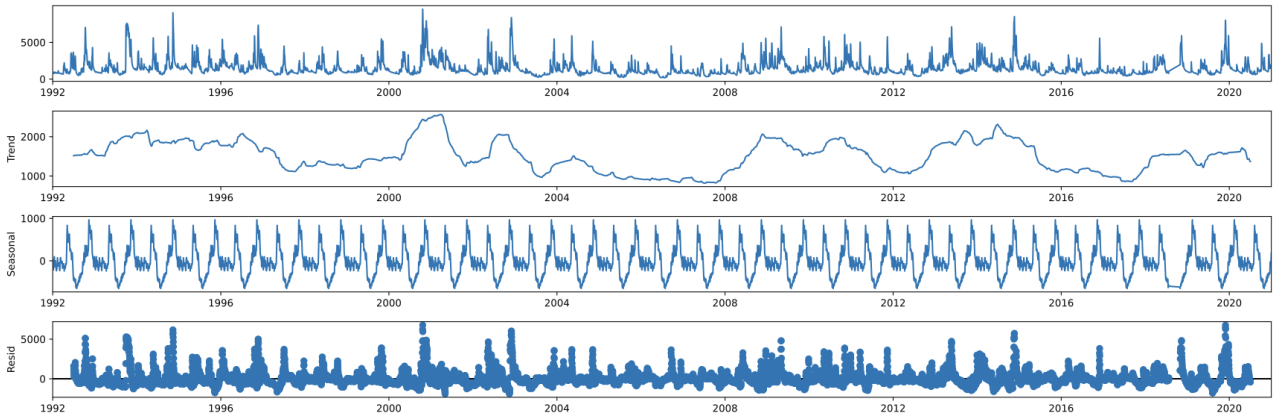

Figure x33: same as Figure x32 but for the measured timeseries.

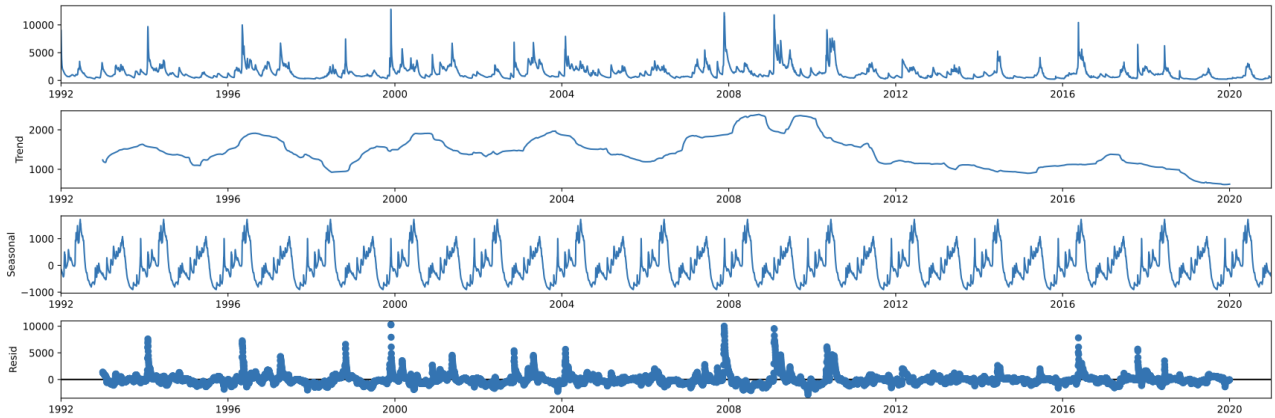

Figure x34: same as Figure x32 but the decomposition was performed using a 730 days moving average. (modeled timeseries)

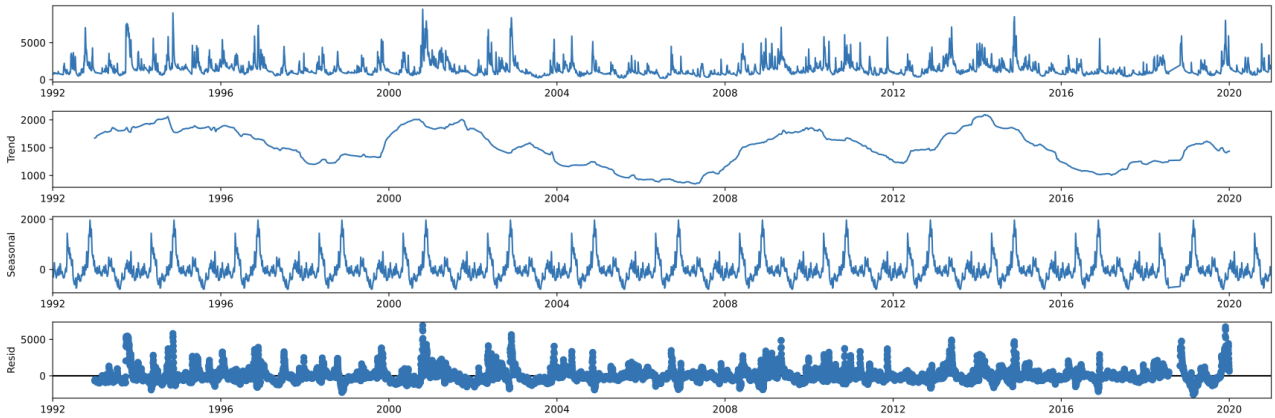

Figure x35: same as Figure x33 but the decomposition was performed using a 730 days moving average. (measured timeseries)

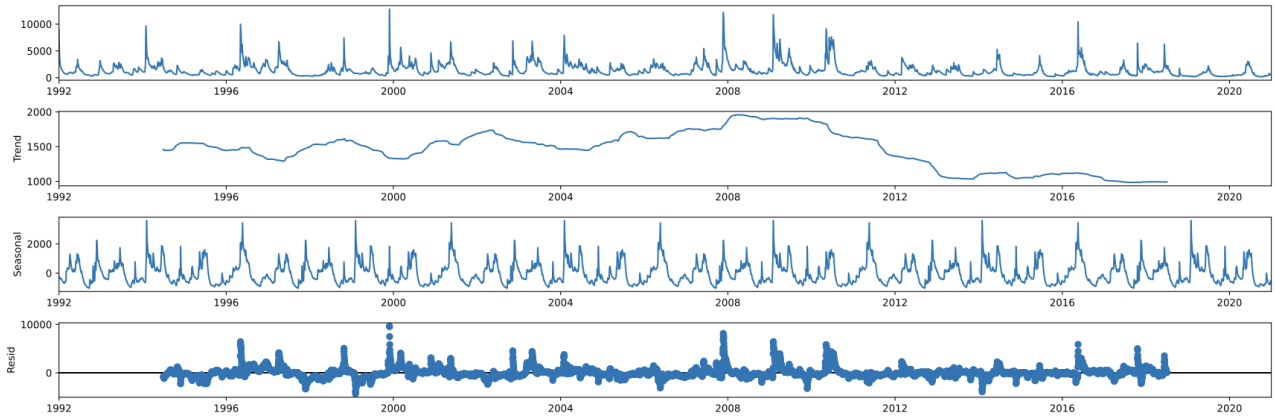

Figure x36: same as Figure x32 but the decomposition was performed using a 1825 days moving average. (modeled timeseries)

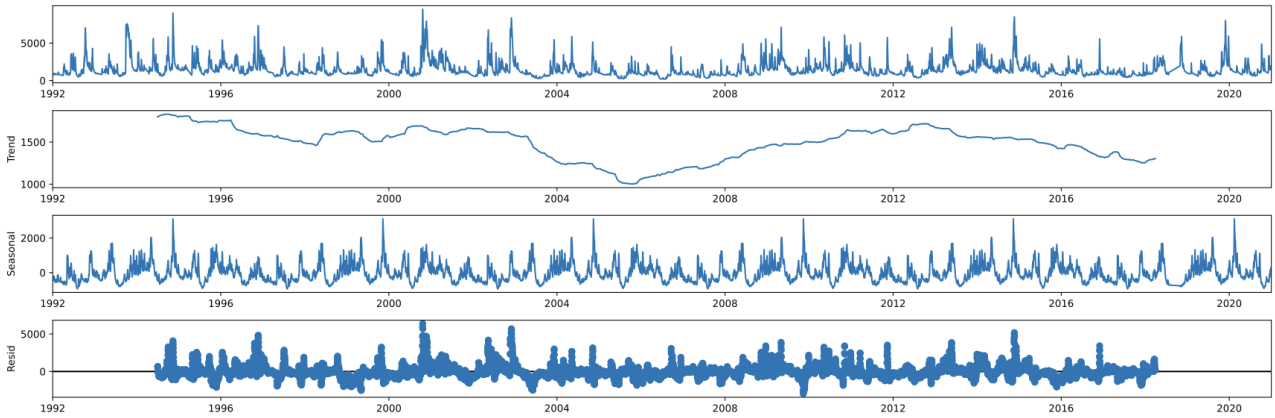

Figure x37: same as Figure x33 but the decomposition was performed using a 1825 days moving average. (measured timeseries)

Data from AdriaClim models WRF, NEMO and WRF-Hydro are used for the dynamical downscaling in ERP considering the period 1992-2020. However due to the known issue of WRF-Hydro in the river discharge for the last period of simulation (2012-2020), data analysis is carried out considering the first twenty years of simulations (1992-2011). We show comparison of the historical simulation results with available observations of salinity, temperature and sea level at Porto Garibaldi station, and between model results and sea level at Porto Corsini stations indicated in Fig. xx. Since the downscaled model is forced by results of climatic simulations, we believe that a good evaluation of the model results should focus on the comparison of variables distributions, more than on time series comparison. distributions for Porto Garibaldi are considered for the period 2010-2011, while the sea level in Porto Corsini is evaluated for the period 1998-2009.

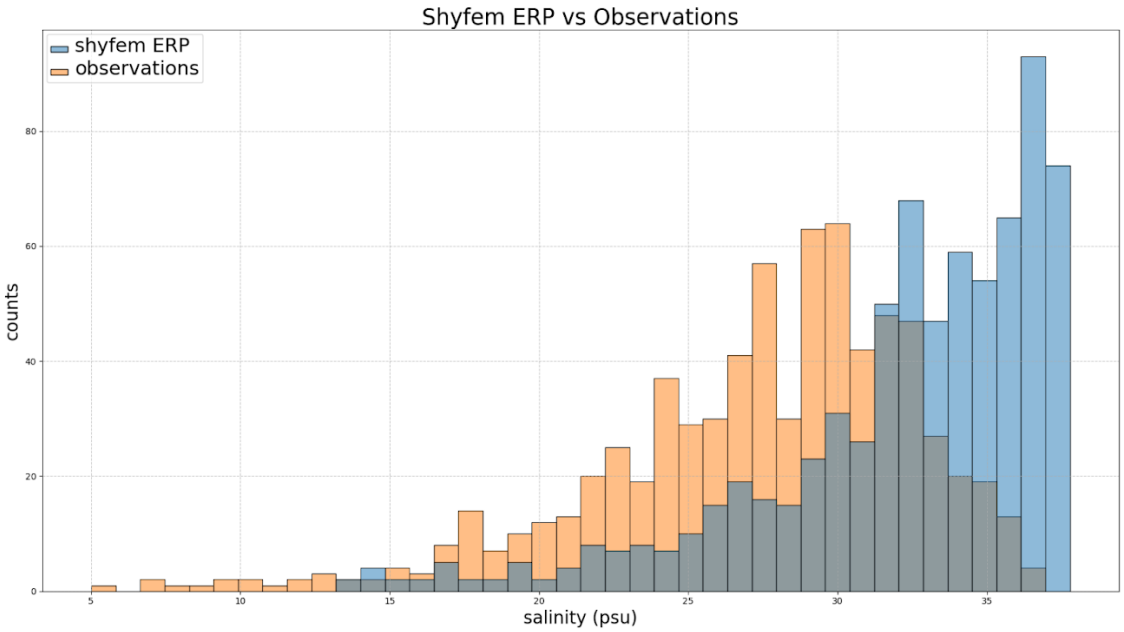

Figure x38: Observed (orange) and modeled (blue) distribution of salinity at Porto Garibaldi station.

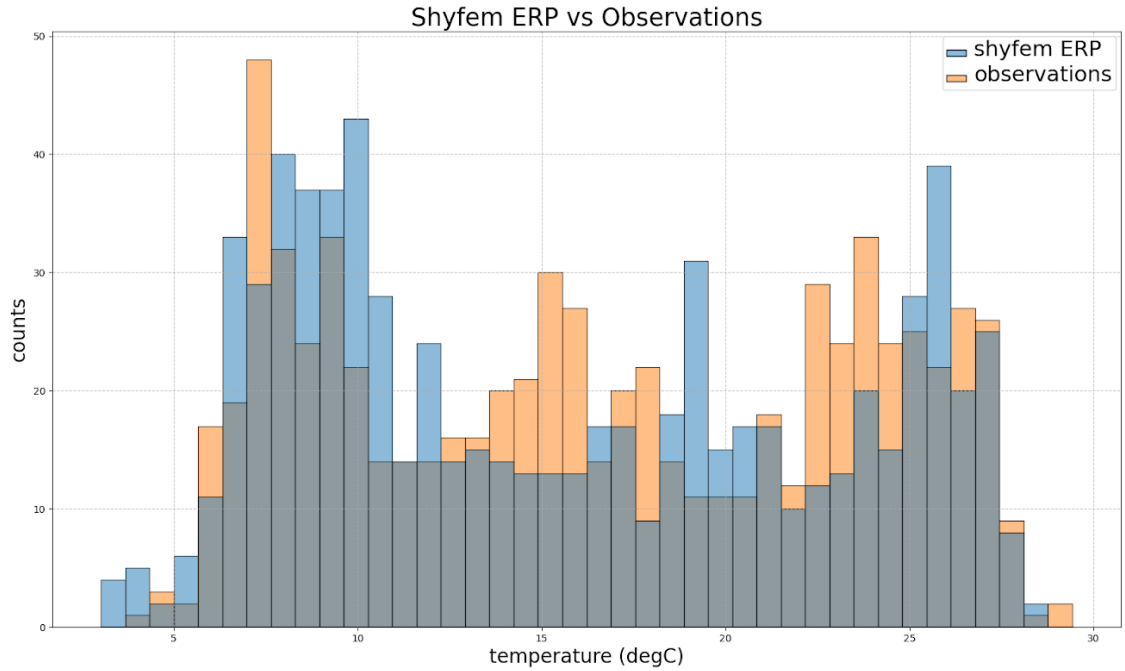

Figure x39: Observed (orange) and modeled (blue) distribution of temperature at Porto Garibaldi station.

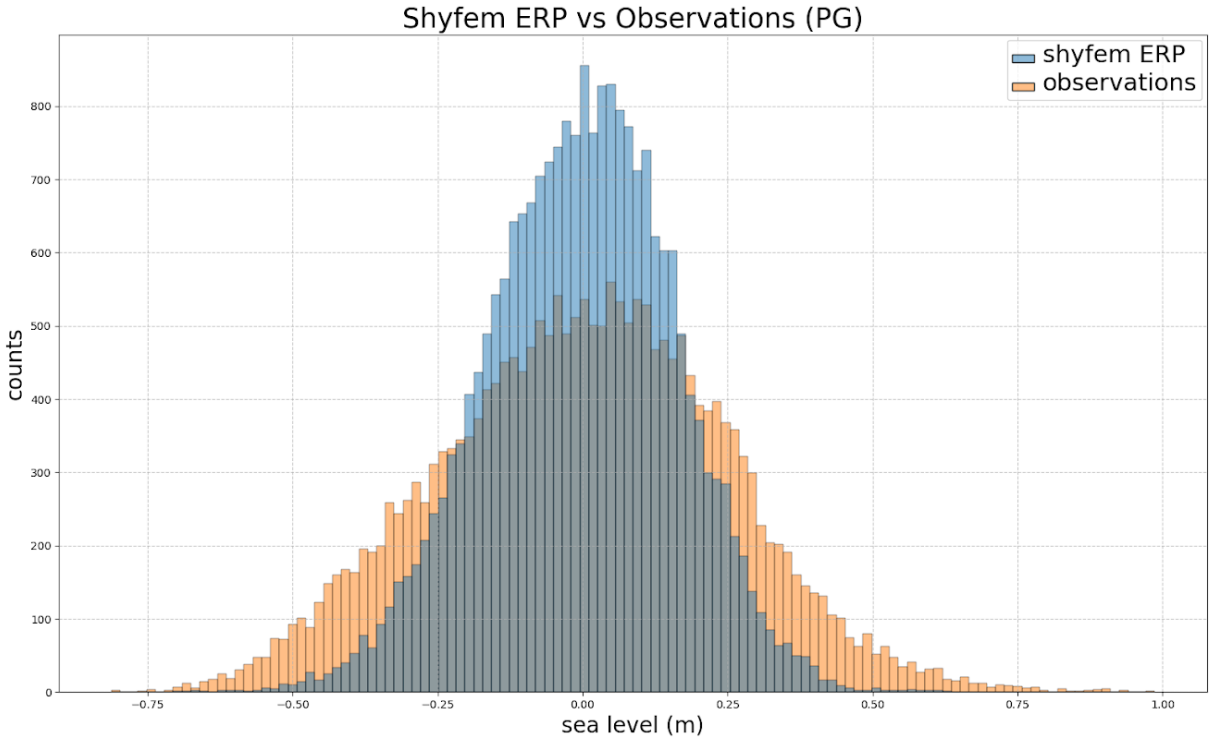

Figure x40: Observed (orange) and modeled (blue) distribution of sea level at Porto Garibaldi station.

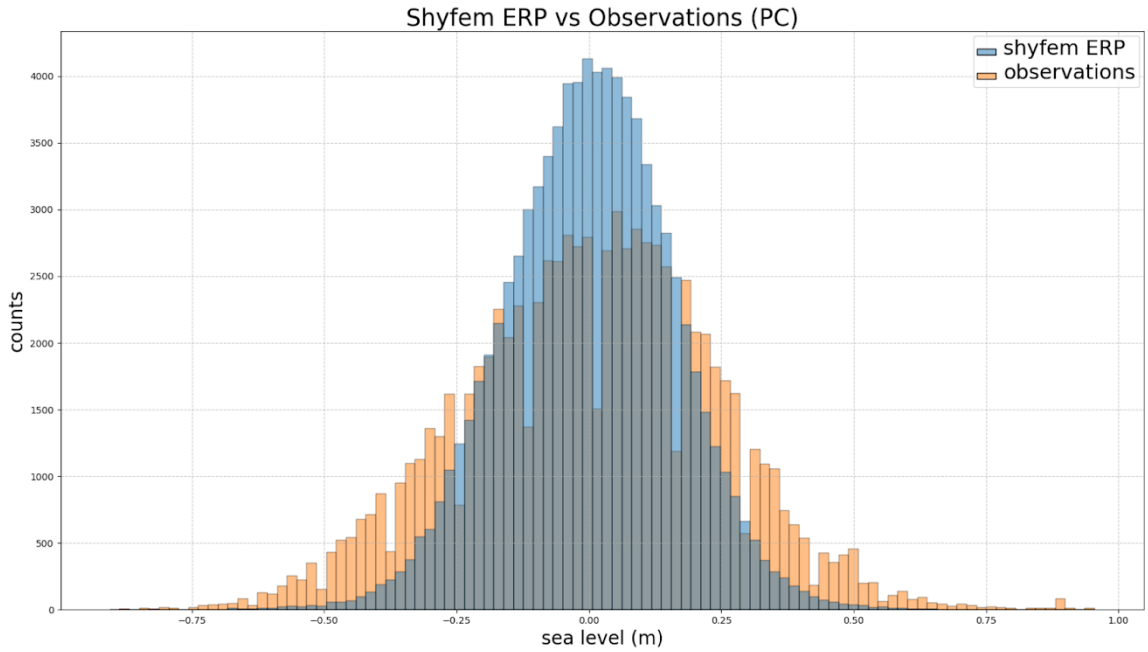

Figurex41: Observed (orange) and modeled (blue) distribution of sea level at Porto Corsini station.

The SHYFEM ERP model has the tendency to be saltier than observed salinity (BIAS = 4.86 psu) in Porto Garibaldi and to miss very low salinity events (Fig. 3.3.2), however the salinity variability shows values comparable with observations, with a standard deviation of σSm= 4.86 psu, comparable to the observed one σSo= 5.30 psu.

Modeled temperature shows satisfactory performance compared to observations (FIg. 3.3.3), with a similar distribution and similar variability (model, σTm= 7.07 C; observations, σTo= 6.89 C). However the model tendency is to be slightly colder than the observed temperature (BIAS= -0.87C).

The results of the sea level show similar results for the two stations. The model has a lower variability (σSSHm= 0.16 m) compared to observations (σSSHo= 0.24 m) in both stations, and the medium to high sea level extremes are underestimated (Fig. 3.3.4, 3.3.5). This could be attributed to an underestimation of the Scirocco events (south-easterly wind) in the WRF wind forcing, since Scirocco is one of the main causes of extreme sea level events in the northern Adriatic Sea.

Aquaculture

1. **Modelling scenarios of *Escherichia coli* contamination to assess the impact on shellfish production areas in Emilia Romagna Pilot**

This study was carried out to determine the potential effects of climate change on the dispersion path of faecal bacteria in the sea and to assess potential effects on the shellfish production areas in the Emilia Romagna Pilot. The study is focused on a single source of pollution with the aim of a general assessment of what can be the change in *Escherichia coli* pollution impacts to be expected in the Climate Change scenario. The area of interest is a coastal stretch of about 12 km that extends about 10 km towards open sea. Its northern boundary is Lido delle Nazioni and its southern one is Riserva Statale Foce Fiume Reno. It includes several shellfish production areas and the mouth of Logonovo channel identified as a source of land-based bacterial pollution (figure 42).

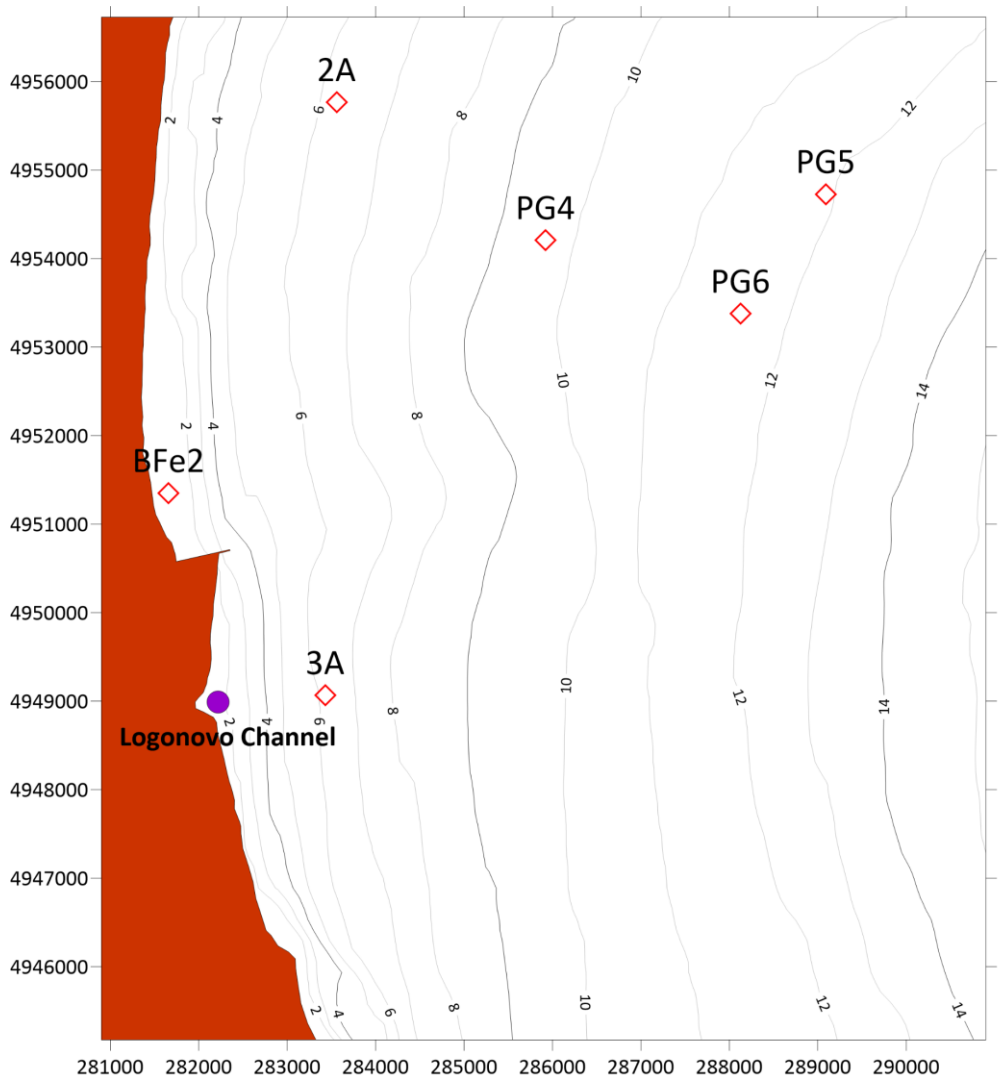

Figure 42. Computational domain of the study. Red squares: shellfish production areas of interest. Purple dot: mouth of Logonovo channel.

Two climatic reference years were considered: 2020 and 2050. 2020 represents the last available year with validated data, while 2050 is a significant year in the future to assess the effects of climate change. This study evaluated the effects of climate change induced by: (a) hydrodynamic variability caused by meteorological and marine forcings such as wind, astronomical and meteorological tides, river-induced currents, and density gradients, and (b) variability in bacterial mortality induced by different environmental conditions of bacterial exposure, particularly solar radiation, salinity, and water temperature.

The scenarios have been implemented in a modelling system composed by Delft3D Flow and Delft3D-WAQ modules. Available data from Adriaclim data repository on ERDDAP data server were used to force the modelling system. Data for the entire year 2020 and the RCP 8.5 scenario for the full year 2050 were used. Current and sea level data were downloaded at various points near the calculation domain from the AdriaClim Adriatic model. Additionally, temperature, salinity, and solar radiation data were downloaded at the same points from the AdriaClim atmospheric model. Subsequently, these data were processed to generate boundary conditions for the numerical models.

A 2DH (two-dimensional horizontal) scheme with vertically integrated variables was chosen for the modelling system. This scheme introduces simplifying assumptions about the hydrodynamic and dispersion processes that occur, mainly related to the formation of thermoclines and hydrodynamic circulation flows for vertical layers. The 2D scheme was adopted to provide a first level of reference analysis that could be meaningful and agile in implementation. A full 3D model would have required to have access to boundary conditions and internal forcing from other AdriaClim products that were not compatible with their release dates.

A computational grid with a resolution of 200 m was defined to ensure numerical stability and efficient execution of the code with a 5 min time step. The model was initialised one month prior to the period of interest to allow for stability from the beginning of the simulation period (January 2020 and January 2050). An appropriate temporal calculation step was chosen. A simulation period of one year was adopted to represent a complete seasonal cycle. Thus, hydrodynamic models for 2020 and 2050 were implemented. The dispersion model, which determines the temporal variation of the contaminant mass, consists of an advective/dispersive component involving hydrodynamic factors, fluid properties, and contaminant concentration, as well as a generation/decay component for *E. coli* bacteria, introduced and dispersed in the sea. Changes between 2020 and 2050 in solar radiation and water temperature were considered in the Mancini equation (1978) for bacterial mortality in the dispersion model. Salinity variation and hydrodynamics are automatically derived from the results of the hydrodynamic model. Other parameters are assumed constant, using default values (see *E. coli* model details). The emission point was set at a location corresponding to the mouth of the Logonovo channel. Since data on the quantities of *E. coli* produced and the outflow rates from the channel were not available, continuous emissions of 10 m^3/s were considered with a reference value of 100 MPN/m^3. The emission was defined and implemented only in the dispersion model.

The hydrodynamic model was implemented using default calibration parameters available in Delft3D-flow, while for the decay rate of *E. coli* pollution in Delft3D-WAQ the formulation proposed by Mancini (1978) was used, taking into account variation of water temperature, salinity and solar radiation.

In order to verify the quality of the modelling output, plumes resulting from the numerical implementation have been compared with satellite images available on Google Earth (Source "Google Earth Image Landsat/ Copernicus"). Results are shown in Figure 43.

15.02.2020

28.02.202

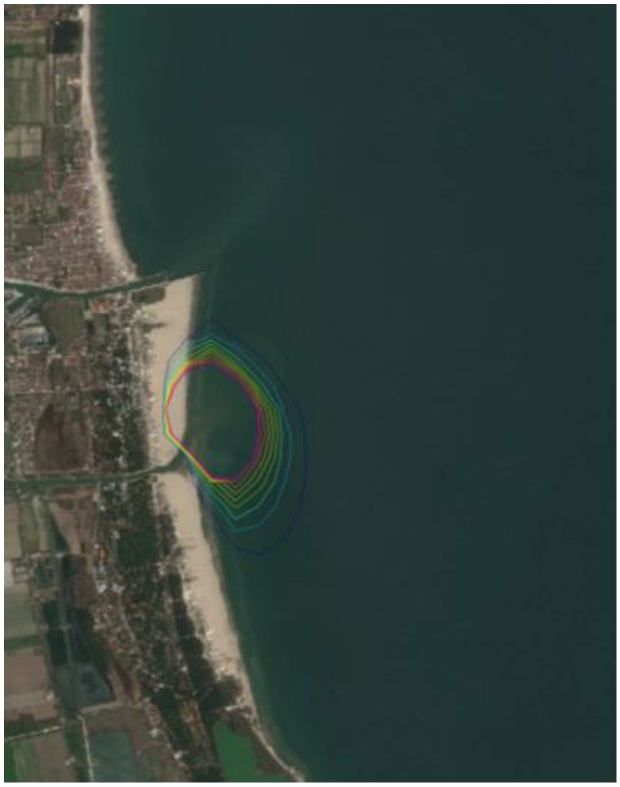	
19.03.2020	03.04.2020

13.05.2020

02.09.2020

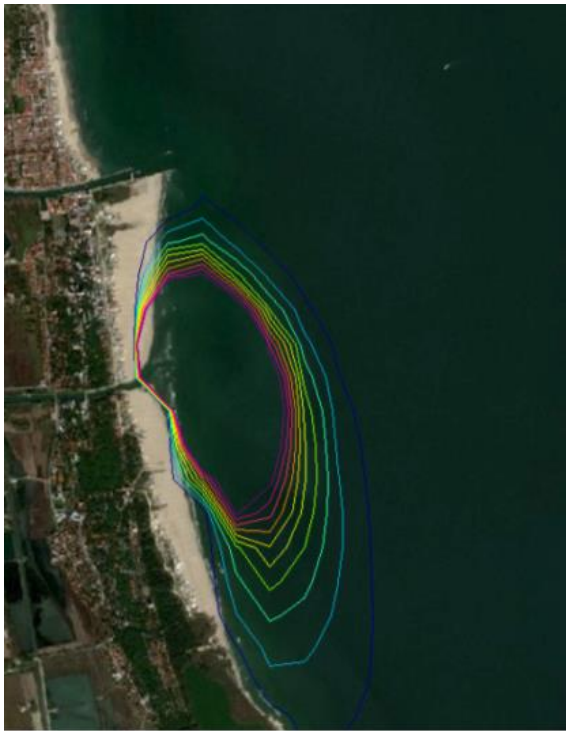

06.01.2020

Figure 43. Qualitative comparison between satellite images from Google Earth (Source "Google Earth Image Landsat/ Copernicus") and the numerical results showing a good agreement between the observed plume from satellite and the output of the modelling system.

In order to make the results as general as possible, the analysed output is the concentration of *E. coli* normalized (time step by time step) with the corresponding value at the mouth of Logonovo channel. As a result, we obtain a value representing a dilution coefficient. Values close to 1 represent no dilution of the pollutant with respect to the concentration at the Logonovo channel mouth whereas values lesser than 1 indicate different degrees of dilution. In particular, concentration values at the mouth may vary from about 5.000 unit/100 ml (about 10^4 unit/100 ml) in standard condition and about 10^9 unit/100 ml in cases of total by-passes from Urban Waste Water Treatment Plants, while reference thresholds for aquaculture are of the order of 10^2. Hence dilution coefficients of about 0.1 indicated a potential impact in case of standard pollution values from the channel. In case of total bypasses this value is 10^-5. The results of the simulations show that climate change will produce a different path of marine dispersion for the plume (Figure 44). The area of impact in standard conditions is very similar, while in the climate change scenario it is wider in the total by-pass case.

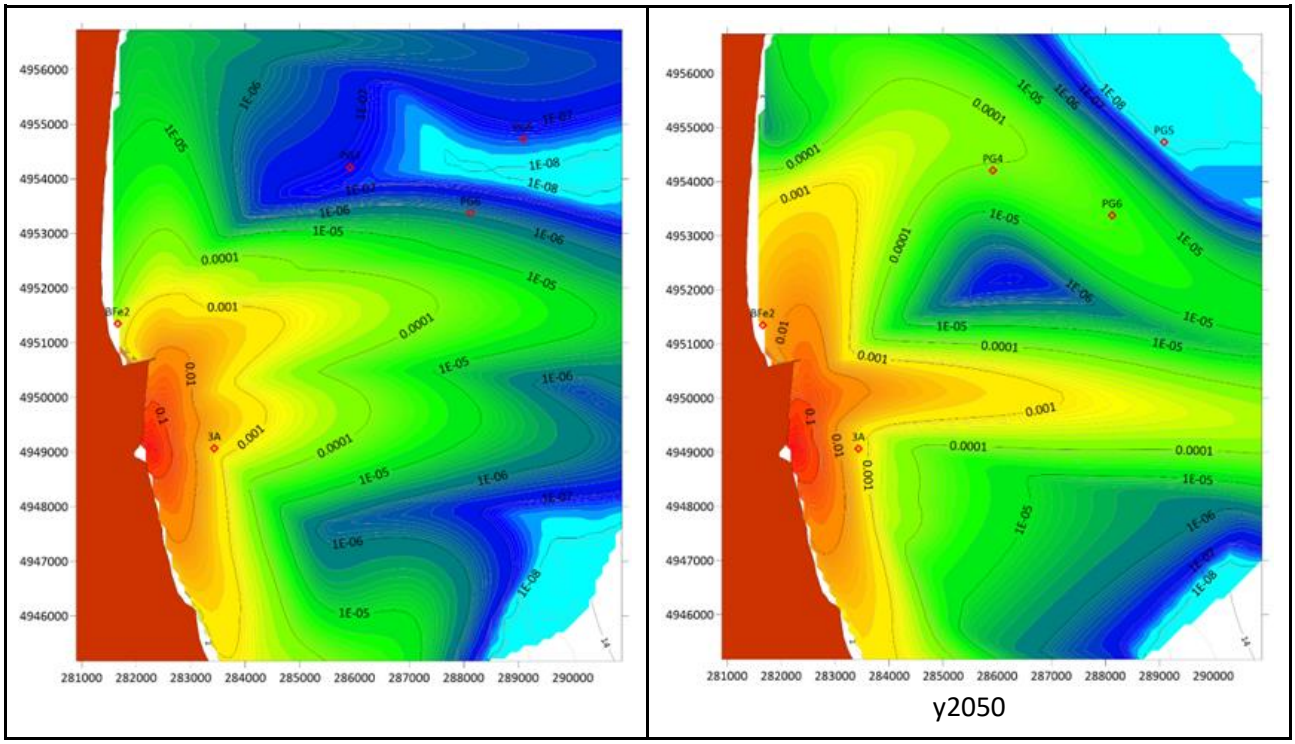

y2020	
Figure 44: Left: Envelope of maxima normalized *E. coli* concentration in the year 2020. Right: Envelope of maxima normalized *E. coli* concentration in the year 2050.	

Focusing on the shellfish production areas, Figure 45 highlights that there is about one order of magnitude resulting from the difference between the normalized concentration in 2050 in respect to 2020 considering maxima, while it is generally lower for mean values.

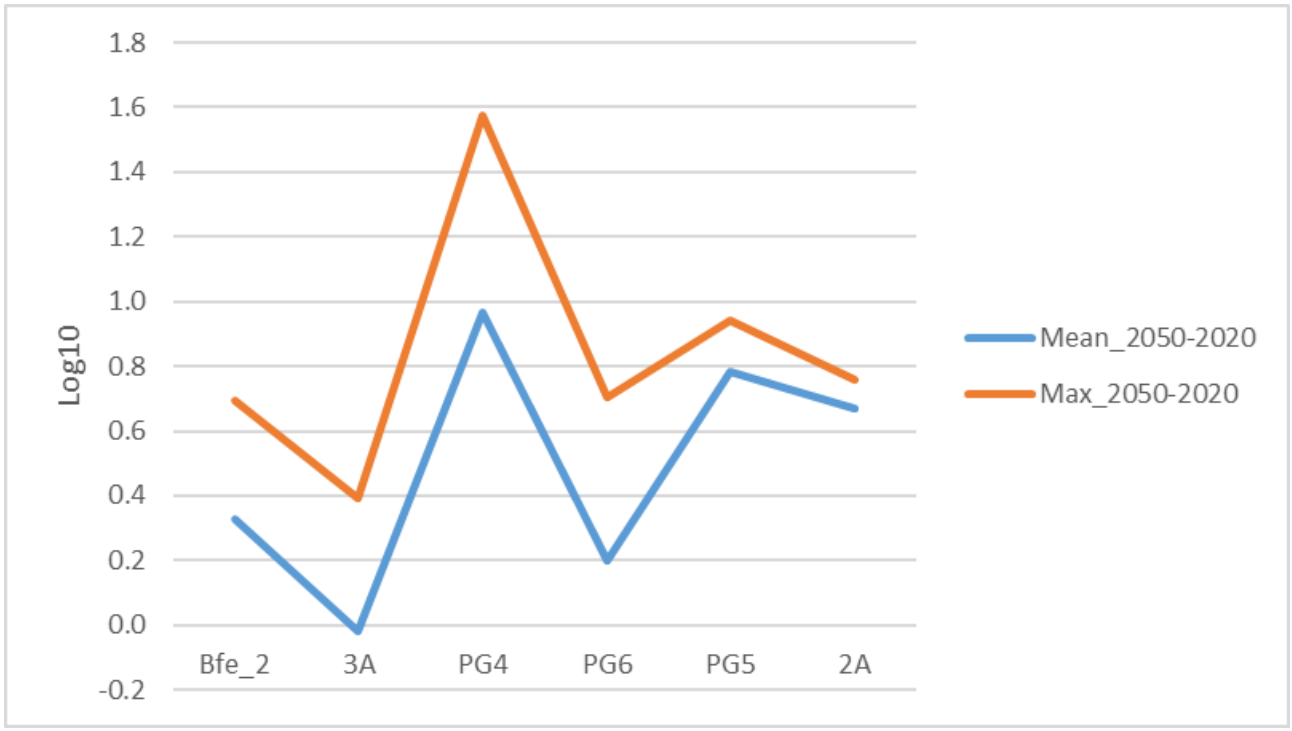

Figure 45: Mean and Maxima of dilution coefficient in the shellfish production areas.

Aquaculture

2. Analysis of suitability for shellfish farming in climate change scenario in Emilia Romagna Pilot

For the PS3 area, an analysis was conducted on environmental variables in relation to their optimal ranges for aquaculture activities according to the national AZA technical guide (ISPRA-MiPAAF, 2020). Both physical factors such as currents, waves, and temperature, as well as biogeochemical parameters including chl-a (chlorophyll-a) and dissolved oxygen, are crucial in determining suitable areas for aquaculture. In this analysis, data from the Adriaclim data repository on Erddap were utilised. These data included information from both historical (1992-2020) and climate change (2022-2050) scenarios.

The parameters were examined by assessing the percentage of events falling within specific ranges considered optimal for aquaculture activities. The analysis focused on the first 5 meters of depth and encompassed the entire study period, as well as an analysis for every season.

Regarding the wave height variable, only historical data were made available at time of analysis, so climate change scenario data were not analyzed. The analysis involved assessing the percentage of occurrences within a broader selection of ranges (to be able to identify also extreme events) and calculating the mean values for the entire examined period (1992-2020) and for each individual season.

Results of the analysis for physical and biogeochemical data in historical and climate change scenario are reported in figure 46. Shellfish growing areas may experience more critical temperature events in climate change scenario along all the Emilia Romagna pilot and GIDAC area. In particular increasing events above 28°C could drive to episodes of eutrophication and anoxia, associated with stress, reducing performance and abnormal mortality of shellfish.

	Variable	Description	Analysis
	Chl-a	% of events within the optimal concentration, first 5 meters of depth, seasonal and annual analysis	>=0.2 mg/m^3
	Dissolved oxygen	% of events within the optimal concentration, first 5 meters of depth, seasonal and annual analysis	>= 6.5 mg/l
	Current speed	% of events between the optimal range, first 5 meters of depth, seasonal and annual analysis	0.03 <= m/s >= 0.1

1992 -2020 (historical) **2022 -2050 (climate change scenario)**	Temperature	% of events between the optimal ranges, first 5 meters of depth, seasonal and annual analysis % of events over and above critical temperature, first 5 meters of depth, annual analysis	18 <= °C >= 26 (fish) 10 <= °C >= 24 (shellfish) 5 <= °C >= 28 (shellfish)
	Wave height*	% of events between ranges, annual analysis	0.0 <= m >= 0.2 0.0 <= m >= 0.7 0.0 <= m >= 2.5 0.0 <= m >= 3.0 2.5 <= m >= 5.0 3.0 <= m >= 5.0 5.0 <= m >= 100
	Wave height	Mean value, seasonal and annual analysis	-

Table 14. Statistical analysis of variables to assess aquaculture suitability from Adriaclim data repository on Erddap, historical (1992-2020) and climate change scenario (2022-2050). *Wave data for CC scenario not available at time of analysis.

Historical (1992-2020)	Climate change scenario (2022-2050)

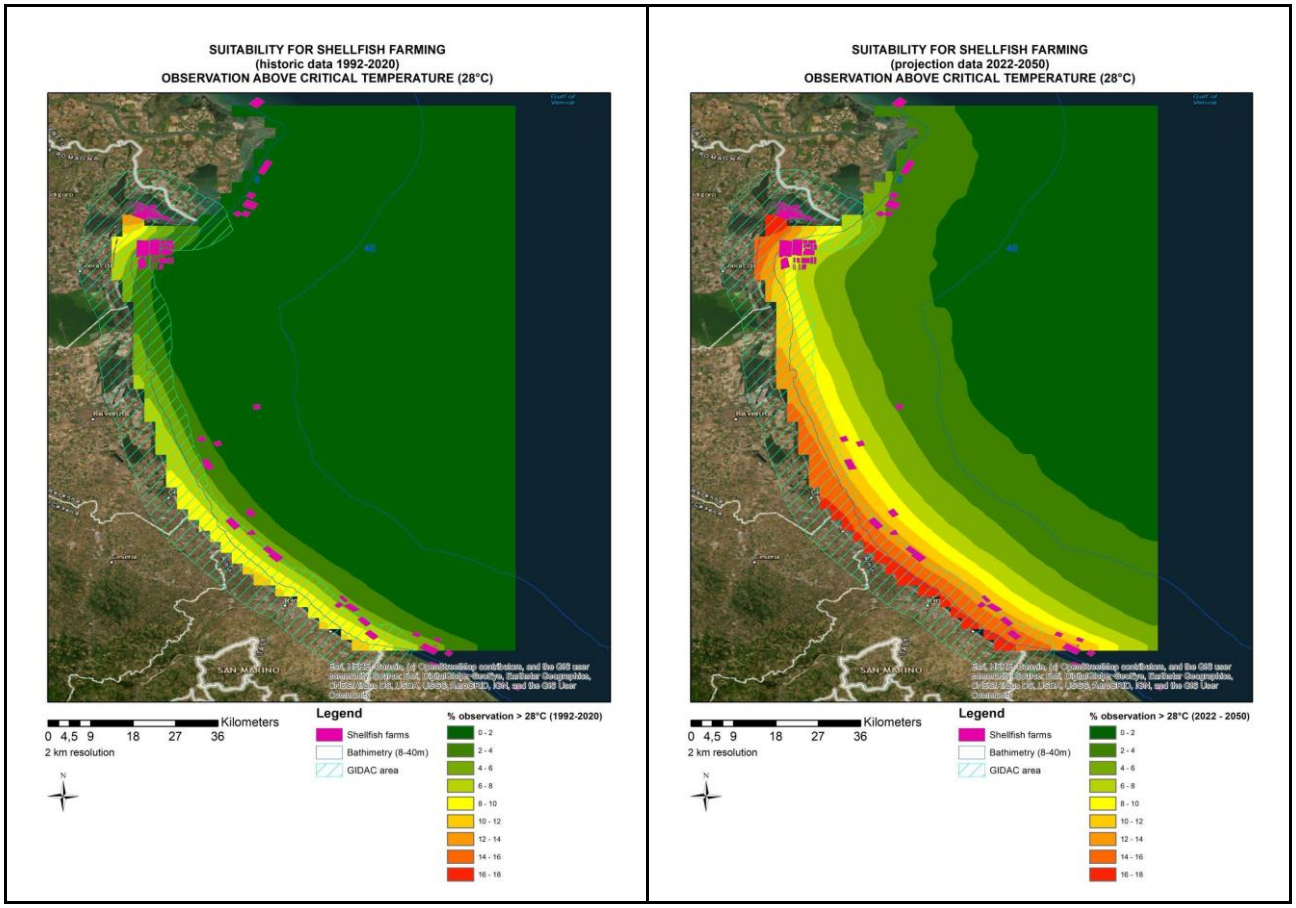
SUITABILITY FOR SHELLFISH FARMING
(historic data 1992-2020)
OBSERVATION ABOVE CRITICAL TEMPERATURE (28°C)
SAN MARINO
Kilometers
0 4,5 9 18 27 36
2 km resolution
N
Legend
Shellfish farms
Bathimetry (8-40m)
GIDAC area
% observation > 28°C (1992-2020)
0 - 2
2 - 4
4 - 6
6 - 8
8 - 10
10 - 12
12 - 14
14 - 16
16 - 18
SUITABILITY FOR SHELLFISH FARMING
(projection data 2022-2050)
OBSERVATION ABOVE CRITICAL TEMPERATURE (28°C)
SAN MARINO
Kilometers
0 4,5 9 18 27 36
2 km resolution
N
Legend
Shellfish farms
Bathimetry (8-40m)
GIDAC area
% observation > 28°C (2022 - 2050)
0 - 2
2 - 4
4 - 6
6 - 8
8 - 10
10 - 12
12 - 14
14 - 16
16 - 18

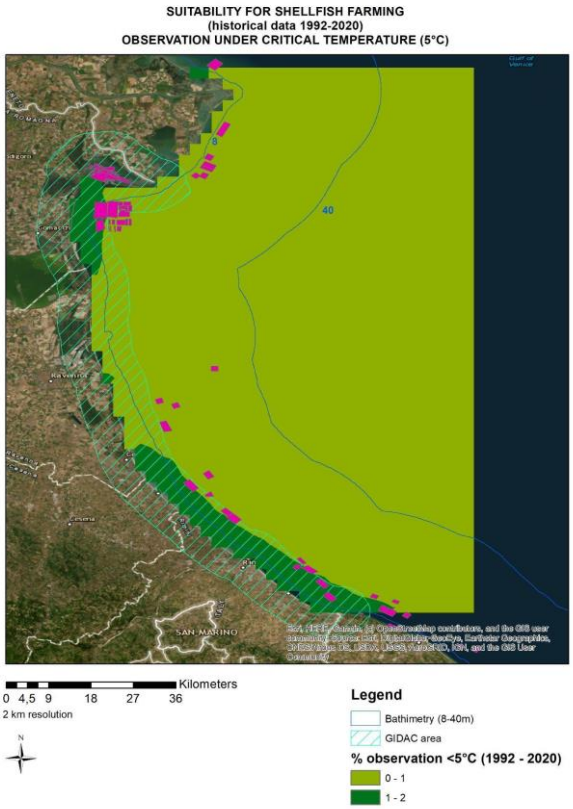
SUITABILITY FOR SHELLFISH FARMING
(historical data 1992-2020)
OBSERVATION UNDER CRITICAL TEMPERATURE (5°C)
8
40
SAN MARINO
Kilometers
0 4,5 9 18 27 36
2 km resolution
N
Legend
Bathimetry (8-40m)
GIDAC area
% observation <5°C (1992 - 2020)
0 - 1
1 - 2

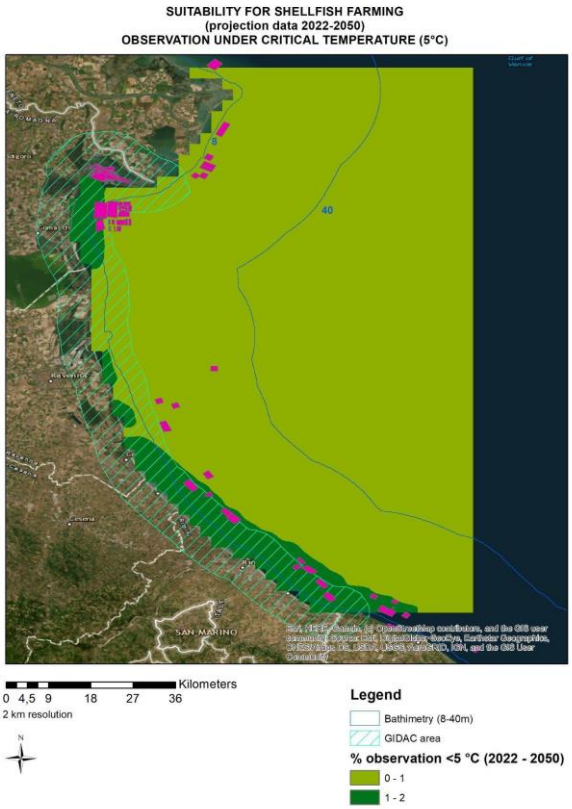
SUITABILITY FOR SHELLFISH FARMING
(projection data 2022-2050)
OBSERVATION UNDER CRITICAL TEMPERATURE (5°C)
8
40
SAN MARINO
Kilometers
0 4,5 9 18 27 36
2 km resolution
N
Legend
Bathimetry (8-40m)
GIDAC area
% observation <5 °C (2022 - 2050)
0 - 1
1 - 2

SUITABILITY FOR SHELLFISH FARMING
(historical data 1992 - 2020)
OBSERVATIONS ABOVE OPTIMAL OXYGEN CONCENTRATION (6,5 mg/l)

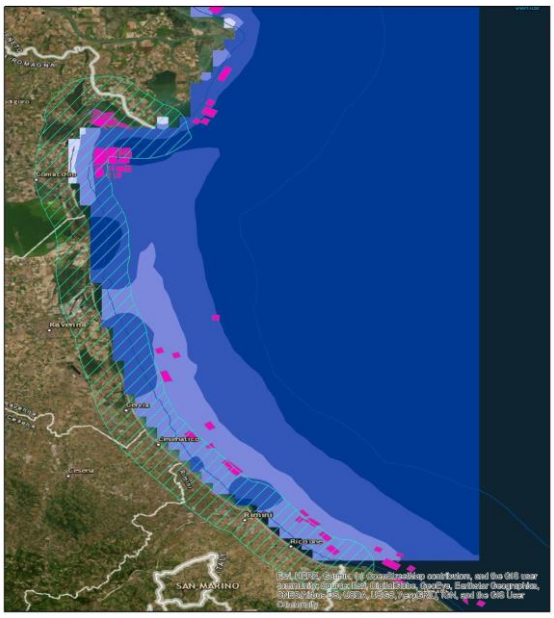

Kilometers
0 5 10 20 30 40
2 km resolution

Legend
GIDAC area
Shellfish farms
Bathimetry (8-40m)
% Obs. OXY ≥ 6.5 mg/l (1992-2020)
80 - 85
85 - 90
90 - 95
95 - 100

SUITABILITY FOR SHELLFISH FARMING
(projection data 2022 - 2050)
OBSERVATIONS ABOVE OPTIMAL OXYGEN CONCENTRATION (6,5 mg/l)

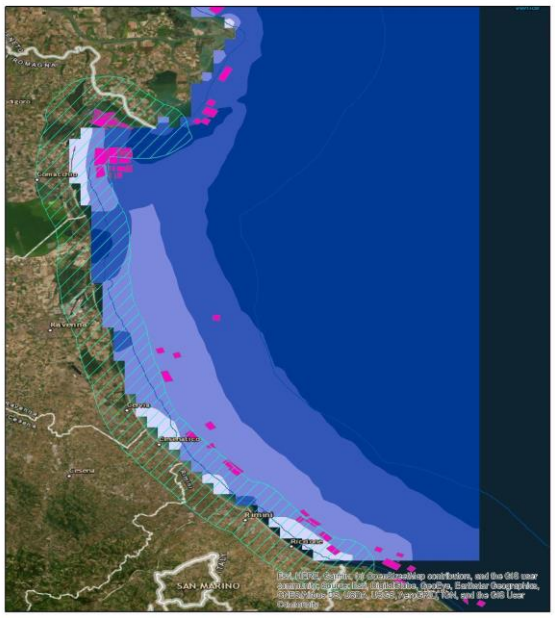

Kilometers
0 5 10 20 30 40
2 km resolution

Legend
GIDAC area
Shellfish farms
Bathimetry (8-40m)
% Obs. OXY ≥ 6.5 mg/l (2022-2050)
80 - 85
85 - 90
90 - 95
95 - 100

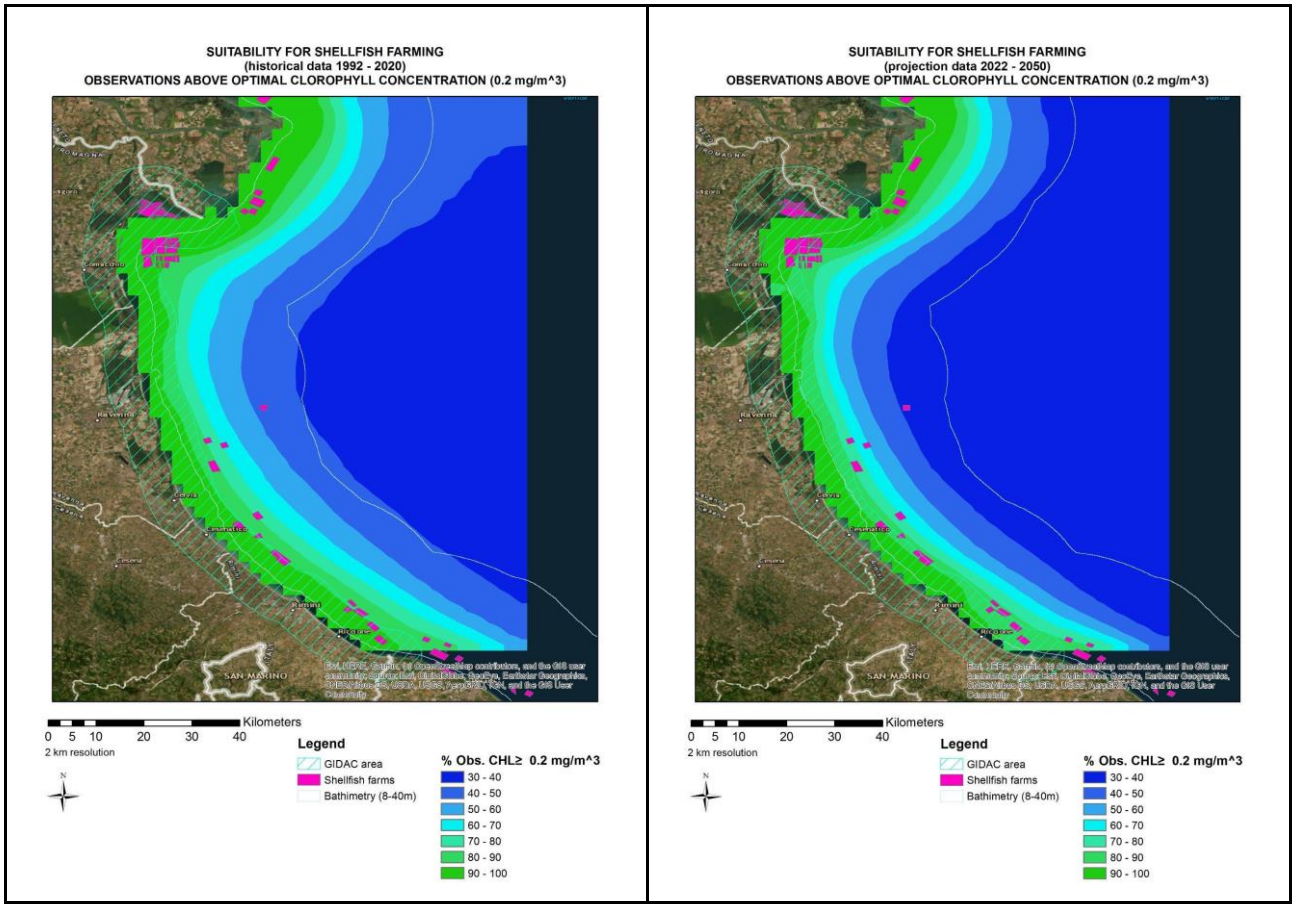
SUITABILITY FOR SHELLFISH FARMING
(historical data 1992 - 2020)
OBSERVATIONS ABOVE OPTIMAL CLOROPHYLL CONCENTRATION (0.2 mg/m^3)
SAN MARINO
Kilometers
0 5 10 20 30 40
2 km resolution
Legend
GIDAC area
Shellfish farms
Bathimetry (8-40m)
% Obs. CHL≥ 0.2 mg/m^3
30 - 40
40 - 50
50 - 60
60 - 70
70 - 80
80 - 90
90 - 100
SUITABILITY FOR SHELLFISH FARMING
(projection data 2022 - 2050)
OBSERVATIONS ABOVE OPTIMAL CLOROPHYLL CONCENTRATION (0.2 mg/m^3)
SAN MARINO
Kilometers
0 5 10 20 30 40
2 km resolution
Legend
GIDAC area
Shellfish farms
Bathimetry (8-40m)
% Obs. CHL≥ 0.2 mg/m^3
30 - 40
40 - 50
50 - 60
60 - 70
70 - 80
80 - 90
90 - 100

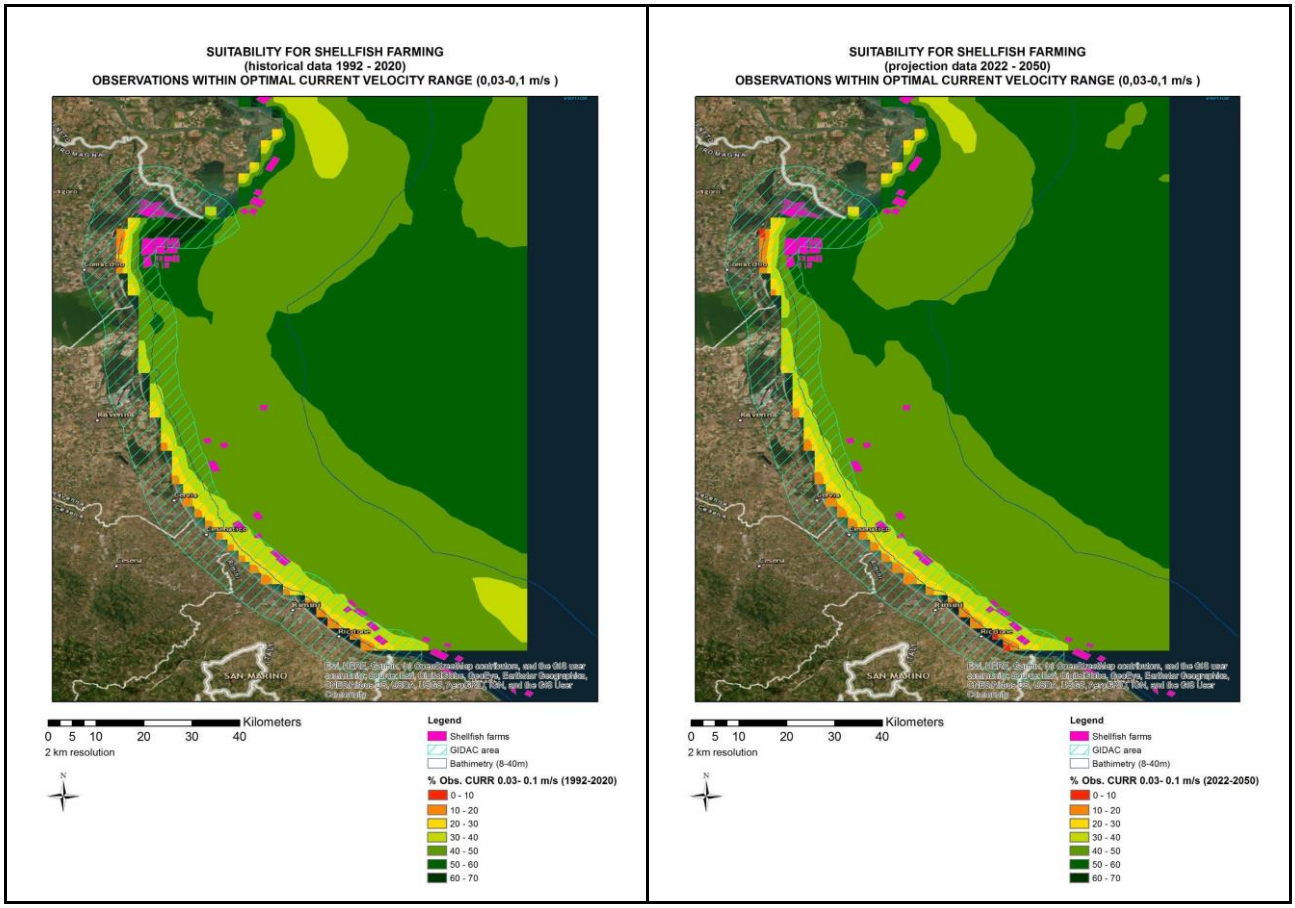

3.4 PS4 Apulia region

Statistics of sea state variables and indicators computed for PS4 from Adriaclim results (historical 1992-2011, projection 2031-2050) and Copernicus Reanalysis (1992-2011 - Table 14).
For the further local downscaling proposed over the Ofanto estuary, a single day comparison of the CMC EBM with a monitoring campaign of the salt wedge intrusion length performed by CNR IRSA has been considered for site-specific calibration (see Del.3.2.1).

Table 15: Statistics computed for PS4 from reanalysis scenario (REA 1992-2011), historical (Hist 1992-2011) and projection (Proj 2031-2050) climate scenario (Hist 1992-2011).

Station	Variable	Trend (units/year)			
		Description	REA 1992-2011	Hist 1992-2011	Proj 2031-2050
Apulia coast	Sea surface temperature (°C)	*Trend in monthly mean values*	*0.052 ± 0.000*	*0.037 ± 0.000*	*0.016 ± 0.000*
		Trend in monthly extreme (p95) values	*0.062 ± 0.000*	*0.037 ± 0.000*	*0.019 ± 0.000*
	Surface salinity	*Trend in monthly mean values*	*0.008 ± 0.000*	*0.010 ± 0.000*	*0.020 ± 0.000*
	Sea surface height (mm)	*Trend in monthly mean values*	*4.60 ± 0.03*	*4.54 ± 0.03*	*3.86 ± 0.02*
		Trend in monthly extreme (p95) values	*4.66 ± 0.03*	*4.51 ± 0.03*	*3.78 ± 0.02*

3.5 PS5 Dubrovnik Neretva area

Table 16: Statistics computed for Neretva (43°N, 17.45°E) station from historical climate scenario (Hist 1992-2020) and climate change RCP85 scenario (RCP8.5 2022-2050).

Station	Variable	Trend (units/year)				
		Description	Obs 1991-2020	REA 1991-2020	Hist 1992-2020	RCP8.5 2022-2050

Neretva station	Sea temperature (°C)	Trend in monthly mean values at 0 m	-	-	-0.0150 ±0.0347	-0.0163 ±00.0363
		Trend in monthly mean values at 10 m		-	-0.0720 ±0.0228	-0.0696 ±00.0235
	Sea level (m)	Trend in monthly mean values (Sea Level calibrated)	-	-	0.0024 ±00.0002	0.0022 ±0.0002
		Trend in monthly mean values (Sea Level calibrated ster avg)	-	-	0.0025 ±00.0003	0.0029 ±0.0003
		Trend in monthly mean values (SSH trend correction)	-	-	0.0030 ±00.0002	0.0030 ±0.0002
	Sea salinity (psu)	Trend in monthly mean values at 0 m		-	0.2795 ±0.0275	0.3070 ±0.0290
		Trend in monthly mean values at 10 m		-	0.0161 ±0.0021	0.0092 ±0.0023

3.6 PS6 Split – Dalmatia area

Table 17: Statistics computed for Stončica station from observations (Obs 1991-2020), historical climate scenario (Hist 1992-2020) and climate change RCP85 scenario (RCP8.5 2022-2050).

Station	Variable	Trend (units/year)

		Description	Obs 1991-2020	REA 1991-2020	Hist 1992-2020	RCP8.5 2022-2050
Stončica station	Sea temperature (°C)	Trend in monthly mean values at 0 m	*No Sign.Trend*	-	0.0106 ±0.0274	0.0084 ±0.0286
		Trend in monthly mean values at 10 m	*No Sign.Trend*	-	0.0246 ±0.0233	0.0273 ±0.0245
		Trend in monthly mean values at 20 m	*No Sign.Trend*	-	0.0382 ±0.0192	0.0441 ±0.0205
		Trend in monthly mean values at 30 m	0.0476	-	0.0366 ±0.0168	0.0447 ±0.0179
		Trend in monthly mean values at 50 m	0.0485	-	0.0297 ±0.0127	0.0393 ±0.0136
		Trend in monthly mean values at 75 m	0.0498	-	0.0316 ±0.0088	0.0375 ±0.0097
		Trend in monthly mean values at 100 m	0.0543	-	0.0372 ±0.0063	0.0419 ±0.0068
Stončica station	Sea salinity (PSU)	Trend in monthly mean values at 0 m	0.0154	-	0.0346 ±0.0026	0.0326 ±0.0029
		Trend in monthly mean values at 10 m	0.0139	-	0.0289 ±0.0013	0.0229 ±0.0013
		Trend in monthly mean values at 20 m	0.0122	-	0.0256 ±0.0011	0.0186 ±0.0010

		Trend in monthly mean values at 30 m	0.0138	-	0.0237 ±0.0010	0.0157 ±0.0009
		Trend in monthly mean values at 50 m	0.0146	-	0.0195 ±0.0008	0.0111 ±0.0008
		Trend in monthly mean values at 75 m	0.0129	-	0.0167 ±0.0007	0.0077 ±0.0007
		Trend in monthly mean values at 100 m	0.0104	-	0.0153 ±0.0006	0.0062 ±0.0006

Table 18: Statistics computed for the Kaštela Bay station ST 101 from observations (Obs 1991-2020), historical climate scenario (Hist 1992-2020) and climate change RCP85 scenario (RCP8.5 2022-2050).

Station	Variable	Trend (units/year)				
		Description	Obs 1991-2020	REA 1991-2020	Hist 1992-2020	RCP8.5 2022-2050
Kaštela Bay station ST 101	Sea temperature (°C)	Trend in monthly mean values at 0 m	*No Sign.Trend*	-	0.0208 ±0.0349	0.0185 ±0.0365
		Trend in monthly mean values at 10 m	*No Sign.Trend*	-	-0.0170 ±0.0235	-0.0294 ±0.0246
		Trend in monthly mean values at 20 m	0.0179	-	-0.0213 ±0.0201	-0.0360 ±0.0215

		Trend in monthly mean values at 30 m	*No Sign.Trend*	-	-0.0225 ±0.0193	-0.0343 ±0.0207
	Sea level (m)	Trend in monthly mean values (Sea Level calibrated)	*-0.0032 ±0.0005*	-	0.0017 ±0.0003	0.0030 ±0.0002
		Trend in monthly mean values (Sea Level calibrated ster avg)	-	-	0.0022 ±0.0003	0.0014 ±0.0003
		Trend in monthly mean values (SSH trend correction)	-	-	0.0031 ±0.0002	0.0027 ±0.0004
	Sea salinity (psu)	Trend in monthly mean values at 0 m	*No Sign.Trend*	-	0.1131 ±0.0117	0.1348 ±0.0127
		Trend in monthly mean values at 10 m	*No Sign.Trend*	-	0.0469 ±0.0026	0.0399 ±0.0024
		Trend in monthly mean values at 20 m	*No Sign.Trend*	-	0.0401 ±0.0022	0.0285 ±0.0021
		Trend in monthly mean values at 30 m	0.025	-	0.0375 ±0.0021	0.0268 ±0.0020

4. References

Cleveland, R. B., Cleveland, W. S., McRae, J.E., and Terpenning, I., 1990. STL: A Seasonal-Trend Decomposition Procedure Based on LOESS. Journal of Official Statistics, 6, 3-73.

Chust, G., González, M., Fontán, A., Revilla, M., Alvarez, P., Santos, M., et al., 2022. Climate regime shifts and biodiversity redistribution in the Bay of Biscay. Sci. Total Environ. 803. doi: 10.1016/j.scitotenv.2021.149622.

Mudelsee, M., 2019. Trend analysis of climate time series: A review of methods. Earth Sci. Rev., 190, 310-322, doi: 10.1016/j.earscirev.2018.12.005.